# Studies of plant innate immunity provide new functional insights on class IIa WRKY transcription factors and reveals a role for two Glucan Synthase-Like genes in gametophyte development

Inaugural-Dissertation

zur

Erlangung des Doktorgrades

der Mathematisch-Naturwissenschaftlichen Fakultät

der Universität zu Köln

vorgelegt von

**Armin Töller**

aus Brühl

**Köln, Januar 2011**

Die vorliegende Arbeit wurde am Max-Planck-Institut für Pflanzenzüchtungsforschung in Köln in der Abteilung für Molekulare Phytopathologie (Direktor: Prof. Dr. P. Schulze-Lefert) angefertigt.



MAX-PLANCK-GESELLSCHAFT



Max-Planck-Institut für
Pflanzenzüchtungsforschung

| | |
|---|---|
| **Berichterstatter:** | Professor Doktor Paul Schulze-Lefert |
| | Professor Doktor Martin Hülskamp |
| **Prüfungsvorsitzender:** | Professor Doktor Ulf-Ingo Flügge |
| **Tag der Disputation:** | 24. Januar 2011 |

**Publications:**

**Armin Töller, Lynette Brownfield, Christina Neu, David Twell, and Paul Schulze-Lefert** (2008) Dual function of Arabidopsis glucan synthase-like genes *GSL8* and *GSL10* in male gametophyte development and plant growth. *The Plant Journal*. **54.** 911-923.

**Tina Jordan, Sabine Seeholzer, Simon Schwizer, Armin Töller, Imre E. Somssich and Beat Keller** (2010) The wheat *Mla* homologue *TmMla1* exhibits an evolutionarily conserved function against powdery mildew in both wheat and barley. *The Plant Journal* **65**, 610-621.

**Takaki Maekawa, Wei Cheng, Laurentiu N. Spiridon, Armin Töller, Ewa Lukasik, Yusuke Saijo, Peiyuan Liu, Qian-Hua Shen, Marius A. Micluta, Imre E. Somssich, Frank L.W. Takken, Andrei-Jose Petrescu, Jijie Chai & Paul Schulze-Lefert** (2011) Coiled-Coil Domain-Dependent Homodimerization of Intracellular MLA Immune Receptors Defines a Minimal Functional Module for Triggering Cell Death (under revision in *Cell Host & Microbe*).

# Summary

**Chapter one**


Plants have evolved a sophisticated innate immune system that is composed of multiple layers. The integration of signals derived from these layers constitutes a crucial prerequisite for efficient defence. Resistance (R) proteins serve as direct or indirect recognition receptors for pathogen-derived isolate-specific effector proteins. Members of the superfamily of WRKY transcription factors regulate plant responses towards pathogens either as activators or repressors. The barley (*Hordeum vulgare*) R protein MLA confers resistance towards the powdery mildew *Blumeria gramins* f. sp. *hordeii*. MLA physically interacts through its N-terminal coiled coil (CC) domain with the transcriptional repressors *Hv*WRKY1 and *Hv*WRKY2 in an effector-dependent manner. This effector-stimulated interaction provides a mechanistic model how plants can integrate defence-related signals from different recognition layers and thereby modulate expression of defence-associated genes. *Arabidopsis thaliana* lacks a functional homologue of MLA and is susceptible towards the powdery mildew *Golovinomyces orontii.* Similar to barley, mutations of the functional homologues of *HvWRKY1* and *HvWRKY2*, namely *AtWRKY18* and *AtWRKY40*, in *Arabidopsis* confer resistance towards *G. orontii*.


In this work I analyzed structural and functional conservation between the transcriptional repressors from barley (*Hv*WRKY1 and *Hv*WRKY2) and their homologues in *Arabidopsis* (*At*WRKY18 and *At*WRKY40). My results revealed that *At*WRKY18 and *At*WRKY40 can associate via a conserved C-terminal motif with selective *R*-gene encoded proteins. Identification of the previously characterized R protein HRT, as putative interactor of *At*WRKY18 and *At*WRKY40, provides a suitable model for further studies.


In addition, genetic studies using the *Atwrky18 AtwrkyY40* double mutant identified differential requirements for the defence-related genes *EDS1*, *CYP81F2*, *PEN2, PEN1* and *PAD3* in pre- and post-invasive resistance towards *G. orontii*. The results support the central role of *EDS1* in plant immunity and indicate a novel *PEN2*-independened function for *CYP81F2* in post-invasive resistance.

The solution structure of the MLA CC domain was used as a basis to further investigate MLA-dependent associations with *Hv*WRKY1 and *Hv*WRKY2. The crystal structure predicts homo-dimerization of the receptor *in vivo*. Analysis of structure-guided targeted amino acid substitution variants of MLA in yeast provided the first evidence for receptor self-association *in vivo*.

## Chapter two

Members of the Glucan Synthase-Like (GSL) family are believed to be involved in the synthesis of the cell wall component callose in specialized locations throughout the plant. I identified two members of the *Arabidopsis GSL* gene family, *GSL8* and *GSL10*, that are independently required for male gametophyte development and plant growth. Analysis of *gsl8* and *gsl10* mutant pollen during development revealed specific malfunctions associated with asymmetric microspore division. *GSL8* and *GSL10* are not essential for normal microspore growth and polarity, but have a novel role in entry of microspores into mitosis. Impaired function of GSL10 also leads to perturbation of microspore division symmetry, irregular callose deposition and failure of generative cell engulfment by the vegetative cell cytoplasm. Silencing of *GSL8* or *GSL10* in transgenic lines expressing gene-specific dsRNAi constructs resulted in a dwarfed growth habit, thereby revealing additional and independent wild-type gene functions for normal plant growth.

# Zusammenfassung

## Kapitel eins

Pflanzen haben ein differenziertes immanentes Immunsystem entwickelt, welches sich aus mehreren Ebenen zusammensetzt. Die Integration von Signalen, die diesen unterschiedlichen Ebenen entstammen, stellt eine entscheidende Voraussetzung für die Effizienz der pflanzlichen Abwehr dar. Resistenzproteine (R Proteine) fungieren als direkte oder indirekte Erkennungsrezeptoren für Pathogen-abgeleitete isolat-spezifische Effektorproteine. Mitglieder der Superfamilie von WRKY Transkriptionsfaktoren regulieren die pflanzliche Immunantwort entweder als Aktivatoren oder Repressoren. Das Gerste (*Hordeum vulgare*) R Protein MLA vermittelt Resistenz gegenüber dem Mehltaupilz *Blumeria gramins* f. sp. *hordeii*. MLA interagiert physikalisch und effektorabhängig durch seine N-terminale Coiled-coil (CC) Domäne mit den transkriptionellen Repressoren *Hv*WRKY1 und *Hv*WRKY2. Diese effektorstimulierte Interaktion bietet ein mechanistisches Modell, aus dem abgeleitet werden kann, wie Pflanzen abwehrverwandte Signale aus unterschiedlichen Ebenen der Pathogenerkennung integrieren und dadurch die Expression Abwehr-assozierter Gene abstimmen können. *Arabidopsis thaliana* besitzt kein funktionales MLA Homolog und ist anfällig gegenüber dem Mehltaupilz *Golovinomyces orontii*. Ähnlich wie im Gerstesystem vermittelt die gleichzeitige Mutation der funktionalen Homologen von *Hv*WRKY1 und *Hv*WRKY2, namentlich *At*WRKY18 und *At*WRKY40, in *Arabidopsis* Resistenz gegenüber *G. orontii*.

In der vorliegenden Arbeit wurde die strukturelle und funktionelle Konservierung zwischen den transkriptionellen Repressoren aus Gerste (*Hv*WRKY1 und *Hv*WRKY2) und ihren Homologen aus *Arabidopsis* (*At*WRKY18 und *At*WRKY40) untersucht. Die Ergebnisse verdeutlichen, dass *At*WRKY18 und *At*WRKY40 - ähnlich wie ihre funktionellen Homologe aus Gerste - in der Lage sind, durch ein C-terminales Motiv mit bestimmten *R* Gen-codierten Proteinen zu assoziieren. Die Identifikation des bereits charakterisierten R Proteins HRT als putativen Interaktionspartner von *At*WRKY18 und *At*WRKY40 stellt ein geeignetes Modell für weitere Untersuchungen dar.

In einer ergänzenden genetischen Studie konnten unterschiedliche Erfordernisse für die der Pflanzenabwehr zugeordneten Gene *EDS1*, *CYP81F2*, *PEN2, PEN1* und *PAD3*, in der prä- und post-invasiven Resistenz von *Arabidopsis Atwrky18 Atwrky40* Doppelmutanten, gegenüber dem Mehltaupilz *G. oronii*, identifiziert werden. Die Ergebnisse bestätigen die zentrale Funktion von EDS1 in der pflanzlichen Immunität und deuten auf eine bislang unbekannte, PEN2 unabhängige Funktion von CYP81F2 hin.

Die Raumstruktur der MLA CC Domäne wurde als Grundlage zur weiterführenden Analyse der MLA-abhängigen Interaktion mit *Hv*WRKY1 und *Hv*WRKY2 genutzt. Die Kristallstruktur deutet auf eine Homo-Dimerisierung des Rezeptors *in vivo* hin. Erste Hinweise für eine Selbstassoziation von MLA *in vivo* erbrachte die Analyse von gerichteten, von der Kristallstruktur abgeleiteten Aminosäureaustausch-Varianten des Rezeptors in Hefe.

**Kapitel zwei**

Es wird angenommen, dass Mitglieder der Familie der Glucan Synthase-Like (GSL) Proteine an der Synthese der Zellwandkomponente Callose in spezifischen Zellkompartimenten innerhalb der Pflanze beteiligt sind. Innerhalb meiner Arbeit habe ich zwei Mitglieder der *GSL* Genfamilie identifiziert, *GSL8* und *GSL10,* die unabhängig voneinander für die Entwicklung des männlichen Gametophyten sowie für das Pflanzenwachstum benötigt werden. Die Analyse der Pollenentwicklung in *gsl8* und *gsl10* Mutanten ließ spezifische Defekte im Kontext der asymmetrischen Zellteilung der Microsporen erkennen. GSL8 und GSL10 sind für das normale Mikrosporenwachstum oder deren Zellpolarität nicht essentiell, haben aber eine bisher unbekannte Rolle für den Eintritt der Mikrospore in die Mitose. Die Beeinträchtigung der Funktion von GSL10 führt zu Störung der Teilungssymmetrie, irregulärer Calloseablagerung und fehlerhafter Umschließung der generativen Zelle durch das Cytoplasma der vegetativen Zelle. Beeinträchtigung der Transkription von *GSL8* und *GSL10* in transgenen Linien mittels genspezifischer dsRNAi Konstrukte führte zum Auftreten von Zwergwuchs bei den entsprechenden Pflanzen. Dieser Befund zeigt zusätzliche unabhängige Genfunktionen von *GSL8* und *GSL10* für das vegetative Wachstum auf.

# Table of contents

# Table of abbreviations

| | |
|---|---|
| % | percent |
| (v/v) | volume per volume |
| (w/v) | weight per volume |
| °C | degrees Celsius |
| µ | micro |
| 4MI3G | 4-hydroxy-indole-3-yl-methyl glucosinolate |
| Å | angström |
| aa | amino acid |
| ABA | abscisic acid |
| *At* | *Arabidopsis thaliana* |
| ATP | adenosinetriphosphate |
| Avr | avirulence |
| B42AD | Blob 42 activation domain |
| *Bgh* | *Blumeria graminis forma specialis hordei* |
| C | carboxy-terminal |
| C24 | *Arabidopsis thaliana* ecotype C24 |
| CC | coiled-coil |
| CMV | *cucumber mosaic virus* |
| Col-0 | *Arabidopsis thaliana* ecotype Columbia-0 |
| CT | carboxy terminal domain |
| *CYP81F2* | cytochrome 81F family member 2 |
| d | days |
| DANN | deoxyribonucleic acid |
| DAPI | 4'-6-Diamidino-2-phenylindole |
| DEPC | diethylpyrocarbonate |
| dH2O | de-ionized water |
| Di17 | *Arabidopsis thaliana* ecotype Dijon-17 |
| DMSO | dimethyl sulfoxide |
| dpi | days post inoculation |
| dSpm | defective Suppressor-mutator |
| *ds*RNAi | double stranded RNA interference |
| DTT | dithiothreitol |

| | |
|---|---|
| *E. coli* | *Escherichia coli* |
| *EDS1* | Enhanced Disease Susceptibility 1 |
| EDTA | ethylenediaminetetraacetic acid |
| EMS | ethyl methane sulfonate |
| ET | ethylene |
| ETI | efector-triggered immunity |
| EtOH | ethanol |
| *f. sp.* | *forma specialis* |
| Fig. | Figure |
| FN | fast neutron |
| g | gram |
| *g* | gravity constant (9.81 ms-1) |
| *GSL10* | Glucan Synthase-Like 10 |
| *GSL8* | Glucan Synthase-Like 8 |
| hpi | hours post inoculation |
| HR | hypersensitive response |
| HRP | horseradish peroxidase |
| *HRT* | hypersensitive response to *turnip crinkle virus* |
| *Hv* | *hordeum vulgare* |
| IG | indole glucosinolates |
| JA | jasmonic acid |
| kD | kilo Dalton |
| l | liter |
| LB | Luria-Bertani |
| Ler | *Arabidopsis thaliana* ecotype Landsberg erecta |
| LexA | DNA binding domain of LexA from *E. coli* |
| LiAc | lithium acetate |
| LRR | leucine rich repeats |
| M | molar |
| min | minutes |
| *MLA* | Milew Locus A |
| n | nano |
| NBS | nucleotide binding site |
| OD | optical density |
| p35S | 35S promoter of CaMV |

| | |
|---|---|
| PAA | polyacrylamide |
| *PAD3* | Phytoalexin Deficient 3 |
| PAGE | polyacrylamide gel-electrophoresis |
| PAMP | pathogen-associated molecular pattern |
| PBS | phosphat buffered saline |
| PCR | polymerase chain reaction |
| *PEN1* | Penetration 1 |
| *PEN2* | Penetration 2 |
| pH | negative logarithm of proton concentration |
| *PMR4* | Powdery Mildew Resistant 4 |
| *Pst* | *Pseudomonas syringae pv. tomato* |
| PTI | PAMP-triggered immunity |
| *pv.* | pathovar |
| R | resistance |
| *RCY1* | resistant to the yellow strain of *cucumber mosaic virus* 1 |
| RNA | ribonucleic acid |
| rpm | rounds per minute |
| *RPM1* | Resistance to *Pseudomonas syringae pv. Maculicola* 1 |
| *RPP8* | *Recognition of Peronospora Aradopsidis* 8 |
| *RPS5* | Resistant to *Pseudomonas syringae* 5 |
| RT | room temperature |
| SA | salicylic acid |
| SAR | systemic acquired resistance |
| SD | synthetic minimal |
| SDS | sodium dodecyl sulphate |
| sec | seconds |
| TCV | *turnip crinkle virus* |
| T-DNA | transfer DNA |
| TIR | Drosophila Toll and mammalian interleukin-1 receptor |
| TMV | *tobacco mosaic virus* |
| TRIS | Tris-(hydroxymethyl)-aminomethane |
| U | unit |
| UV | ultraviolet |
| V | Volt |
| VIGS | virus induced gene silencing |

| WD | WRKY DNA binding domain |
| WRKY18 | WRKY transcription factor 18 |
| WRKY40 | WRKY transcription factor 40 |
| wt | wild-type |

# Chapter I

**Structural and functional analysis of class IIa WRKY transcription factors in basal and R protein-mediated plant immunity**

**Contributions:**

Figures 1.7 and 1.8 are taken from Maekawa et al. (under review in Cell Host & Mircobe); Immuno-blot analyses using αLexA antibody in Fig. 1.10 and αLexA and αB42AD antibodies in Fig. 1.11 were performed by Dr. Takaki Maekaw (MPIPZ; Köln); description of the MLA-CC domain (1.2.7) is based on Maekawa et al. (under review in Cell Host & Mircobe).

## 1.1  Introduction

As in mammals, plants have to combat a large variety of different pathogens and pests such as viruses, bacteria, fungi, oomycetes and insects throughout their life cycle (Dangl and Jones, 2001). This plethora of invading microbes represents a wide range of different life styles and infection strategies.  Pathogenic bacteria employ natural openings e.g. stomata and hydathodes, or wound sites to enter the plant tissue and proliferate in the apoplast. Some biotrophic fungi and oomycetes invaginate feeding structures (haustoria) into the plasma membrane of their living host cell. Necrotrophy instead is associated with the feeding of the pathogen on dead plant tissue (Jones and Dangl, 2006). Despite this, disease is a rather rare case in nature. In fact, most plant species are resistant towards a wide range of potential pathogens (Nürnberger et al., 2004). This is accomplished because plants have evolved a sophisticated multi-layered immune system to sense microbial invaders and to mount appropriate defence responses (Jones and Dangl, 2006).  However, the underlying mechanisms that enable plants to integrate signals from different defence layers, including extra- and intracellular perception, transcriptional reprogramming and the delivery of anti-microbial compounds, in order to restrict a specific pathogen are still poorly understood.

### 1.1.1  Non-host resistance

The phenomena that a plant species is resistant towards all genetic variants of a pathogen species is termed "species" or "non-host" resistance (NHR) and defines the pathogen as non-adapted (Lipka et al., 2008). Infrequent changes in the host range of phytopathogens indicate the integrity of this species immunity (Heath, 2000). The durability of NHR is believed to be the consequence of several successive layers that comprise constitutive plant barriers and inducible host reactions (Thordal-Christensen, 2003; Nürnberger and Lipka, 2005).

Activation of defence responses essentially requires perception of the potential pathogen by the host and the ability to differentiate "self" from "non-self". Therefore, plants possess a surveillance system of pattern recognition receptors (PRRs). PRRs residing at the plasma membrane usually consist of an extracellular ligand-binding-domain, often comprising leucine-rich repeats (LRR), a single trans-membrane domain and an inter-cellular serine/theronine kinase-signalling domain. Such PRRs were termed receptor-like kinases (RLKs). In the model plant *Arabidopsis thaliana* (*Arabidopsis; At*) genome 610 RLKs and 56 receptor-like proteins (RLPs), which are of similar structure but lack the kinase domain, have

been identified (Bittel and Robatzek, 2007). PRRs perceive so called microbe-associated molecular patterns (MAMPs), which constitute highly conserved molecular signatures, that identify whole classes of microbes but are absent from the host (Boller and Felix, 2009). Currently, the best characterized PRR/MAMP pair in plants is the *Arabidopsis* Flagellin Sensing 2 (FLS2) receptor that recognizes a 22 amino acid epitope (flg22) from bacterial flagellin (Felix et al., 1999; Gómez-Gómez and Boller, 2000). The role of FLS2 in plant defence is underpinned by the observation that *fls2* mutant plants exhibit enhanced disease susceptibility towards bacterial infections (Zipfel et al., 2004). Elongation Factor-Tu Receptor (EFR) constitutes another PRR described in the literature to mount defence responses upon recognition of the epitope elf18 from bacterial EF-Tu (Zipfel et al., 2006). Chitin, the major component of fungal cell walls, is known as an elicitor of plant defence since many years (Boller, 1995). More recent publications show that the RLK CERK1 is essential for the chitin response in *Arabidopsis* (Petutschnig et al., 2010).

Generally, MAMP-triggered activation of PRRs induces rapid ion fluxes across the plasma membrane, the generation of reactive oxygen species (ROS), nitric oxide (NO) and ethylene, as well as the subsequent synthesis of antimicrobial compounds and the deposition of callose (Zipfel and Felix, 2005; Bittel and Robatzek, 2007). Signalling from the activated receptor to downstream components often involves MAPK cascades (Asai et al., 2002; Menke et al., 2005; Zipfel and Felix, 2005; Suarez-Rodriguez et al., 2007). The signal transduction culminates in transcriptional reprogramming of defence-related genes that frequently involve the action of WRKY-type transcription factors (Asai et al., 2002; Zipfel et al., 2004; Andreasson et al., 2005; Journot-Catalino et al., 2006; Xu et al., 2006; Shen et al., 2007). Successful growth inhibition of a potential pathogen by these processes, initiating from PRR activation, is termed MAMP-trigged immunity (MTI).

Epidermal waxes and carbohydrate-rich cell walls display complex designs, which constitute the first physical barrier for invading pathogens (Sarkar et al., 2009). Many haustoria-forming fungal parasites cross this barrier by penetrating the cell wall. Plants respond to such entry attempts by a rearrangement of their actin cytoskeleton followed by redistribution of secretory-pathway organelles towards the site of fungal host cell entry (Schmelzer, 2002; Takemoto et al., 2003). This leads to the deposition of *de novo* synthesized cell wall components, such as cellulose, *β*-1,3-glucan (callose), pectins and phenolics in the paramural space (Aist, 1976). These local appositions are termed papilla and are thought to reinforce the cell wall in order to restrict the invading pathogen. Although phytopathogenic bacteria do not enter their host cell, cell wall remodelling in *Arabidopsis* occurs as well in response to bacterial pathogens, as in the interaction with non-adapted

*Pseudomonas syringae* (*Ps*) *pv. phaseolicola* (Lipka et al., 2008). Synthesis of papilla-associated callose in *Arabidopsis* requires *Glucan Synthase-Like* (*GSL*) *5* (Jacobs et al., 2003; Nishimura et al., 2003). In contrast to the intuitive assumption of fortification, *gsl5* mutants, that lack papilla-associated callose, are actually more resistance towards the adapted powdery mildew fungi *Erysiphe cichoracearum* and *Golovinomyces orontii* (Vogel and Somerville, 2000; Jacobs et al., 2003; Nishimura et al., 2003).

*Arabidopsis PEN* (Penetration) gene products have been identified to limit the entry success of non-adapted powdery mildews like *Blumeria gramins* f. sp. *hordei* (*Bgh*) and *Erysiphe pisi* (Collins et al., 2003; Lipka et al., 2005; Stein et al., 2006). Consistent with the reorganization of the secretory pathway, *PEN1* was shown to encode a plasma membrane-resident syntaxin that focally accumulates in papilla formed in response to non-adapted and adapted powdery mildews (Collins et al., 2003; Meyer et al., 2009). PEN1 assembles with SNAP33 and VAMP721/722 into a ternary SNARE (soluble *N*-ethylmalemide-sensitive attachment protein receptor) complex that is thought to tether vesicles containing unknown cargo to the plasma membrane (Kwon et al., 2008). *Arabidopsis* plants deficient in *pen1* exhibit enhanced entry of the non-adapted hemibiotrophic oomycete *Phytophthora infestans* and impaired basal resistance to the necrotrophic ascomycete *Plectosphaerella cucumerina* (Lipka et al., 2005; Stein et al., 2006). Since *pen1* mutants still show GSL5-dependent callose deposition at fungal entry sites as well as in haustorial encasements, the coordination of the timely and localized delivery of defence-related compounds probably requires multiple pathways (Meyer et al., 2009).

In fact, components of a second secretory pathway have been identified, including PEN2 and PEN3, which are required for flg22-stimulated GSL5-mediated extracellular accumulation of callose in *Arabidopsis* seedlings (Clay et al., 2009). *PEN2* encodes a glycoside hydrolase that, together with the plasma membraneresident ATP (adenosine triphosphate)-binding cassette (ABC) transporter PEN3, is part of an entry control mechanism that mediates broad spectrum anti-fungal defence (Lipka et al., 2005; Stein et al., 2006). PEN2 localizes to peroxisomes that focally accumulate at incipient entry sites of *Arabidopsis* cells inoculated with the non-adapted barley (*Hordeum vulgare; Hv*) powdery mildew *Bgh* (Lipka et al., 2005). Recently, PEN2 was shown to act as an atypical myrosinase in the activation of 4-methoxyindol-3-ylmethylglucosinolate (4MI3G), a tryptophan-derived indol glucosinolate (Bednarek et al., 2009). Glucosinolates are sulfur-rich, anionic natural products that upon hydrolysis by endogenous myrosinases produce several different products (e.g., isothiocyanates, thiocyanates, and nitriles). The hydrolysis products have diverse biological activities, e.g., as defence compounds. For humans these compounds

function as cancer-preventing agents, biopesticides, and flavour compounds (Halkier and Gershenzon, 2006). The final step in 4MI3G biosynthesis is mediated by the P450 monooxygenase CYP81F2 that converts indol-3-ylmethylglucosinolate (I3G) to 4MI3G. Consistently, *cyp81f2* mutants, that lack 4MI3G, were found to be more susceptible to non-adapted powdery mildew fungi (Bednarek et al., 2009). Generally, the activation of glucosinolates occurs through a tissue damage-trigger, which allows mixture of the compartmentalized enzyme with the substrate. This mechanism of glucosinolate generation is particularly effective against chewing herbivores (Halkier and Gershenzon, 2006). The glucosinolate-activation pathway described for PEN2 occurs in intact tissue, demonstrating its role in anti-microbial defence (Bednarek et al., 2009; Clay et al., 2009). These findings are further supported by several recent publications describing the activity of glucosinolates in plant microbial interactions (Consonni et al., 2010; Sanchez-Vallet et al., 2010; Schlaeppi et al., 2010).

Beside glucosinolates, phytoalexins are antimicrobial secondary metabolites produced *de novo* by plants in response to biotic and abiotic stresses (Bailey and Mansfield, 1982). To date 44 phytoalexins have been isolated from cultivated and wild crucifers (Pedras et al., 2010). The major phytoalexin of *Arabidopsis* is camalexin (3-thiazol-2-yl-indole). Camalexin formation is induced upon infection with biotrophic and necrotrophic pathogens, including bacteria, viruses, fungi and oomycetes (Glawischnig, 2007). The biosynthesis of camalexin originates, as is the case for 4MI3G, from tryptophan. The final step, the conversion of dihydro-camalexic acid to camalexin, is mediated by the P450 enzyme Phytoalexine Deficient 3 (Schuhegger et al., 2006). Analyses of *pad3* mutants, which lack camalexin, indicate that accumulation of this phytoalexin contributes to disease resistance to some pathogens, whereas it has no effect on others (Kliebenstein, 2004; Ferrari et al., 2007). More recent publications implicate a sequential role for glucosinolates and camalexin in pathogen restriction (Bednarek et al., 2009; Schlaeppi et al., 2010). Based on these findings camalexin is thought to act later in defence, potentially after microbial host cell entry.

To date, NHR is best characterized for the incompatible interaction of *Arabidopsis* with the non-adapted biotrophic mildew fungi *Bgh* and *E. pisi*. Mutant plants affected in pre-invasive resistance, like *pen1*, *pen2* and *pen3* that exhibit enhanced entry-rates of these two non-adapted pathogens, are still resistant. This is due to a second post-invasive defence layer that contributes to NHR (Lipka et al., 2005). Post-invasive immunity is often associated with a localized cell death response at the site of infection. This very rapid and localized hypersensitive reaction (HR) of the host cell consequently interferes with the biotrophic lifestyle of these mildew fungi. Execution and control of this cell death reaction depends on

the lipase like proteins Enhanced Disease Susceptibility 1 (EDS1), Phytoalexin Deficient 4 (PAD4) and Senescence-Associated Gene 101 (Lipka et al., 2008). Genetic and biochemical analysis revealed theses proteins to constitute a regulatory node that is essential for the activation of salicylic acid (SA) signalling and isolate-specific immunity mediated by a subset of resistance (R) proteins (Wiermer et al., 2005). SA-mediated defence responses are mainly effective against biotrophic pathogens, whereas jasmonic acid (JA)- or ethylene (ET)-mediated responses are predominantly active against necrotrophs and herbivorous insects (Glazebrook, 2005). Crosstalk between these phytohormone signalling pathways is believed to fine tune defence responses towards encountered pathogens (Pieterse and Dicke, 2007). Single mutants in *eds1*, *pad4* or *sag101* are only marginal compromised in NHR towards *Bgh* and *E. pisi*. Combination of mutants affected in pre- and post-invasive resistance however act synergistically. This was demonstrated by the successful colonization by *E. pisi* of *Arabidopsis pen2* pad4 *sag101* triple mutants (Lipka et al., 2005). Therefore, NHR toward biotrophic powdery mildews is thought to act though two successive multi-component defence layers (Lipka et al., 2008).

## 1.1.2 NBS-LRR receptor-mediated immunity

Pathogens that successfully overcome non-host defence encounter an additional, basically intracellular, layer of the plant immune system, mainly operational through resistance (*R*) gene-encoded cultivar-specific immune receptors. R proteins perceive specific effector molecules delivered by the pathogen into the host cell mainly to increase their own fitness (Jones and Dangl, 2006). Such effector molecules were originally termed avirulence factors (Flor, 1971). Perception of an avirulence factor by its R protein counterpart results in the activation of a robust immune response leading to resistance. Such a host pathogen interaction is defined as incompatible and the pathogen is defined as avirulent.

Intracellular *R* gene products generally belong to the class of NBS-LRR proteins. They were named after their central nucleotide binding site (NBS) and C-terminal LRR domains and constitute a subfamily of STAND (signal transduction ATPases with numerous domains) NTPases, found in archea, bacteria, fungi, plants and animals (Lelpe et al., 2004). Their NBS domains show homology to human APAF1 (Apoptotic Protease Activating Factor 1), the central component of the human apoptosome and its *Caenorhabditis elegans* ortholog CED4 (*Caenorhabitis elegans* death 4;(van der Biezen and Jones, 1998). In plants, NBS-LRR proteins are subdivided into two classes based on their N-terminal domains. One class possesses an N-terminal Toll/Interleukin1 receptor (TIR) domain with homology to the

intercellular signalling domains of Drosophila Toll and mammalian Interleukin1 receptors (TIR-NBS-LRR), whereas the other contains a coiled-coil (CC) domain (Dangl and Jones, 2001).

R proteins perceive their cognate effectors either directly (Receptor Ligand Model) or indirectly by monitoring the integrity of their cellular targets (Rafiqi et al., 2009). Direct recognition was originally shown for the rice (*oryza sativa; Os*) CC-NB-LRR Pi-ta that confers resistance to the Avr$_{Pita}$ effector from *Magnaporthe grisea* (Jia et al., 2000). In contrast, the *Arabidopsis* CC-NB-LRR protein RPS5 recognizes the degradation of the protein kinase PBS1 by the *Ps* effector protein HopAR1 (Shao et al., 2003), and modifications of the negative defence regulator RIN4 by the *Ps* effectors Avr$_{Rpm1}$, Avr$_B$ or Avr$_{Rpt2}$ are monitored by the *Arabidopsis* R proteins RPM1 and RPS2 (Axtell and Staskawicz, 2003; Mackey et al., 2003). Effector-mediated R protein activation induces a pattern of cellular responses (including an increase in cytosolic calcium, depolarisation of the plasma membrane, a localised ROS burst and NO production), that show significant overlap with those triggered by PRR activation (Nimchuk et al., 2003; Nürnberger et al., 2004). Effector recognition is prevalently associated with the death (HR) of the host cell. HR constitutes a significant cost for the plant. Therefore, it seems apparent that the mechanism underlying R protein activation must be tightly regulated.

Forward genetic screens in *Arabidopsis* and tobacco identified components of the eukaryotic chaperon machinery as required for several R protein functions (Schulze-Lefert, 2004). HSP90 (Heat Shock Protein 90) for example is required for resistance mediated by *Arabidopsis* RPM1 and tobacco N, and association of HSP90 with both receptors has been shown *in planta* (Hubert et al., 2003; Takahashi et al., 2003). The co-chaperon-like proteins RAR1 (Required for MLA12 Resistance) and SGT1 (Suppressor of the G2 allele of SKP1), which are essential for resistance mediated by some R proteins, can form complexes with HSP90 (Takahashi et al., 2003). SGT1 and HSP90 interact with barley MLA and positively affect receptor abundance (Bieri et al., 2004). RPM1 requires RAR1 and HSP90 for resistance against *Ps*, whereas HRT-mediated *Turnip crinkle virus* (TCV) resistance occurs independent of RAR1 and SGT1 (Austin et al., 2002; Hubert et al., 2003; Chandra-Shekara et al., 2004). More recently the ATPase CRT1 (Compromised Recognition of TCV) was shown to be required for HRT-mediated TCV resistance and to interact with several R proteins, including HRT (Kang et al., 2008). Interestingly, CRT1 can associate with HSP90 and overexpression experiments with wild-type and mutant forms of RCY1 suggest preferential association of CRT1 with immune receptors prior to their effector-triggered activation (Kang et al., 2010). The presence of R proteins in such multi-component

complexes might, apart from correct protein folding and stabilization, facilitate conformational changes required for their activation (Rafiqi et al., 2009).

The NBS domain of plant R proteins has been proposed to function as a molecular switch. In this model, transition between the active and inactive conformation of the receptor is achieved by ADP/ATP exchange and subsequent hydrolysis of ATP. More precisely, the R protein is believed to exist in the absence of its cognate effector in an inactive, ADP bound state. The recognition event stimulates the exchange of ADP to ATP and adoption of the active conformation, associated with the release of its signalling potential. The ATPase function of the protein attenuates the signalling function and returns the protein to its inactive state (Takken et al., 2006). Consistent with this idea, the crystal structure of human APAF1 revealed ADP bound to its nucleotide binding pocket and biochemical analysis implicate the ATPase activity in downstream signalling (Riedl et al., 2005). Nucleotide binding requires the conserved ATPase WALKER A (P-loop) motif and several R proteins, including I2, N, L6, RPS2 and RPS5, impaired in nucleotide binding by a P-loop mutation, are rendered inactive (Dinesh-Kumar et al., 2000; Tao et al., 2000; Tameling et al., 2002; Ade et al., 2007). Furthermore, some R proteins affected in ATP hydrolysis by a mutation in a second conserved motif (WALKER B), have been found to be auto-active (Tameling et al., 2002; Ade et al., 2007; van Ooijen et al., 2008). Thus, ATP binding rather than its hydrolysis is critical for receptor activity. CED4 was found to preferentially bind ATP (Yan et al., 2005) and the recently described octameric crystal structure of the CED4 apoptosome, together with *in vitro* studies, suggest CED4 activity to occur independent of ATP hydrolysis (Yan et al., 2005; Qi et al., 2010). Therefore, different mechanisms of R protein activation might as well exist in plants.

CED4 forms an asymmetric dimer that adopts its octameric structure in a stimulus-dependent manner (Yan et al., 2005; Qi et al., 2010). In plants, homomeric assemblies of R proteins have been reported *e.g.* for N and RPS5 (Mestre and Baulcombe, 2006; Ade et al., 2007). The TIR-NBS-LRR immune receptor N confers resistance to tobacco mosaic virus (TMV) upon recognition of the p50 helicase domain of the TMV replicase protein (Erickson et al., 1999b; Erickson et al., 1999a). Transient expression of N in *Nicotiana benthamiana* followed by immunoprecipitation indicates receptor oligomerization in the presence of the elicitor. Inactive P-loop mutants of N are inhibited in elicitor-dependent oligomerization, whereas mutations in a second conserved motif, RNBS-A, did not affect N coprecipitation, but still impaired resistance (Mestre and Baulcombe, 2006). Previous studies described a contribution of SGT1 and EDS1 to N-mediated resistance (Peart et al., 2002a; Peart et al., 2002b). Virus-induced gene silencing (VIGS) of *EDS1* did not affect N oligomerization,

whereas in SGT1 silenced plants self-association was undetectable (Mestre and Baulcombe, 2006). The authors concluded that oligomerzation of N is an early event in response to TMV, that occurs upstream of EDS1 and is not exclusively capable for resistance.

Several genetic analyses show that mutation in the downstream component *eds1* mainly interfere with resistance mediated by TIR-NB-LRR type R proteins, whereas most characterized CC-NB-LRR immune sensors depend on the plasma membrane-anchored protein NDR1 (Parker et al., 1996; Aarts et al., 1998; Feys et al., 2001). Despite this paradigm some exceptions have been reported. HRT encodes a CC-NB-LRR protein that inhibits the spread of TCV in an *EDS1*-dependent manner (Chandra-Shekara et al., 2004). A second example is RPW8. This atypical R protein requires *EDS1* to confer broad spectrum powdery mildew resistance but lacks the NB-LRR domains (Xiao et al., 2001). EDS1 mutants are hypersusceptible to virulent pathogens, indicating a role in basal defence (Parker et al., 1996). EDS1 and PAD4 are required equally for SA induction and their transcriptional activation is in turn stimulated by SA. This positive feedback loop is thought to be essential for defence amplification (Falk et al., 1999; Jirage et al., 1999; Feys et al., 2001). EDS1-deficient plants are completely compromised in the initiation of HR-associated cell death, whereas PAD4 mutants develop cell death that, in many cases, is not capable to restrict pathogen growth (Feys et al., 2001). This suggests a more prominent role for EDS1 in accomplishing defence responses. However, the signal transduction pathway downstream of R protein activation is still poorly understood.

### 1.1.3 MLA-mediated resistance

The polymorphic barley *MLA* locus encodes allelic CC-NBS-LRR type immune receptors each recognizing a distinct isolate-specific effector of the pathogenic powdery mildew fungus *Bgh* (Seeholzer et al., 2010). To date more than 30 *MLA* resistance specificities have been reported. This locus, located on chromosome H1, encodes the largest number of known R proteins to *Bgh* (Jorgensen, 1994). The extreme functional diversification at this locus constitutes a good source for genetic analysis.

MLA immune receptors share >90% sequence identity (Halterman et al., 2001; Shen et al., 2003; Halterman and Wise, 2004). Analysis of the nucleotide diversity of a MLA cDNA library, containing 23 receptor variants, identified 34 sites of positive selection, that were predominantly located in the LRR. The domain-restrictive nature of this positive selection site pattern implicates the LRR domain in effector recognition and moreover, suggests direct

recognition of the effector by MLA (Seeholzer et al., 2010). This is in agreement with previous experiments, using reciprocal domain swap chimeras of MLA1 and MLA6 that show distinct LRRs to mediate effector-specificity (Shen et al., 2003). Together theses data provide strong evidence for direct recognition of the cognate effectors through the polymorphic LRR domain encoded by allelic *MLA* variants. Resistance mediated by MLA is coincident with the appearance of an HR. The timing of HR initiation, mediated by MLA, was found to be variable between different alleles. MLA1 and MLA6 mount a quick cell death response at the stage of haustorium differentiation, whereas MLA3, MLA7 and MLA12 initiated HR much slower, at the stage of secondary hyphae elongation (Freialdenhoven et al., 1994; Boyd et al., 1995). On the other hand, MLA12 overexpression induces rapid effector-dependent defence responses (Shen et al., 2003). This suggests MLA steady state levels to be critical for effective defence and is further supported by the requirement of HSP90, RAR1 and SGT1 for different MLA resistance specificities (Shen et al., 2003; Bieri et al., 2004).

Cell-autonomous localisation studies, using fluorescent-tagged MLA10 identified the protein in the nucleus and in the cytosol. After inoculation with avirulent *Bgh* isolates, the nuclear pool of MLA10 was found to be enriched and similar results were observed by immuno-blot analyses with transgenic *MLA1-HA* plants. Nuclear exclusion of MLA10, by fusing the protein to a nuclear export signal, compromised resistance to *Bgh*, indicating a requirement of the nuclear MLA pool for defence (Shen et al., 2007). Nucleocytoplasmic localisation was reported for other immune receptors, like the TIR-NBS-LRR proteins RPS4 and N (Burch-Smith et al., 2007; Wirthmueller et al., 2007). Nuclear accumulation of the TIR-NB-LRR receptor N is required for HR initiation (Burch-Smith et al., 2007). The N receptor is thought to interfere with the transcriptional machinery by interaction with distinct members of the squamosa promoter-like (SPL) family of transcription factors (Shen and Schulze-Lefert, 2007). Interestingly, another TIR-NB-LRR R protein, RRS1, possesses a C-terminal WRKY domain extention that is shared by all WRKY transcription factors and binds to a *cis*-regulatory DNA element, termed W-box (Ülker and Somssich, 2004; Noutoshi et al., 2005). RSS1 interacts in the nucleus with its cognate effector PopP2 derived from the bacterial pathogen *Ralstonia solanacearum*, and a mutation in its WRKY domain results in conditional activation of defence responses and loss of W-box binding (Rushton et al., 2010). Beside RRS1, *At*WRKY16 and *At*WRKY19 belong to the same class of NBS-LRR-WRKY proteins. Therefore, these immune receptors may enable a mechanistic shortcut in effector-triggered R protein activation, leading to transcriptional reprogramming (Rushton et al., 2010).

Yeast 2-hybrid experiments, using the highly invariant CC domain fragment ($MLA_{1-46}$) of MLA, identified two sequence related WRKY transcription factors, *Hv*WRKY1 and

11

*Hv*WRKY2, as putative interactors of MLA. A combination of fluorescence lifetime imaging (FLIM) and Förster resonance energy transfer (FRET) confirmed the physical interaction of MLA10 with *Hv*WRKY2 in the nucleus of living cells in an effector-dependent manner. *Hv*WRKY1 and *Hv*WRKY2 show rapid transient transcript activation in compatible and MLA-specific incompatible interactions with *Bgh* as well as in response to flg22 treatment. Transcriptional knock-down of *Hv*WRKY1 and *Hv*WRKY2 enhanced resistance to *Bgh*, indicating that both WRKY factors function as repressors in MAMP-triggered immunity (Eckey et al., 2004; Shen et al., 2007). These findings suggest a model in which effector-stimulated MLA receptors can interfere with WRKY repressor functions and thereby de-repress MAMP-triggered immune responses. The resulting amplification of the immune response is thought to be sufficient for driving the host cell into suicidal death and to mediate resistance (Shen et al., 2007; Shen and Schulze-Lefert, 2007).

### 1.1.4  WRKY transcription factors

The superfamily of WRKY transcription factors consists of 74 members in *Arabidopsis*, 109 in rice, 66 in papaya (*Carica papaya*) and 104 in poplar (*Populs spp.*), and represents one of the ten largest families of transcription factors in higher plants (Ülker and Somssich, 2004; Eulgem and Somssich, 2007; Ross et al., 2007; Rushton et al., 2010).

All WRKY factors share their characteristic DNA binding domain, called the WRKY domain. The WRKY domain is about 60 amino acid residues in length. It contains at the N-terminus the almost invariant eponymous peptide signature WRKYGQK, whereas the C-terminal part harbours an atypical zinc finger motif (either $Cx_{4-5}Cx_{22-23}HxH$ or $Cx_7Cx_{23}HxC$). The first solution structure of a WRKY domain was reported by Yamasaki et al. (2005). The WRKY domain of *At*WRKY4 consists of a four-stranded-β-sheet in which the zinc coordinating residues Cys/His form a zinc binding pocket and the WRKYGQK motif sticks out of the domain surface (Yamasaki et al., 2005). A second crystal structure using a longer fragment of *At*WRKY1, revealed a similar structure containing an additional fifth β-sheet (Duan et al., 2007). Binding experiments using different WRKY factors defined the W-box (TTGACC/T) as the minimal consensus for DNA binding, whereas adjacent sequences might communicate binding site preferences (Rushton et al., 1996; Ciolkowski et al., 2008). W-boxes are statistically overrepresented in the promoters of *WRKY* genes, indicating auto- and cross-regulation as important components in the WRKY network (Dong et al., 2003). Based on available data, it is thought that the WRKY motif binds the W-box by entering the mayor groove of the DNA (Yamasaki et al., 2005). So far however, neither the crystal

structure of a full length WRKY protein nor a WRKY domain co-crystal with its DNA-binding site has been reported.

WRKY factors are engaged in many plant processes, including germination, senescence and response to abiotic stresses such as cold and drought (Rushton et al., 2010). Extensive studies over the past decade however have revealed that the major line of action of this transcription factors family is in regulating plant responses towards pathogens (Eulgem and Somssich, 2007; Pandey and Somssich, 2009). WRKY factors constitute a complex cross-linked network that is crucial for regulation of the defence transcriptome. Some WRKY factors, like *At*WRKY25 and *At*WRKY33, can be phosphorylated via MPK4, indicating their role in early MAMP-triggered defence responses (Andreasson et al., 2005; Eulgem and Somssich, 2007). Transcript levels of *PcWRKY1* the parsley ortholog of *At*WRKY33, increases very rapidly and transiently upon MAMP treatment of cells. *Pc*WRKY1 represses its transcription by binding to W-boxes in its own promoter, but positively stimulates *PR1* gene expression (Turck et al., 2004). *At*WRKY33 is a positive regulator of resistance towards the necrotrophic fungi *Alternaria brassiciciola* and *Botrytis cinerea* (Zheng et al., 2006). Mutants compromised in *At*WRKY33, in turn are more susceptible towards both pathogens and show reduced expression levels of the jasmonate-regulated defensin *PDF1.2* (Zheng et al., 2006). *At*WRKY70 was identified as a central component modulating the balance between SA and JA signalling and is required for RPS4-mediated resistance (Li et al., 2006; Knoth et al., 2007). Expression of AtWRKY70 depends on SA and at later time points on NPR1, whereas its early activation appears to be NPR1 independent (Li et al., 2004). NPR1 regulates the expression of several other *WRKY* genes, including *AtWRKY18*, *AtWRKY53* and *AtWRKY54* (Wang et al., 2008). *At*WRKY53 exhibits dual functionality. *AtWRKY53* mutants show delayed disease symptom development upon infection with *R. solanacearum*, whereas they were more susceptible towards *Ps* (Murray et al., 2007; Hu et al., 2008). Additionally, some WRKY factors have been reported to exert redundant functions in defence. Loss-of-function mutants of *AtWRKY11*, for instance, are more resistant to virulent and avirulent *Ps* strains and this effect is enhanced in *Atwrky11 Atwrky17* double mutant plants (Journot-Catalino et al., 2006). Several recent reports describe WRKY-dependent defence responses in other plants, thereby emphasizing the role of this transcription factor family in plant immunity. One should however mention that many of current reports, particularly those in rice, employ strong ectopic overexpressor lines to deduce WRKY functions in plant defence. More rigorous tests will be required in the future to determine whether these results can be verified under native conditions.

### 1.1.5  *At*WRKY18 and *At*WRKY40 in plant immunity

WRKY factors are organized in three groups, based on the number of WRKY domains and the structure of their zinc finger motif. Group II members contain the $Cx_{4-5}Cx_{22-23}HxH$ zinc finger motif and one WRKY domain. This group is further sub-divided based on their primary amino acid sequences (Eulgem et al., 2000). Members of subgroup IIa possess an N-terminal leucine zipper motif and representatives of this subclade, *e.g. Hv*WRKY1 and *Hv*WRKY2, are engaged in homomeric associations *in vivo* (Eulgem et al., 2000; Shen et al., 2007). The *Arabidopsis* group IIa consists of three members namely, *At*WRKY18, *At*WRKY40, and *At*WRKY60 (Eulgem et al., 2000). Deletion studies identified the leucine zipper of these three WRKY factors to mediate both homo- and heteromeric-associations, indicating potential functional diversification via such interactions (Xu et al., 2006). Single mutants of these WRKY factors behaved almost similar to wild-type in response to different pathogens, although resistance towards *Ps* DC3000 was slightly increased in *Atwrky18* plants (Berger et al., 2006; Shen et al., 2007). A different study using the *Atwrky18* mutant, however reported enhanced susceptibility in response to *Ps maculicola* (Wang et al., 2008). These different observations might result from different experimental procedures and/or *Ps* strains used for the analyses.

Interestingly, *Atwrky18 Atwrky40* double and *Atwrky18 Atwrky40 Atwrky60* triple mutant plants are almost fully resistant towards the adapted powdery mildew *G. orontii* (Shen et al., 2007). This indicates *At*WRKY18 and *At*WRKY40 to act redundantly as repressors of basal defence. Consistently, *Atwrky18 Atwrky40* mutants showed enhanced resistance toward *Ps* DC3000 (Xu et al., 2006). Both transcription factors are thought to mediate transcriptional repression through different complex mechanisms. This is indicated by the observation that defence-related genes, including several members of the *JAZ* repressor family, were up-regulated prior to infection, whereas other pathogen-responsive genes, such as *EDS1*, showed an exaggerated transcriptional activation post-infection. Moreover, transcriptional regulators constituted one of the largest groups of differentially regulated genes in the double mutant compared to the wild-type (Pandey et al., in press).

*At*WRKY40 binds to W-box containing regions in the promoters of *EDS1* and *JAZ8*, suggesting that AtWRKY18 and AtWRKY40 may interfere with the balance of SA and JA signalling (Pandey et al., in press). This is supported by expression analysis of SA-induced *PR1* and JA-regulated *PDF1.2* in wild-type and *Atwrky18 Atwrky40* mutants after infection with hemibiotrophic *Ps* DC3000 and the necrotrophic fungus *B. cinerea* (Xu et al., 2006). *Atwrky18 Atwrky40* double mutants accumulate strongly elevated levels of camalexin after *G.*

*orontii* infection, and this difference might explain the enhanced pre-invasion resistance of the double mutant towards *G. orontii* (Pandey et al., in press). In sum these data suggest both WRKY factors to function in a feedback repression system that controls basal defence. Nevertheless, it remains still unclear how the observed alteration in the *Atwrky18 Atwrky40* mutant background contribute to *G. oronii* resistance.

### 1.1.6 Thesis aims

The effector-dependent nuclear association of the immune sensor MLA with the WRKY class IIa transcriptional repressors *Hv*WRKY1 and *Hv*WRKY2 provides a mechanistic model how plants can integrate signals from different layers of their innate immune system (Shen et al., 2007). In chapter one I investigate the possible conservation of this mechanism between mono- and dicotyledonous plants by the identification of potential R protein clients of *At*WRKY18 and *At*WRKY40, the functional homologues of *Hv*WRKY1 and *Hv*WRKY2 in the model plant *Arabidopsis thaliana*. Furthermore, I analyze the molecular basis of *G. orontii* resistance in the *Atwrky18 Atwky40* double mutant plant by testing the contribution of some key early signalling components, using a genetic approach. Based on the unpublished solution structure of the coiled-coil domain of MLA, initial studies regarding the homo-dimerization of the receptor were performed (Maekawa et al., under review in Cell Host & Microbe).

*Arabidopsis* cells that undergo death in response to host cell entry of non-adapted powdery mildew fungi deposit callose along their entire cell margins. These encasements were absent in *glucose synthase-like* (*gsl5*) mutant plants, which rather showed a punctate callose pattern of cells, reminiscent of plasmodesmata (Jacobs et al., 2003). The initial goal of my second project was to identify GSL proteins (encoded by 12 gene members in Arabidopsis) that contribute to these putative plasmodesmata-associated callose depositions. In the course of these studies unexpected observations encouraged me to pursue the function of two highly sequence-related *GSL* genes in the male gametophyte. Molecular components similarly, a member of the MLO protein family originally discovered in powdery mildew resistance, was recently reported to be involved in pollen tip reception (Kessler et al., 2010). These data provide interesting examples of how common molecular components can be integrated into distinct cellular response pathways here, plant defence and reproduction. It also reiterates recent studies linking development to defence (Kazan and Manners, 2009). The results of this project are presented in chapter two.

## 1.2 Results

### 1.2.1 The conserved C-terminus of *Hv*WRKY2 is the potential *in vivo* target of MLA

Barley *Hv*WRKY1 and *Hv*WRKY2 are structurally related to *Arabidopsis At*WRKY18 and *At*WRKY40. Virus-induced gene silencing (VIGS) experiments suggest that both WRKY factors act as repressors in basal defence. The intercellular CC-NB-LRR type immune receptor mildew A (MLA) confers isolate specific resistance in barley towards the powdery mildew *Blumeria graminis f. sp. hordii* (*BGH*). Perception of its cognate *BGH* effector stimulates nuclear association of MLA with *Hv*WRKY1 and WRKY2 (Shen et al., 2007). An N-terminal truncated fragment of barley *Hv*WRKY2 (WRKY2$_{178-319}$), still containing its DNA binding- (WRKY-domain) and C-terminal (CT) domain, was found by Shen et al. (2007) to be sufficient for association with the N-terminus of the MLA coiled-coil (CC) domain (MLA$_{1-46}$) in yeast (see also Fig. 1.2). Sequence alignment analysis of *Hv*WRKY1, *Hv*WRKY2 and related *Arabidopsis* transcription factors *At*WRKY18 and *At*WRKY40 revealed strong conservation within the WRKY domain as well as in the CT region within and across both plant phyla (Shen et al., 2007; Fig. 1.1a). Clustering of conserved amino acids in the CT region(s) of related barley and *Arabidopsis* WRKY factors potentially indicate an evolutionary preserved function.

Specific binding of WRKY factors to W-box containing DNA sequences is predicted to bury the WRKY domain deeply into the major groove of the DNA (Yamasaki et al., 2005; Duan et al., 2007). Thus, I hypothesized the CT domain to be sufficient for the association with MLA. To test this assumption I separately cloned the WRKY- and CT domain from *HvWRKY2* (Fig. 1.1b). Fusions of *Hv*WRKY2$_{178-242}$ and *Hv*WRKY2$_{243-319}$ with the activation domain of B42 were co-expressed with MLA$_{1-46}$ fused to the LexA DNA binding domain in yeast and tested for an interaction phenotype. Under induced conditions (for details see materials & methods) yeast growth (indicative for association between prey and bait constructs) was only detectable for transformants containing *Hv*WRKY2$_{243-319}$ but not *Hv*WRKY2$_{178-242}$ (Fig. 1.2a). Immuno-blot analysis using LexA and B42AD specific anti-sera detected all fusion proteins as being expressed at similar levels (Fig. 1.2b). Thus, the C-terminal domain of *Hv*WRKY2 is sufficient to associate with MLA$_{1-46}$ in yeast. Furthermore these data implicate the conserved C-terminus of *Hv*WRKY2 as the *in vivo* target of MLA.
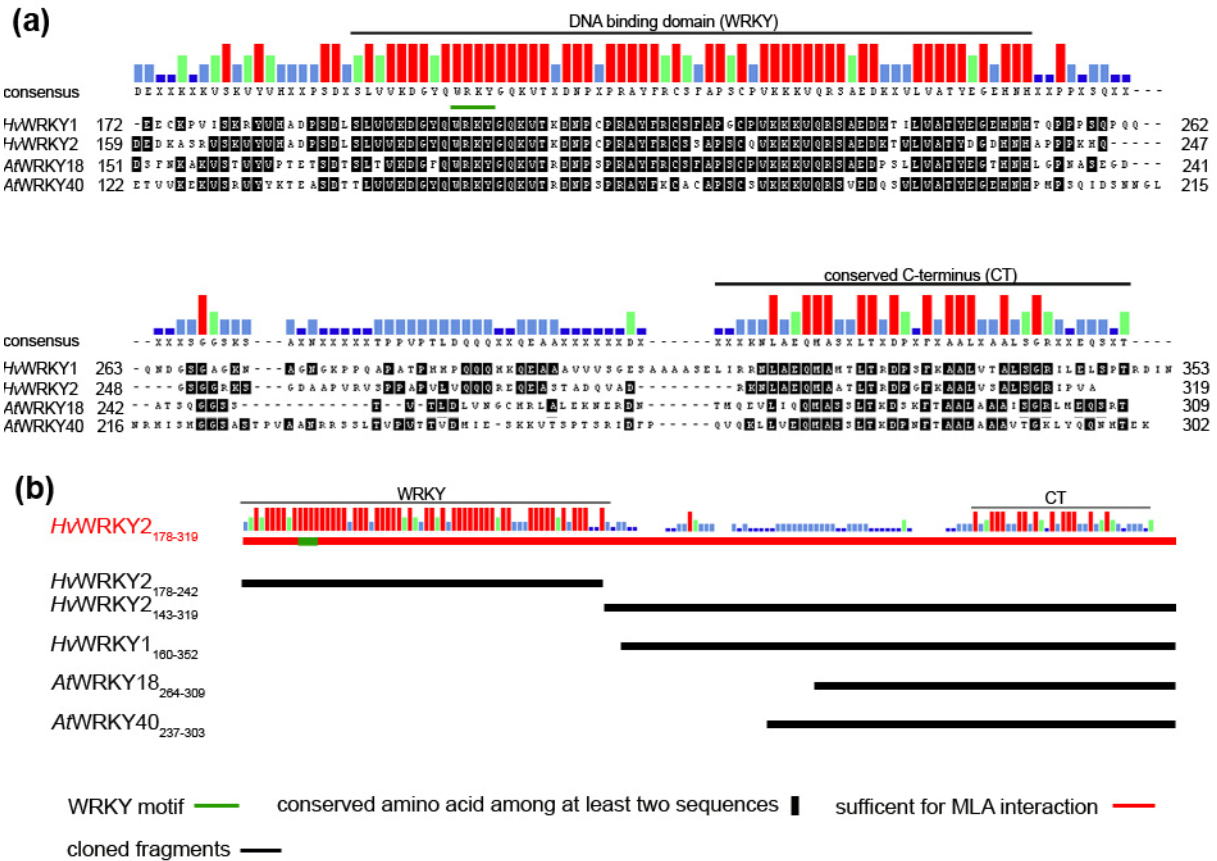
**Figure 1.1: Alignment analysis of barley *Hv*WRKY1, *Hv*WRKY2 and Arabidopsis *At*WRKY18 and *At*WRKY40 proteins.** (a) Sequence alignment of the C-terminal half of barley *Hv*WRKY1 and *Hv*WRKY2 with Arabidopsis *At*WRKY18 and *At*WRKY40. High sequence conservation was found within the DNA binding domains (WRKY domain) and among the extreme C-termini (CT). (b) Construct design for yeast 2-hybrid interaction studies with MLA. The fragment *Hv*WRKY2$_{178-309}$, previously reported to be sufficient to interact with the MLA-CC domain, is indicated in red. Newly generated constructs of *Hv*WRKY2, *Hv*WRKY1 and of the two related *Arabidopsis* WRKY proteins *At*WRKY18 and *At*WRKY40 are indicated in black.
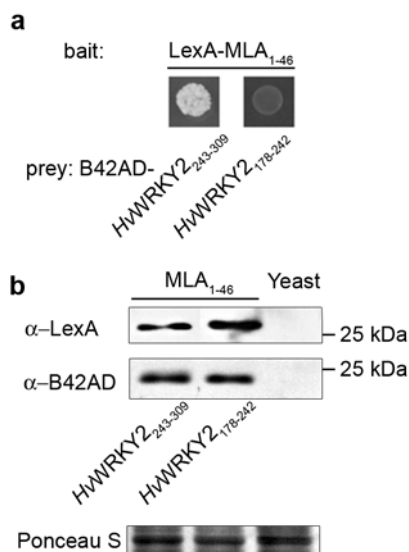


**Figure 1.2: The conserved C-terminus of *Hv*WRKY2 is sufficient to interact with MLA$_{1-46}$ in yeast.** (a) Yeast 2-hybrid growth phenotypes indicating association of MLA$_{1.46}$ with the extreme C-terminus of *Hv*WRKY2 (WRKY2$_{243-309}$) but not with the WRKY domain (WRKY2$_{178-242}$). (b) Accumulation of bait and prey fusion proteins in yeast. Log-phase growing yeast were used for total protein extraction. Equal amounts of protein were subjected to immuno-blot analysis using bait (LexA) and prey (B42AD) specific antibodies.

18

## 1.2.2 Association of *At*WRKY18 and *At*WRKY40 with the MLA-CC domain in yeast

I found *Hv*WRKY2-CT to be sufficient to associate with MLA$_{1-46}$. Thus, the related *Arabidopsis* transcription factors *At*WRKY18 and *At*WRKY40 might as well possess coiled-coil binding specificities among their conserved CTs. Therefore, I first tested whether *At*WKY18-CT and *At*WRKY40-CT were able to bind MLA$_{1-46}$ in yeast. LexA DNA binding domain fusions with *At*WRKY18$_{164-309}$ (*At*WRKY18-CT) and *At*WRKY40$_{237-303}$ (*At*WRKY40-CT) as well as with *Hv*WRKY1$_{260-353}$ (*At*WRKY1-CT; Fig. 1.1b) were co-expressed with MLA$_{1-46}$ fused to the B42 activation domain and assayed for yeast-growth after 72h. Consistent with my results for *Hv*WRKY2-CT, *Hv*WRKY1-CT was found to associate (indicated by yeast growth) with MLA$_{1-46}$ (Fig. 1.3a). Interestingly, *At*WRKY18-CT and *At*WRKY40-CT also showed a growth phenotype similar to *Hv*WRKY1-CT, indicative for association with MLA$_{1-46}$ (Fig. 1.3a). Immuno-blot analysis using bait and prey specific anti-sera demonstrated that all fusion proteins accumulate (Fig. 1.3b). The capability of both *Arabidopsis* WRKY-CTs to associate with barley MLA$_{1-46}$ might denote, together with their structural conservations, sustained functional competence(s) between barley and *Arabidopsis* WRKY factors. Currently the functional homologue of the R protein MLA in *Arabidopsis* remains elusive. Nevertheless, the Arabidopsis genome contains 62 putative CC-NBS-LRR R protein encoding genes (Meyers et al., 2003). Thus, it seems reasonable to assume that a specific sub-group of *Arabidopsis* CC domain possessing intracellular immune receptors, like barley MLA, can associate with *At*WRKY18 and *At*WRKY40 *in vivo* and thereby modulate defence responses.
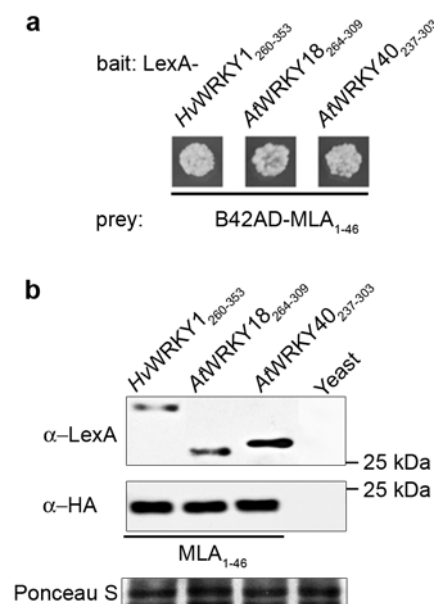


**Figure 1.3: Association of the *At*WRKY18 and *At*WRKY40 C-termini with MLA$_{1-46}$ in yeast.** (a) Yeast growth phenotypes indicating association of MLA$_{1-46}$ with the conserved C-terminus of *Hv*WRKY1 as well as with related *At*WRKY18 and *At*WRKY40. (b) Equal amounts of total protein extracts derived from log-phase growing yeast were subjected to immuno-blot analysis. Fusion proteins were detected by the use of specific anti-sera.

### 1.2.3 Identification of *At*WRKY18 and *At*WRKY40 interacting candidate CC domains encoded by NBS-LRR *R* genes from *Arabidopsis*

To identify such putative interactors I aimed at cloning all coiled-coil domains from CC-NBS-LRR proteins encoded by the *Arabidopsis* genome and subsequently test for association with *At*WRKY18-CT and *At*WRKY40-CT in a targeted yeast 2-hybrid approach. To reduce the number of candidates, I excluded genes with imperfect CC- predictions and putative pseudogenes (based on the program COILS: http://www.ch.embnet.org/software/COILS_form.html and Meyers et al., 2003). Out of the 45 remaining CC-NBS-LRR candidate genes I successfully cloned 28 coiled-coil domains from the ecotype Columbia. Cloned candidate CC regions fused to the activation domain of B42 were co-expressed in yeast, either with AtWRKY18-CT or *At*WRKY40-CT LexA DNA binding domain fusions. Interactions were scored +, ++, or +++ according to the rate of growth under induction conditions after 72h (Tab.1). Among the 28 candidates the CC domains encoded by At1G51480, At1G59124 and At5G43730 exhibited the most prominent growth phenotypes upon co-expression with both WRKY-CTs. A similar phenotype was observed for the CC domain of At5G63020 upon co-expression only with *At*WRKY18-CT. Moderate growth was detected after co-expression of the CC domains encoded by At3G14460, At4G10780, At5G43470 and At5G47250 with *At*WRKY18-CT and *At*WRKY40-CT, and for At5G66900 only with *At*WRKY18-CT. A weak interaction phenotype upon co-expression with *At*WRKY18-CT and *At*WRKY40-CT was observed for the coiled-coil domains of At1G62630 and At1G63360. The CC domains encoded by At3G14470 and At5G04720 displayed weak interaction phenotypes only upon co-expression with *At*WRKY40-CT (Tab. 1).

A phylogenetic analysis of the candidate interacting CC domains, described above, revealed clustering into two groups. Representatives of the three strongest interacting candidates (At1G51480, At1G59124 and At5G43730) fell into both clusters (Fig. 1.4). Increasing sequence distance in this analysis was found to correlate with decreasing growth phenotypes in the yeast 2-hybrid screen. Interestingly, MLA-CC was found to cluster together with the CC domain encoded by *rpp8* (15,4% identity) (Fig. 1.4). Among identified candidate loci, to date, only *RPP8* has been shown to harbor an *R* gene mediating resistance specificity. In the ecotype Landsberg functional *RPP8* is required for full resistance against the oomycete *Hyaloperonospora arabidopsidis*, whereas in the ecotypes C24 und Dijon17 the corresponding genes *RCY1* and *HRT* confer resistance against the viral pathogens cucumber mosaic virus and turnip crinkle virus, respectively (Cooley et al., 2000; Kachroo et al., 2000). So far no resistance specificity has been described for *rpp8* in the ecotype Columbia.

Together these data suggest the existence of two distinct phylogenetic subgroups of CC domains that potentially can associate with *At*WRKY18 and WRKY40 *in vivo*. Additionally, barley MLA-CC, which was found to be capable of associating with *At*WRKY18 and *At*WRKY40 in yeast, shares at least weak *in silico* homology with one of these subgroups. Further structural and functional information on CC domain-encoding NBS-LRR *R* genes may help to substantiate these findings.

**Table 1.1: Interaction study of Coiled-coil domains encoded by *Arabidopsis* CC-NB-LRR genes with WRKY18 and WRKY40 in yeast**

| gene identifier | title | cloned fragment | interaction with WRKY18 | interaction with WRKY40 | resistance phenotype | reference |
|---|---|---|---|---|---|---|
| AT1G12210 | RFL1 (RPS5-like1) | 1-151 | | n.d. | | Warren et. al 1995 |
| AT1G12220 | RPS5 | 1-145 | | | *Pseudomonas syringae* | Simonich and Innes 1995 |
| AT1G12280 | | 1-173 | | | | |
| AT1G12290 | | 1-161 | | n.d. | | |
| AT1G51480 | | 88-228 | +++ | +++ | | |
| AT1G53350 | | 1-166 | | | | |
| AT1G58390 | RPM1 homolog | 1-155 | | + | | |
| AT1G59124 | PRM1 homolog (RF45) | 1-161 | +++ | +++ | | |
| AT1G59620 | PRM1 homolog (CW9) | 1-116 | | | | |
| AT1G59780 | | 1-150 | | | | |
| AT1G61190 | | 1-157 | | | | |
| AT1G61310 | | 1-151 | | | | |
| AT1G62630 | putative RPS2 | 1-154 | + | + | | |
| AT1G63350 | | 1-151 | | | | |
| AT1G63360 | | 1-151 | + | + | | |
| AT3G07040 | RPM1 | 1-159 | | | *Pseudomonas syringae* | Grandt et. al 1995 |
| AT3G14460 | | 1-177 | ++ | ++ | | |
| AT3G14470 | | 1-171 | | + | | |
| AT3G46530 | RPP13 | 1-156 | | | *Peronospora aradopsidis* | Bittner-Eddy et. al 1999 |
| AT4G10780 | | 1-160 | ++ | ++ | | |
| AT5G04720 | | 1-193 | | + | | |
| AT5G43470 | RPP8 | 1-164 | ++ | ++ | *Peronospora aradopsidis, Cucumber mosaic virus, Turnip crinkle virus* | Cooley et. al 2000, Kachroo et. al 2000, Takahashi et. al 2002 |
| AT5G43730 | | 1-155 | +++ | +++ | | |
| AT5G47250 | | 1-163 | ++ | ++ | | |
| AT5G47260 | | 1-157 | n.d. | | | |
| AT5G63020 | | 1-169 | +++ | | | |
| AT5G66900 | | 1-163 | ++ | | | |
| AT1G58602 | | 1-153 | | | | |

| | Interaction phenotype | |
| --- | --- | --- |
| | WRKY18 | WRKY40 |
| At1G51480 | +++ | +++ |
| At5G43730 | +++ | +++ |
| At5G47250 | ++ | ++ |
| At4G10780 | ++ | ++ |
| At1G62630 | + | + |
| At1G63360 | ++ | ++ |
| At5G63020 | +++ | |
| At1G59124 | +++ | +++ |
| At5G43470 (rpp8) | ++ | ++ |
| HvMLA10 | ++ | ++ |
| At3G14460 | ++ | ++ |
| At3G14470 | | + |
| At5G04720 | | + |
| At5G66900 | ++ | |
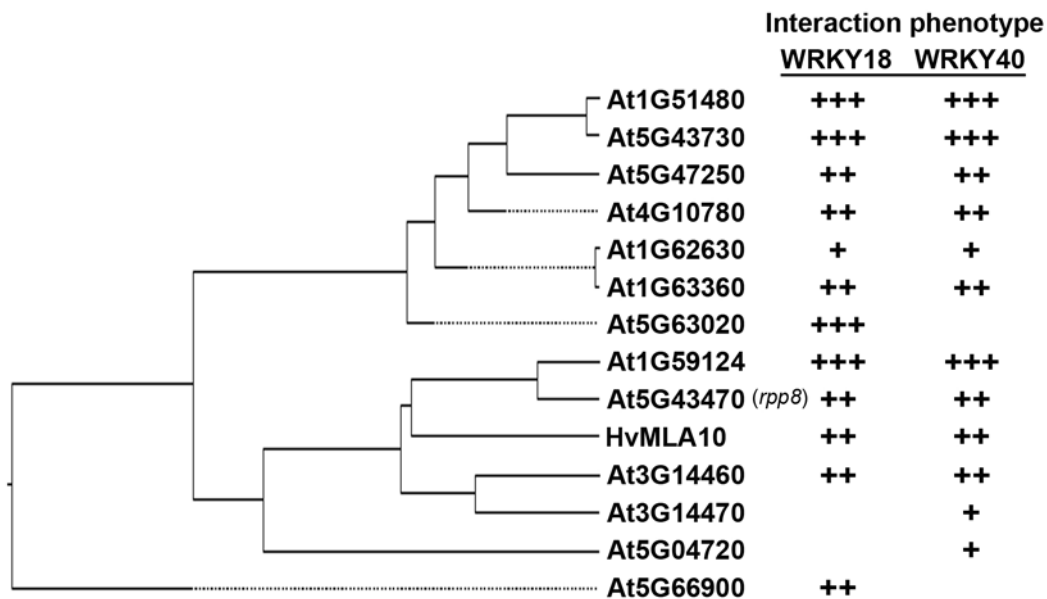
**Figure 1.4: Phylogenetic analysis of candidate *At*WRKY18 and *At*WRKY40 interacting CC domains of *Arabidopsis* R proteins.** Amino acid sequences (1-120) of CC domains indentified as putative interactors of *At*WRKY18 and *At*WRKY40 in yeast were analyzed with *clustalW*. Yeast 2-hybrid growth rates (indicative of interaction intensity) with *At*WRKY18 and *At*WRKY40 were scored as + low, ++ medium and +++ strong, respectively. Clustering of CC sequences was found to correlate with yeast growth phenotypes in the presence of *At*WRKY18 and *At*WRKY40.

## 1.2.4 Different yeast 2-hybrid interaction phenotypes of RPP8 family member CC domains with *At*WRKY18 and *At*WRKY40 indicate *in vivo* specificity

Among my candidate interactors with *At*WRKY18-CT and *At*WRKY40-CT I found the CC domain of RPP8 (rpp8-CC). The *RPP8* gene from ecotype Columbia is to date uncharacterized, whereas resistance specificities for this locus have been reported in other accessions. Thus it is conceivable that other members of the RPP8 family, which share at least 95% sequence identity with rpp8-CC (data not shown), as well can associate with *At*WRKY18-CT and *At*WRKY40-CT. To test this hypothesis I cloned the CC domains of functional *R* genes encoded by the RPP8 locus from the accessions Landsberg (Ler), Dijon17 (Di17) and C24. Fusions of *RPP8*-CC (Ler), *HRT*-CC (Di17) and *RCY1*-CC (C24) with the B42 activation domain were co-expressed with *At*WRKY18-CT, *At*WRKY40-CT as well as with *Hv*WRKY1-CT fused to the LexA DNA binding domain in yeast. Equal amounts of co-expressing yeast were allowed to grow for 72h under induction conditions prior to analysis (Fig. 1.5a-b). For all three WRKY-CT domains the strongest growth phenotype was found with HRT-CC (Di17), whereas the growth phenotypes with RPP8-CC (Ler) and RCY1-CC (C24) were weaker and resembled those of rpp8-CC (Col) (Fig2.5a, data for *At*WRKY18-

CT not shown). To exclude possible allelic variations among the different ecotypes at the *At*WRKY18 and *At*WRKY40 loci, the relevant genomic regions of Ler, Di17 and C24 were sequenced. No variations among the different ecotypes were found. Thus, minor changes within the amino acid sequences of CC domains encoded by the *RPP8* locus in different accessions are likely the cause for the different association intensities with tested *At*WRKY-CTs in yeast. Together, these data suggest conserved association specificities among related *Arabidopsis* and barley *At*WRKY-factors toward distinct CC domains of NBS-LRR R proteins.
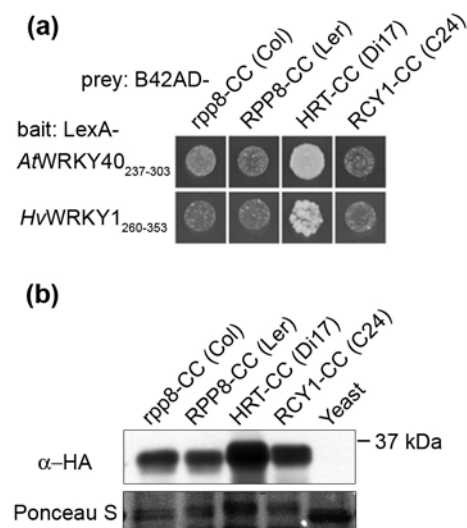


**Figure 1.5: Preferential interaction of related *Arabidopsis* and barley WRKY factors with HRT-CC.** (a) Yeast co-expressing different RPP8 loci-encoded CC domains together with *Arabidopsis* or related barley WRKY-CT constructs as indicated. Different growth phenotypes indicate preferential association of HRT-CC with the WRKY factors constructs. (b) Equal amounts of total protein extracts derived from log-phase grown yeast were subjected to immuno-blot analysis. Prey (B42AD) fusion proteins were detected with an HA specific antiserum (for accumulation of bait fusion proteins in yeast see fig. 2.4).

HRT confers resistance against turnip crinkle virus (Kachroo et al., 2000) and this resistance requires, other than RPP8- and RCY1-mediated resistance specificities, functional EDS1 (Takahashi et al., 2002). In the context of the data recently published by Pandey et al. (in press) this result provides a link between *At*WRKY18- and *At*WRKY40-mediated transcriptional regulation and EDS1-dependent signalling in plant immunity.

## 1.2.5 Post-invasive resistance towards *Golovinomyces orontii* in *Atwrky18 Atwrky40* double mutants is independent of pre-invasive defence but requires EDS1 and CYP81F2

To further analyze the implicated role of functional EDS1 in the *At*WRKY18 *At*WRKY40-mediated modulation of the basal defence (see above), I choose the compatible interaction of Arabidopsis with *G.orontii* as a model. In susceptible *Arabidopsis* wild-type plants *AtWRKY18* and *AtWRKY40* transcripts rapidly accumulate (~4h) after infection with adapted

*G. orontii* and show fungal entry rates of >83% 48 hours post infection (hpi). At later stages the fungus undergoes several rounds of asexual reproduction and subsequent re-infections to colonize the plant. In contrast, fungal entry rates in *Atwrky18 Atwrky40* double mutants, which lack *AtWRKY18* and *AtWRKY40* transcripts, were significantly reduced to 35%. These plants show resistance at later stages (8 days post infection; dpi), since the fungus fails to colonize the plant (Pandey et al., in press). However, it remains elusive whether this late post-invasive resistance is dependent on decreased fungal entry efficiency and how EDS1 might contribute to this.

To answer these questions I crossed the *Atwrky18 Atwrky40* genotype with *Arabidopsis* mutant variants, impaired in pre-invasive defence and *eds1*, to generate the appropriate triple mutants. 4 week old homozygous F3 plants were infected with *G. orontii* and assayed for host cell entry efficiency and fungal growth phenotypes 48 hours and 8 days post infection, respectively. Wild-type plants displayed fungal entry rates of ~90% whereas the host cell entry efficiency in *Atwrky18 Atwrky40* mutants was significantly reduced to ~60% (Fig. 1.6a). Susceptibility in the wild-type was associated with successful fungal reproduction on the leaf surface 8 days post infection. However, resistant *Atwrky18 Atwrky40* plants showed only occasional faint fungal sporulation at leaf margins (Fig. 1.6b). In contrast, all single mutants used for triple mutant generation (*eds1*, *pen1*, *pen2*, *pad3* and *cyp81f2*), exhibited wild-type-like fungal entry rates (~90%) and colonization phenotypes (Fig. 1.6a-b). Triple mutants carrying either a mutation in *pen2* or *pad3* showed wild-type-like penetration rates but the fungus failed to reproduce on infected leaves at later stages (Fig. 1.6b). Thus, PEN2 and PAD3 functions seem to be required for limiting host cell entry but are dispensable in establishing *Atwrky18 Atwrky40*-dependent post-invasive resistance. In contrast, *PEN1* appears not to be required for limiting fungal host cell entry since *Atwrky18 Atwrky40 pen1* mutants displayed *wrky18 wrky40*-like fungal entry rates (~60%). At later infection stages, resistance was associated with the appearance of large necrotic leaf areas on *Atwrky18 Atwrky40 pen1* plants, whereas *Atwrky18 Atwrky40* mutants showed only a few defined small necrotic leaf speckles (Fig. 1.6a-b). PEN1 syntaxin accumulates in papillae underneath fungal appressoria and papillae formation is delayed in *pen1* mutants (Assaad et al., 2004). Therefore *PEN1* contributes in some way to *Atwrky18 Atwrky40*-mediated resistance.

Pandey et al. (in press) showed that *At*WRKY40 binds to W-boxes in the 5` regulatory region of *EDS1 in vivo*. Interestingly, *Atwrky18 Atwrky40 eds1* triple mutants appeared wild-type-like at both time points assayed post infection, indicating a requirement for *EDS1* in pre- and post-invasive powdery mildew resistance (Fig. 1.6a-b).
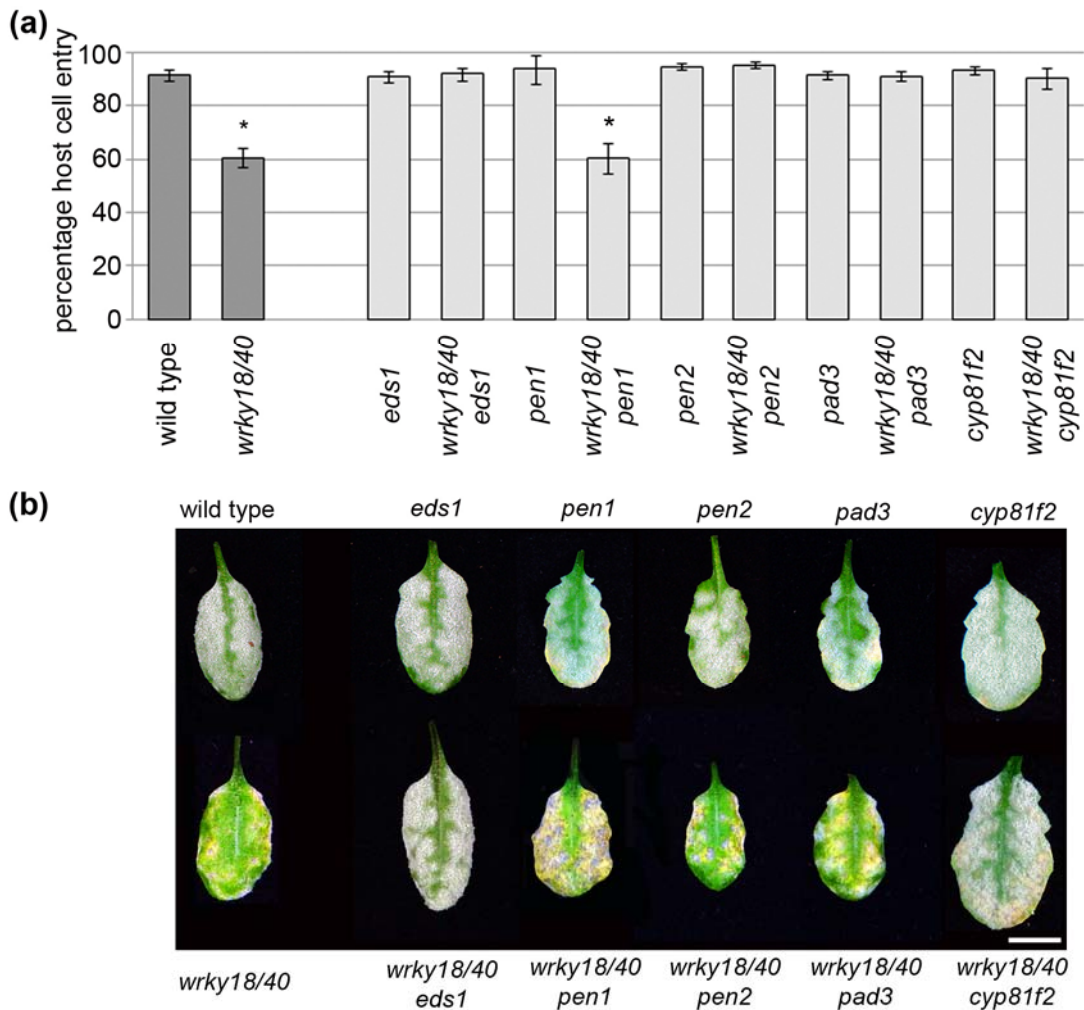
**Figure 1.6: Leaf infection phenotypes of different mutants following infection with *G. orontii*.**
(a) Percentage of fungal host cell entry on 4-week old wild-type, *Atwrky18 Atwrky40*, and indicated single and triple mutants 48h post infection. Asterix t<0,005; based on students t-test  (b) Macroscopic infection phenotypes 8 days post infection on 4-week old wild-type, *Atwrky18 Atwrky40*, single and corresponding triple mutants. Bar: 1cm.

Surprisingly, mutation of *CYP81F2* rendered *Atwrky18 Atwrky40* mutant plants as susceptible as wild-type with respect to both, pre- and post-invasive defences (Fig. 1.6a-b). *CYP81F2* encodes a P450 monooxygenase that catalyses the conversion of indole-3-yl-methyl glucosinolate (I3G) to 4-hydroxy-indole-3-yl-methyl glucosinolate (4MI3G). 4MI3G is activated by the atypical myrosinase PEN2 thereby inducing broad-spectrum anti-fungal defence (Bednarek et al., 2009). PAD3 (CYP71A13) catalyzes the final step in camalexin synthesis (Nafisi et al., 2007). These data therefore implicate both secondary metabolites, camalexin and 4MI3G, as components of *Atwrky18 Atwrky40*-mediated pre-invasive defence. Strikingly, different requirements for *CYP81F2* and *PEN2* in *Atwrky18 Atwrky40*-mediated

powdery mildew resistance further suggest the existence of a so far unknown function of CYP81F2.


## 1.2.6 The MLA10-CC domain forms a homo-dimer


Oligomerization of NBS domain-containing proteins, such as human APAF-1 and nematode CED-4, provide an established paradigm for the formation of signalling complexes. Similarly, some plant R proteins have been described to form homomeric assemblies prior to or post effector recognition (Mestre and Baulcombe, 2006; Ade et al., 2007; Danot et al., 2009; Gutierrez et al., 2010). Studies on tobacco N (TNL), tomato Prf (novel N-terminal domain) and *Arabidopsis* RPS5 (CNL) provide evidence for their N-terminal domain-mediated homo-oligomerization. However, both the structural basis for this as well as the relevance for ETI remains elusive. Recently our collaborator Jijie Chai (Beijing, China) solved the crystal structure of the invariant CC domain (residues 1-120) of barley MLA by Single-wavelength Anomalous Diffraction (SAD) at a resolution of 2.0 Å (Maekawa et al.; under review in Cell Host & Microbe). The final atomic model comprises residues 6–120. As predicted from the primary sequence, the monomeric structure of the CC domain is mainly α-helical and contains two long anti-parallel α-helices linked by a short loop (Fig. 1.7a-b), thereby forming a helix-loop-helix structure. No electron density was observed corresponding to the five residues 91-95 likely due to a disorder of this region in solution (Fig. 1.7a-b). In the crystals, two protomers of the CC domain pack symmetrically mainly through the interior-lined residues in the CC monomer (Fig. 1.7a). Assembly of the CC domain dimer resembles two springs slammed together and such an intertwined packing arrangement gives rise to an extensive dimer interface, generating the burial of 7,950 Å$^2$ surface area (Fig. 1.7a). This large buried surface area suggests that the CC domain dimer would be highly stable and likely intrinsically inseparable.
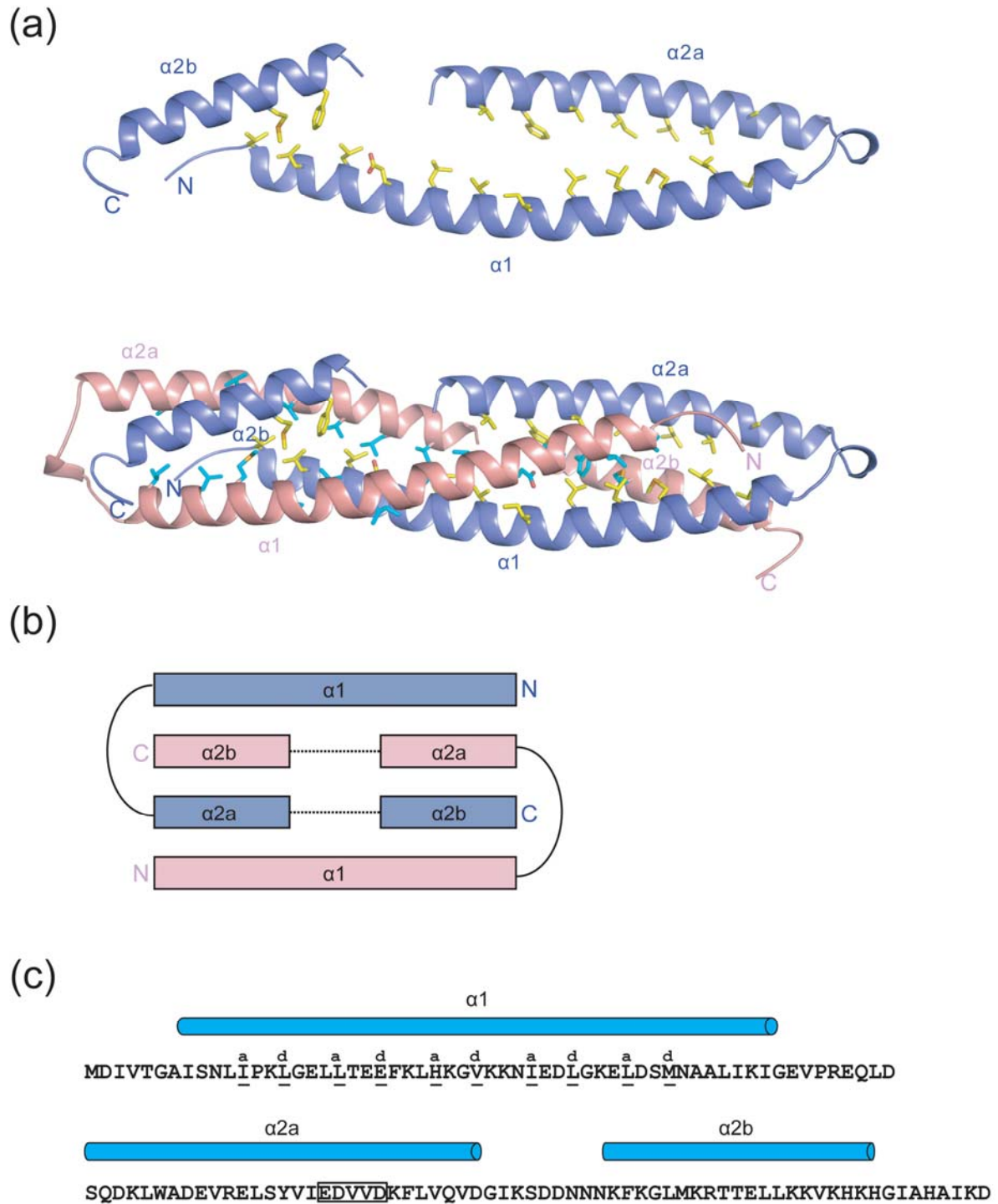
**Figure 1.7: The MLA10 CC$_{5-120}$domain forms a homo-dimer.**

(a) Ribbon diagram of the MLA10 CC domain; monomer top; dimer bottom. (b) Simplified topology of the CC dimer. (c) Amino acid sequence of MLA10$_{1-120}$. Blue tubes indicate areas with α-helical structure, a and d denote the position within the haptad repeat(s) of αI; the black frame highlights the EDV a conserved motif involved in intra-domain interactions. Taken from Markawa et al.; under review in Cell Host & Microbe.

A large portion of the two α-helices are involved in homo-dimerization of the CC domain. The helix α1 (residues 12-44) forms a parallel two-stranded coiled-coil fold in the dimer structure (Fig. 2.8a). Coiled-coil formation in the CC domain is primarily dependent on Ile12, Leu15, Leu19, Glu22, His26, Val29, Ile33, Leu36, Leu40, and Met43 from the heptad repeat sequences (Fig. 1.8a). These residues are located either at a or d (Fig. 1.7c) positions that make hydrophobic contacts with those from the other helix, which are characteristic of the interactions observed in other coiled-coil structures (Kohn et al., 1997). The ends of the coiled-coil slightly splay apart and, together with the N-terminal half of helix α2b and the C-terminal third of helix α2a, form short antiparallel four-helix bundles (Fig. 1.8b). In total 20 residues from both CC protomers form a network of van der Waals interactions within one helical bundle. Leu11, Leu15, Leu18, Phe99, Met103 and Ser106 from one monomer and Leu36, Glu39, Met43, Ser73, Ile76 and Val80 from the other one, that reside at the center of one helical bundle, constitute the core of hydrophobic interactions within one helix bundle (Fig. 1.8b). To further strengthen dimerization of the CC domain, the proximal C-terminal end of α2b makes tight hydrophobic contacts with the C-terminal end of α1a and the N-terminal end of α2a from the other CC monomer (Fig. 1.8c). In addition, the hydrogen bonds formed between Lys116 and His117 from the loop C-terminal to the helix α2a in one monomer and Asp59 and Asp62 in the other monomer contribute to CC domain dimerization, respectively (Fig. 1.8c).
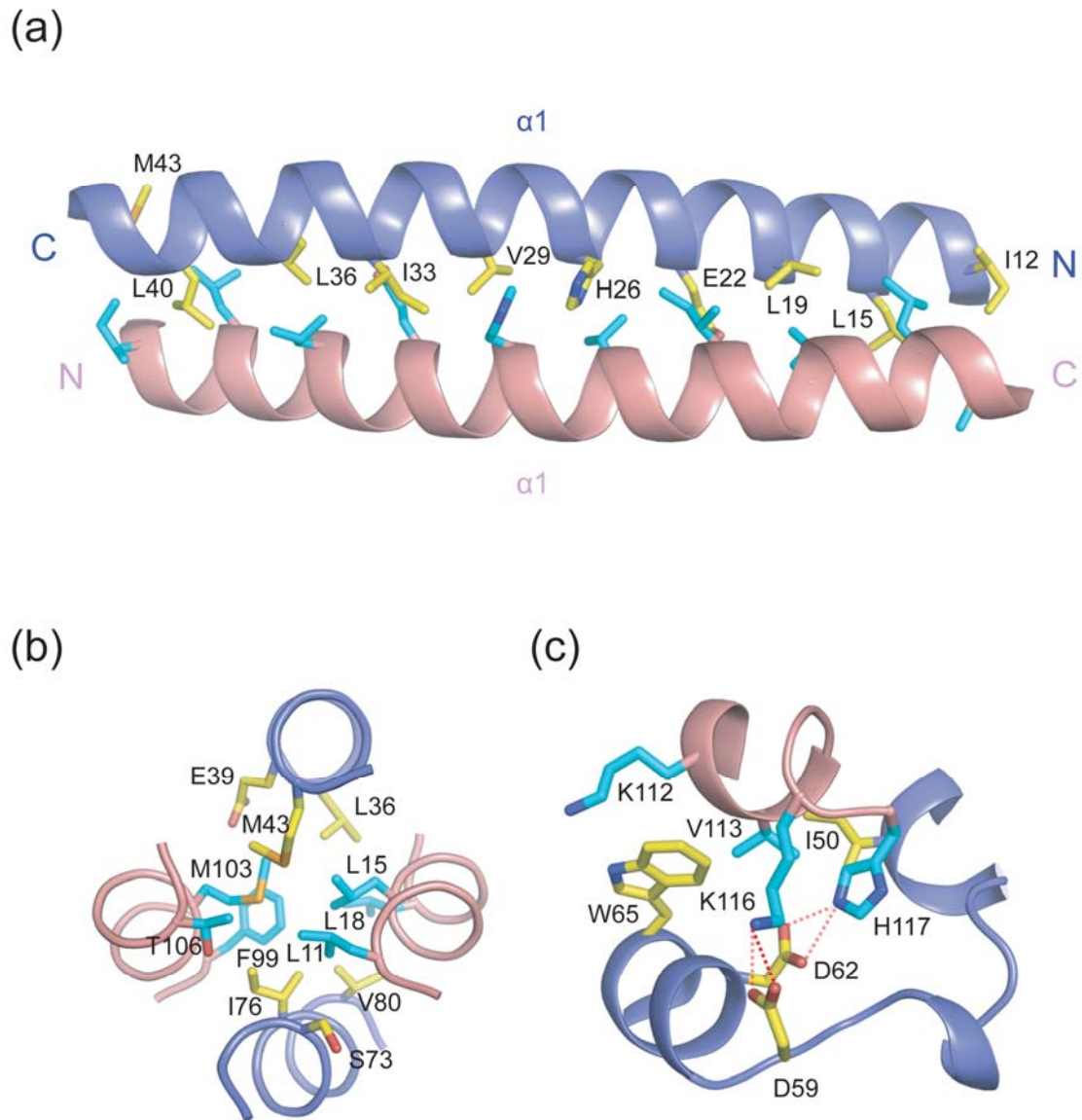
**Figure 1.8: Predicted hydrophobic contacts between the two MLA10 coiled-coil protomers.**
(a) Hydrophobic contacts within helix α1 of both protomers involves the residues I12, L15, L19, E22, H26, V29, I33, L36, L40 and M43 that locate at position a or d within the heptad repeat. (b) Core van der Waals interactions within a four helical bundle, consisting of ends of both helices α1 and helix α2a and helix α2b from different protomers. The contacts involve L11, I15, L18, F99, M103 andT106 form one- and L36, E39, M43, S73 and I76 from the other monomer. (c) The hydrogen bonds formed between K116 and H117 from one- and D59 and D62 from the other monomer contribute to the dimer formation. Taken from Markawa et al..; under review in Cell Host & Microbe.

## 1.2.7 MLA self-association in plants and yeast

To study potential MLA self-association *in planta,* Dr. T. Maekawa (MPIPZ, Köln) generated stable transgenic barley plants co-expressing *MLA1-HA* and *MLA1-Myc* from single copy transgenic lines each expressing functional *MLA1-HA* or *MLA1-Myc* (Bieri *et al*., 2004). By the use of total leaf protein extracts he could demonstrate co-immunoprecipitation (co-IP) of MLA1-HA and MLA1-Myc. Analysis of protein extracts prepared from co-expressing plants at several time points post inoculation with *Bgh* indicate that self-association of MLA1 is not the consequence of effector-triggered receptor activation, but rather to occur in naïve plants (Full experimental data, figures and methods are described in Maekawa et al.; under review in Cell Host & Microbe). To further investigate the role of the CC domain in MLA self-association, I employed the yeast 2-hybrid assay. For this, bait (LexA) and prey (B42AD) fusion constructs expressing full-length (FL) and truncated *MLA10* variants were generated. Co-expression of identical bait and prey fusion constructs revealed self-interactions of $MLA10_{1-225}$. No self-interactions were detected for MLA10 full-length, $MLA10_{1-523}$ and $MLA10_{1-46}$ (Fig. 1.9a). Protein analysis using bait (LexA) and prey (B42AD) specific anti-sera identified $MLA10_{1-225}$ and $MLA10_{1-46}$ fusion proteins. We failed to detect LexA-$MLA10_{1-523}$ and both $MLA10_{FL}$ fusion variants (Fig. 1.9b). Lack of detection of these proteins might reflect their instability or their accumulation below detection limit(s) in yeast. Irrespectively, theses data indicate MLA self-association *in vivo*. To gain further knowledge about the mechanistics of MLA self association $MLA10_{1-225}$ was used for further detailed analysis in yeast.
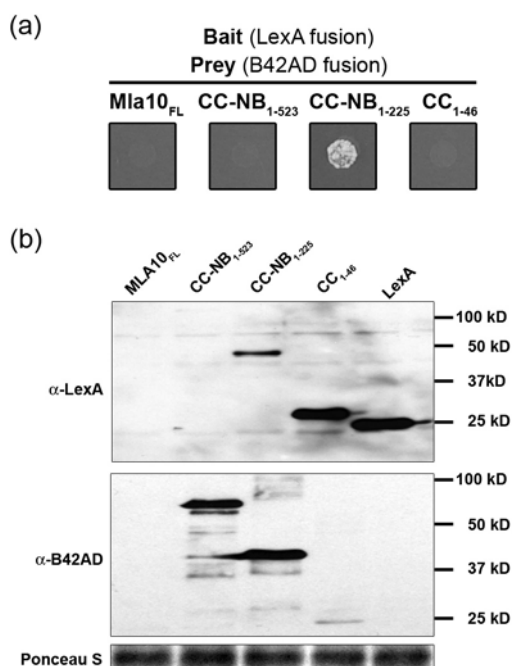


**Figure 1.9: MLA10 self associates in yeast.**
(a) Self-interaction of MLA. Yeast two hybrid results of bait fusions of the LexA DNA binding domain and prey fusions of the B42 activation domain with identically truncated MLA10 variants. Yeast growth indicates interaction. (b) Accumulation of bait and prey fusion proteins in yeast. LexA DNA binding domain and B42 activation domain fused to identical MLA constructs were co-expressed in yeast. Overnight cultures were used for total protein extraction. Equal protein amounts were subjected to immuno-blot analysis using LexA (α-LexA) and B42 (α-B42AD) specific anti-sera.

### 1.2.8 Functional analysis of the MLA10 CC dimer interface by structure-guided mutagenesis

To define the functional significance of the dimeric interface found in the MLA10-CC structure (Fig. 1.7 and 1.8) I took advantage of 17 available amino acid substitution variants. Each of theses variants targets an individual residue lining the interior between the protomers by a substitution to glutamic acid (Fig. 1.10a). Substitution of these residues is predicted to be thermodynamically unfavorable, possibly destabilizing the dimeric structure (corresponding MLA10 full-length clones were generated and kindly provided by Dr. T. Maekawa). For analysis identical MLA10$_{1-225}$ bait and prey constructs were co-expressed in yeast. Out of these 17 targeted single substitutions, three located in helix α1 (I33E, L36E, and M43E) resulted in loss of MLA10$_{1-225}$ self-interactions, whereas interactions were still detectable to varying degrees upon co-expression of eight other variants (L11E, L15E, L18E, L25E, V29E, V69E, L72E, and I76E; Fig. 1.10a). The colony growth phenotype of five substitutions (L19E, F23E, F99E, M103E, and L110E) could not be examined, due to auto-activity of the bait constructs (yeast cells grew in the absence of prey on selective media; data not shown). Overall this data show that all amino acid substitutions tested weaken MLA10$_{1-225}$ self-association whilst only three variants in helix α1 disrupt this phenotype.

MLA-mediated isolate-specific *Bgh* resistance is thought to involve nuclear association of the MLA-CC domain with the WRKY factors *Hv*WRKY1 and *Hv*WRKY2 (Shen et al., 2007). To improve our understanding of the MLA WRKY association in the context of MLA-CC homo-dimerization, I tested MLA10$_{1-225}$ substitution variants for altered association phenotype(s) with *Hv*WRKY1-CT in yeast. Surprisingly, all MLA10$_{1-225}$ prey (B42AD) variants showed an impaired interaction phenotype with the *Hv*WRKY1$_{260-353}$ bait (LexA) fusion, except for L18E (Fig. 1.11a). Immuno-blot analysis with bait and prey specific antibodies indicated similar expression levels for all fusion proteins. Since Shen et al. (2007) previously showed that MLA10$_{1-46}$, representing helix α1, is required and sufficient for the MLA WRKY interaction, CC dimerization in general cannot be essential for the heteromeric association. Nevertheless, MLA self-association *in vivo* might regulate accessibility of helix α1 for the WRKY interaction. Dr. T. Maekawa used the transient single cell expression system in barley leaf epidermal cells to analyze the significance of the single amino acid substitution variants in MLA triggered immunity. He biolistically transformed barley epidermis cells with MLA10 wild-type and substitution variant constructs. After inoculation with the *Bgh* A6 isolate

expressing cognate *Avr_A10* the frequency of fungal haustoria formation was estimated.
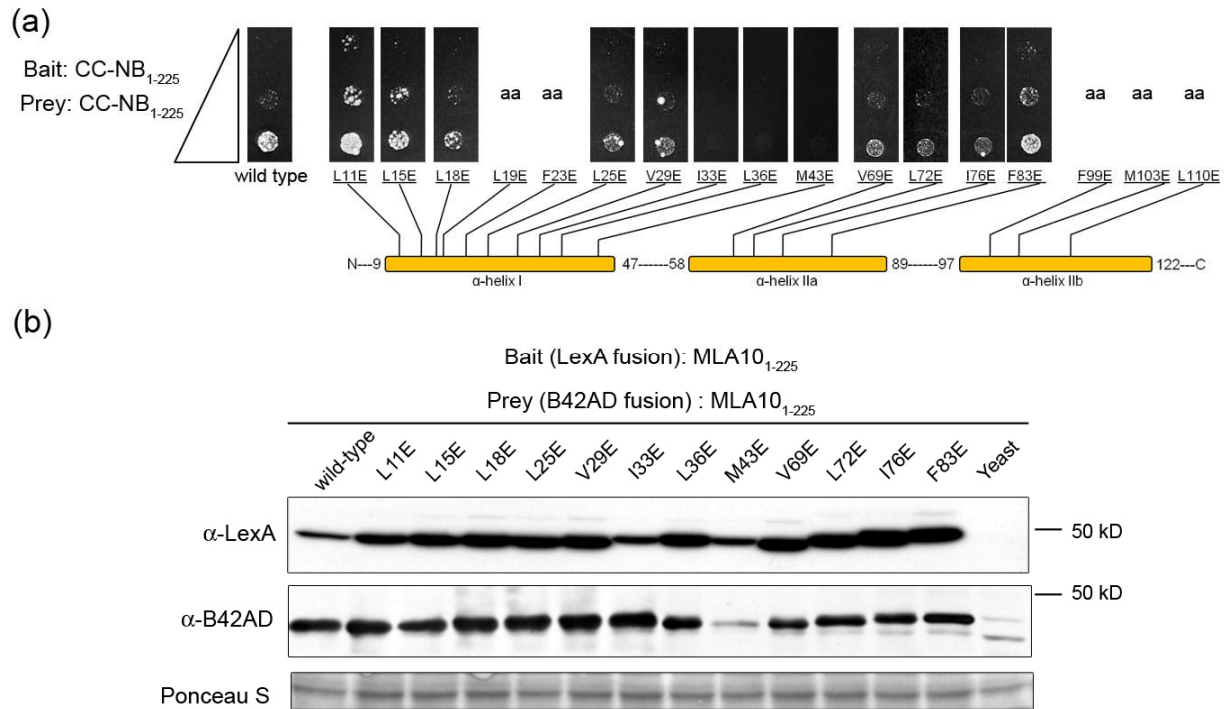


**Figure 1.10: Structure guided mutant analysis of MLA10 CC self association.**
(A) Single amino acid substitutions in the CC domain disrupt MLA10 CC homo-dimer formation in yeast. Amino acids indicated in the cartoon were substituted for glutamate. Amino acids 1-225 from all substitution mutants were cloned into yeast two-hybrid bait and prey vectors and co-expressed in yeast, respectively. aa auto-activity of yeast bait constructs (interaction phenotype could not be evaluated). Triangle indicates decreasing yeast concentrations. (B) Accumulation of bait and prey fusion proteins in yeast. LexA DNA binding domain and B42 activation domain fused to identical MLA constructs were co-expressed in yeast. Overnight cultures were used for total protein extraction. Equal protein amounts were subjected to immuno-blot analysis using LexA (α-LexA) and B42 (α-B42AD) specific antisera.

Notably, only the targeted substitution variant L18E as well as the naturally occurring variant G37R (Seeholzer et al., 2010) retained disease resistance activity (Full experimental data, figures and methods are described in Maekawa et al.; under review in Cell Host & Microbe). In summary, these data provide a link between CC dimerization, WRKY factors and MLA-mediated disease resistance.
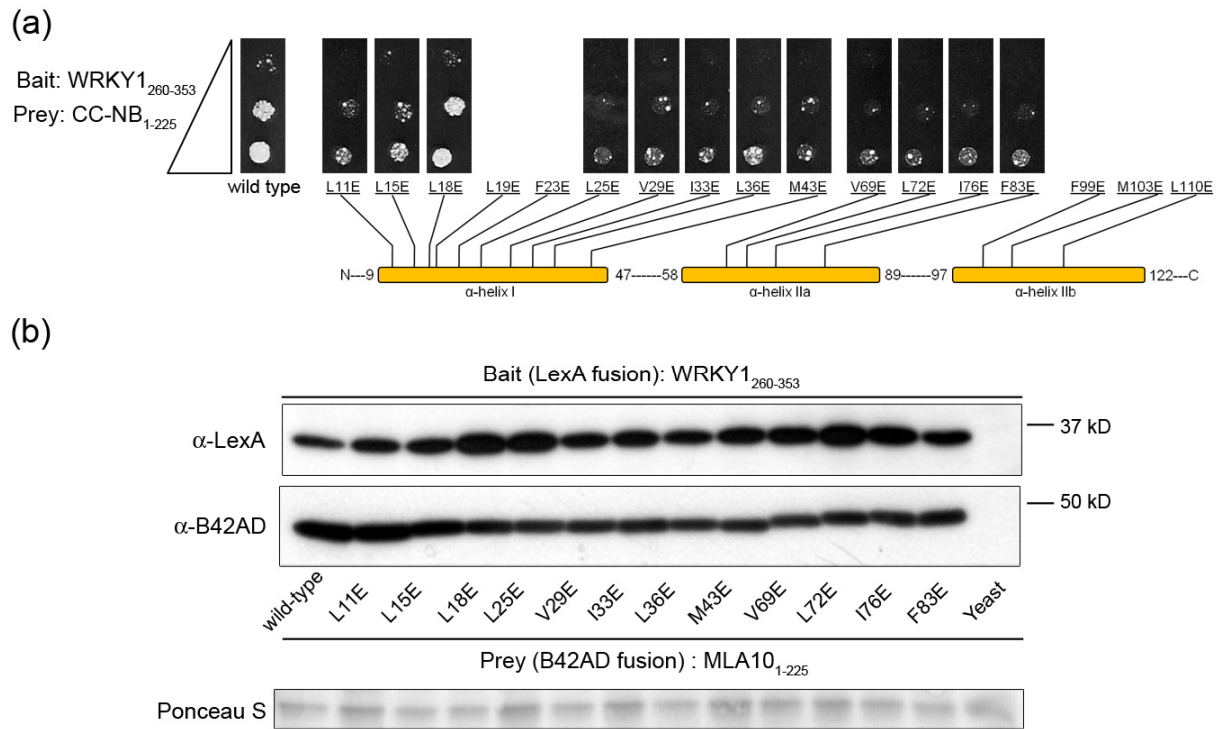
**Figure 1.11: Analysis of the *Hv*WRKY1-CT association with MLA10-CC amino acid substitution variants.** (a) Single amino acid substitutions in the MLA10-CC domain compromise the association with *Hv*WRKY1 in yeast. The C-terminus of *Hv*WRKY1 fused to the LexA DNA binding domain was co-expressed with MLA10$_{1-225}$ amino acid substitution variants fused to the B42 activation domain in yeast. Triangle indicates decreasing yeast concentrations. (b) Accumulation of bait and prey fusion proteins in yeast. LexA DNA binding domain and B42 activation domain fusion constructs (described above) were co-expressed in yeast. Overnight cultures were used for total protein extraction. Equal protein amounts were subjected to immuno-blot analysis using LexA (α-LexA) and B42 (α-B42AD) specific antisera.

## 1.3 Discussion

### 1.3.1 Coiled-coil domain binding abilities are retained among the conserved C-termini of related barley and *Arabidopsis* WRKY-factors

The nuclear association of barley MLA with *Hv*WRKY1 and *Hv*WRKY2 provides a direct mechanistic link how distinct R protein-derived signals are integrated into the plants basal defence machinery. A truncated version of *Hv*WRKY2 possessing its WRKY and CT domains was shown to be sufficient to associate with MLA (Shen et al., 2007). WRKY factors bind W-box containing DNA sequences through their WRKY domain (Eulgem et al., 1999) and combined crystal structure analysis and *in silico* modeling suggest this domain to be deeply buried into the major grove of the DNA (Yamasaki et al., 2005). The CT constitutes a short stretch (~40) of amino acids that is conserved among relatet *Hv*WRKY1, *Hv*WRKY2 and *At*WRKY18, *At*WRKY40 transcription factors (Shen et al., 2007; Fig. 1.1). In this work I identified association of MLA with the CT but not with the WRKY domain thereby identifying the C-terminal structures of *Hv*WRKY1 and *Hv*WRKY2 as the potential *in vivo* targets of MLA (Fig. 1.2, Fig. 1.3). I further explored whether conservations in the amino acid sequence among the CT domains of related *Arabidopsis* WRKY factors 18 and 40 constitute a potentially preserved binding specificity. A targeted yeast 2-hybrid experiment revealed association of both *Arabidopsis* WRKY factor CT domains with MLA (Fig 1.3). Thus, dicotyledonous *At*WRKY18 and *At*WRKY40 probably share a conserved binding specificity, among their so far functionally uncharacterized CT domains, with their related monocotyledonous barley WRKY factors 1 and 2. This result is supported by the work of Mangelsen et al. (2008), which indicates that structurally related WRKY factors from monocots and dicots share retained protein functional competences. Nevertheless, to date an *Arabidopsis* homologue of MLA has not been identified.

In *Atwrky18 Atwrky40* mutants the transcription of defence related genes is exaggerated in a pathogen-dependent manner (Xu et al., 2006; Shen et al., 2007; Pandey et al., in press), and these plants are resistant towards the adapted powdery mildew *G. orontii*. Therefore, both WRKY factors were thought to be part of a feedback repression system, similar to *Hv*WRKY1 and *Hv*WRKY2, in basal defence (Shen et al., 2007). In any case, a general direct repressor function of *At*WRKY18 and *At*WRKY40 seems rather unlikely, since *Atwrky18 Atwrky40* plants do not constitutively express defence related genes (Shen et al., 2007; Pandey et al., in press). The transient expression of defence responsive genes is the outcome of a complex interplay of distinct repressors and co-activators (Lopez-Maury et al., 2008) and this is supported by the recent studies of Pandey et al. (in press). Moreover,

*At*WRKY18 and *At*WRKY40 might exert associations with other CC domains encoded by *NBS-LRR R* genes and thereby modulate defence responses towards pathogens other than *G. orontii*.

### 1.3.2  *At*WRKY18 and *At*WRKY40 are competent to associate with distinct *R* gene encoded coiled-coil domains

Since *At*WRKY18 and *At*WRKY40 can associate with the coiled-coil domain encoded by barley MLA in yeast, I further analyzed the association abilities of these WRKY factors with coiled-coil domains encoded by *Arabidopsis R* genes. A newly generated candidate library of 28 CC domains was exemplary tested in yeast for association with *At*WRKY18-CT and *At*WRKY40-CT and 13 putative interactors identified (Tab. 1.1), which clustered into two phylogenetic subgroups, indicating the competence of *At*WRKY18 and *At*WRKY40 to associate with distinct structurally related *R* gene-encoded coiled-coil domains (Fig. 1.4). Previous MEME (Multiple Expectation Maximization for Motif Elicitation; Bailey and Elkan, 1995) analysis of the CC domains encoded by *Arabidopsis NBS-LRR* genes identified twenty motifs, based on conserved sequence patterns. Two of these (motif 1 and 7) were found coincident with the CC pattern predicted by COILS (Meyers et al., 2003). Consistently, the two subgroups of putative interactors can be specified as possessing either motif 1 (bottom group in Fig. 1.4) or motif 7 (top group in Fig 1.4). Whether *Hv*MLA possesses motif 1 could not be addressed, since the explicit definition of this motif was not available. Additionally, most members shared up to five other sequence patterns (described by Meyers et. al., 2003) in a subgroup-dependent manner. To date only the EDVID motif, which is highly conserved among CC domains of NBS-LRR proteins (including MLA, RX and HRT), has been functionally characterized (Rairdan et al., 2008). The EDVID motif of Resistance to potato virus X (RX) mediates intermolecular interactions that depend on its NB-ARC2 and LRR domains, whereas poorly conserved sequences at the N-terminus of the CC and flanking the EDVID motif mediate binding to the RanGTPase activating protein 2 (RanGAP 2) that is required for RX function (Sacco et al., 2007; Tameling and Baulcombe, 2007; Rairdan et al., 2008). This latter observation suggests a large interacting surface rather than a short defined sequence motif for the intermolecular association with RanGAP 2 (Rairdan et al., 2008).

Consistent with this, single amino acid substitution mutants within the CC of MLA10 were found to attenuate but not to inhibit the association with *Hv*WRKY1 in yeast (Fig. 1.11; Maekawa et al., under review in Cell Host & Microbe). Similar to RX and RanGAP 2 the R proteins RPS2 and RPM1 interact with RIN4 in the absence of their cognate effectors (Boyes

et al., 1998; Axtell et al., 2001; Mackey et al., 2002; Sacco et al., 2007) and such pre-formed complexes are thought to function as recognition platforms for their cognate AVR proteins (Collier and Moffett, 2009). Different from these, the nuclear association between MLA10 and *Hv*WRKY factors has been described as a post-recognition event, requiring activated MLA10 (Shen et al., 2007). Furthermore, involvement of the EDVID motif in the association of CC domains with WRKY factors is rather unlikely, since the minimal fragment of MLA-CC (MLA$_{1-46}$), required to associate with *Hv*WRKY1 and *Hv*WRKY2, lacks this region (Shen et al., 2007; Fig. 1.2; Fig. 1.3). However, a contribution of the EDVID motif in the CC-WRKY association cannot be completely excluded, and further *in vivo* studies are required to shed light on the molecular basis of how WRKY factors can associate with *R* gene-encoded CC domains.

### 1.3.3 Preferential association with HRT in yeast links *At*WRKY18 and *At*WRKY40 with EDS1-dependent *Turnip crinkle virus* resistance

Among the loci encoding candidate CC domains only *RPP8* (At5g43470; Tab. 1.1) has been described to harbor certain resistance specificities among three ecotypes different from the analyzed accession Columbia (McDowell et al., 1998; Cooley et al., 2000; Takahashi et al., 2002). Functional analysis of the promoter region of resistance-mediating *RPP8* (Landsberg), *HRT* (Di17), *RCY1* (C24) and functionally uncharacterized Columbia *RPP8* by Mohr et al. (2010) identified three conserved W-boxes matching the stringent consensus sequence TTGACT (Euglem et al., 2000). Mutations within these *cis* regulatory DNA elements, known to prevent WRKY factor binding (Du and Chen, 2000; Yu et al., 2001; Kim and Zhang, 2004), abolished almost completely *RPP8* basal and pathogen-induced expression (Mohr et al., 2010). W-boxes in the promoter of parsley *PcWRKY1* have been shown to be continously occupied by WRKY factor complexes, but their composition appears to be altered in a stimuli-dependent manner (Turck et al., 2004). Thus, regulation of basal and defence-induced responses through W-box containing sequences in the *RPP8* locus maybe likely achieved through the action of different WRKY factors. Whether *At*WRKY18 and *At*WRKY40 bind to W-box containing sequences in the promoter region of the *PRR8* locus remains to be determined. The limited information on the expression of *RPP8* in Arabidopsis plants under various treatments is due to the fact that At5g43470 (*RPP8*) is not detected by any probe set on the Affymetrix 22k chip.

The yeast 2-hybrid analyses, presented in this work, indicate specific association of *At*WRKY18 and *At*WRKY40 with HRT (the gene product encoded by At5g43470 in the ecotype Di17; Fig. 1.5). High selectivity for downstream targets can be seen as a prerequisite

for R proteins, encoded by At5g43470, to mediate resistance to such striking different pathogens as viruses (HRT and RCY1) and oomycetes (RPP8). Furthermore, this data are consistent with the preliminary observation that *RPP8-* mediated resistance toward *H. arabidopsidis Emco5* is most likely achieved independently of *At*WRKY18 and *At*WRKY40 (data not shown).

The CC domains (amino acid residues 1-120) encoded by At5g43470, in the accessions Columbia, Landsberg, C24 and Di17, share a minimum of 95 % identity. High sequence conservation among CC domains was recently reported for the large allelic series of MLA immune receptors (Seeholzer et al., 2010). Functional studies of the MLA-CC domain indicate that already single amino acid substitution renders the MLA protein inactive (Maekawa et al., under review in Cell Host & Microbe) and similar results have been reported for RCY1 (Sekine et al., 2006). Further, single amino acid substitution variants of MLA10-CC strongly diminish the association with *Hv*WRKY1 in yeast (Fig. 1.11). Together these data suggest a high degree of invariant functional constraints acting on *R* gene-encoded CC domains. In addition, this assumption is further supported by preferential binding of *Hv*WRKY1 to HRT in yeast (Fig. 1.5). Sequencing analysis verified the C-termini of *At*WRKY18 and *At*WRKY40 to be absolutely conserved among the four relevant ecotypes. Therefore, the stronger association phenotype of *At*WRKY18 and *At*WRKY40 with the CC domain of HRT in yeast is likely to reflect *in vivo* specificity.

HRT exhibits the only RPP8 locus-encoded R protein whose function is dependent on EDS1 (Chandra-Shekara et al., 2004). Interestingly, EDS1 was shown to be a direct target of *At*WRKY40. *EDS1* transcripts accumulate, after pathogen challenge, in the *Atwrky18 Atwrky40* mutant background to higher levels than in wild-type (Panday et al., 2010). Thus, putative de-repression of *At*WRKY18 and *At*WRKY40 by interaction with HRT might act on downstream components of TCV resistance, such as EDS1. The second *RPP8* locus-encoded viral resistance specificity, mediated by RCY1, was shown to be independent of EDS1 (Takahashi et al., 2002). Therefore, RCY1 resistance towards cucumber mosaic virus (CMV) employs a pathway different from EDS1. This might also explain why RCY1 apparently seems not to associate with *At*WRKY18 and *At*WRKY40. EDS1 is required for HRT-mediated resistance to TCV and together with SA it is required for the induction of a HR at the site of viral infection (Chandra-Shekara et al., 2004; Venugopal et al., 2009). A member of the GHKL ATPase/kinase superfamily, CRT1, was shown to associate with HRT and other R proteins like Rx, RPS2 and SSI4 (Kang et al., 2008) and these interactions are disrupted when these proteins become activated (Kang et al., 2010). Mutation and silencing experiments revealed CRT1 to interfere with both, HRT-mediated HR and resistance. This

implicates CRT1 to function at an early point in HRT-mediated resistance before the branch leading to HR and pathogen restriction splits (Kang et al., 2008). In turn, these results suggest a later role for *At*WRKY18 and *At*WRKY40, acting in the EDS1-dependent branch of HRT-mediated viral immunity. Interestingly, high SA levels led to a PAD4-dependent up regulation of *HRT* expression and to the ability to overcome the repressive effect of RRT in TCV resistance (Chandra-Shekara et al., 2004).

Another GHKL family member is the cytosolic molecular chaperon HSP90, which is required for resistance mediated by the R proteins N, RPS2, RPS4 and RPM1 (Hubert et al., 2003; Takahashi et al., 2003; Liu et al., 2004b). HSP90 associates with RAR1 and SGT1b, which in turn are required for resistance specificities mediated by a variety of different R proteins, including barley MLA (Shen et al., 2003; Bieri et al., 2004; Liu et al., 2004a). Therefore such interactions were believed to be required for the formation of proper R protein-containing signalling complexes (Liu et al., 2004b) and CRT1 might act in the same way on HRT (Kang et al., 2008). HRT localizes to the plasma membrane (Jeong et al., 2010) and CRT1 was found in endosome-like vesicles suggesting a role for this subcellular compartment in R protein signalling and/or activation (Kang et al., 2010). *At*WRKY18 and *At*WRKY40 were shown to localize mainly to the nucleus (Xu et al., 2006). Several studies have shown that activated R proteins, like MLA10, N and RPS4, can enter the nucleus (Shen and Schulze-Lefert, 2007) Therefore, HRT activation and potential translocation might depend on CRT1, whereas at least parts of the R protein-mediated downstream signalling probably depends on the nuclear association with *At*WRKY18 and *At*WRKY40.

Another model is provided by the recent findings of (Shang et al., 2010). They show that rising ABA concentrations stimulate the association of *At*WRKY40 with the cytosolic fraction of the chloroplast membrane-residing magnesium-protoporphyrin IX chelatase H subunit (CHLH/ABAR). Extrachloroplastic ABA levels increase up to five-fold in the interaction of tobacco with five different strains of tobacco mosaic virus (Whenham et al., 1985). A more recent study shows that mutants deficient in ABA sensing or synthesis were more susceptible towards the soil-borne oomycete pathogen *Pythium irregulare* and ABA levels were elevated after pathogen challenge in the wild-type (Adie et al., 2007). Together these data provide an intriguing though still highly speculative alternative model of how WRKY factors can associate with HRT outside of the nucleus.

Notably, a still not fully characterized line of the *Atwrky18 Atwrky40* mutant expressing barley *Hv*WRKY1 under control of the 35S CaMV promoter is phenotypically more susceptible than the *Atwrky18 Atwrky40* double mutant to both, *G. orontii* and TCV (data not

shown; Preedep Kachroo, personal communication). Detailed analysis of the contribution of *At*WRKY18 and *At*WRKY40 to HRT-mediated TCV resistance has to be part of future analysis and requires the generation of new, carefully selected, genetic material.

### 1.3.4  EDS1 is required for *Atwrky18 Atwrky40*-mediated pre- and post-invasive *G. orontii* resistance

I identified the R protein HRT as potential interaction partner of *At*WRKY18 and *At*WRKY40 (Fig. 2.5). This links both WRKY factors with EDS1-dependent TCV resistance. *At*WRKY40 targets W-box containing sequences in the EDS1 promoter (Pandey et al., in press). A role of the immune regulator EDS1 in *Atwrky18 Atwrky40*-mediated resistance was substantiated by my analysis of newly generated *Atwrky18 Atwrky40 eds1* triple mutants with respect to early (48h) and late (8d) infection phenotypes with *G. orontii*. Consistent with the previously reported role of EDS1 in basal defence against virulent (host-adapted) biotrophic and hemi-biotrophic pathogens (Falk et al., 1999; Feys et al., 2001; Lipka et al., 2005), *eds1 Atwrky18 Atwrky40* triple mutants were found to restore wild-type-like host cell entry rates (48 h) after pathogen challenge (Fig. 1.6a). EDS1 influences transcriptional reprogramming in *Arabidopsis* plants challenged with avirulent *Pst DC3000* AvrRps4 (Bartsch et al., 2006) and such EDS1-dependent transcriptional reprogramming was shown to require pathogen-induced enrichment of the nuclear pool of EDS1 (Garcia et al., 2010). Transcript levels of EDS1-dependent up-regulated genes like *EDS1*, *PAD4* and *FMO1* (Bartsch et al., 2006; García et al., 2010) were also found to be elevated at early time points (4-8 h) following *G. orontii* infection, in resistant *Atwrky18 Atwrky40* plants compared to the susceptible wild-type (Pandey et al., in press). Therefore, it would be interesting to monitor EDS1 nuclear and cytoplasmic steady state levels in wild-type and *Atwrky18 Atwrky40* mutants. Elevated *EDS1* transcript levels were found to be transient in the *Atwrky18 Atwrky40* background and resembled those of the wild-type after 24 hpi (Pandey and Mann, 2000). Thus, transcriptional up-regulation of *EDS1*, prior to or coincident with the fungal penetration attempts in *Atwrky18 Atwrky40* mutants (Pandey et al., in press) is likely to contribute to *Atwrky18 Atwrky40*-mediated pre-invasive resistance.

At later infection stages (8 dpi) wild-type-like susceptibility was restored on *Atwrky18 Atwrky40 eds1* mutants infected with *G.orontii* (Fig. 1.6b) indicating an additional requirement for EDS1 in the establishment and/or maintenance of *Atwrky18 Atwrky40*-mediated resistance towards the adapted powdery mildew. These early and late EDS1-dependent responses might represent two different processes, since post-invasive resistance can be

separated from pre-invasive fungal host cell entry restriction in the *Atwrky18 Atwrky40* background (see below). EDS1 and its sequence-related interacting partner PAD4 act upstream of SA in basal defence as well as in ETI as part of a positive feedback loop, since SA can rescue defence gene activation in *eds1* and *pad4* mutants and induces *EDS1* expression (Vlot et al., 2009). *AtWRKY18* and *AtWRKY40* transcription levels were found to be induced in wild-type plants upon treatment with the endogenous phytohormone signalling molecules SA and methyl jasmonate (MeJA) as well as after treatment with the bacterial MAMP flg22 within 4 h (Pandey et al., in press). In contrast *G. orontii*-induced early accumulation of *AtWRKY18* and *AtWRKY40* transcripts were reported to be independent of *isochorismate synthase 1* (Chandran et al., 2009), which is responsible for approximately 90 % of the pathogen- and UV-induced host SA production (Wildermuth et al., 2001; Garcion et al., 2008). In contrast, accumulation of transcripts for both WRKY factors at later infection stages was found to be *ICS1* dependent (Chandran et al., 2009). This may implicate the transcriptional induction of *AtWRKY18* and *AtWRKY40* to depend on differentially derived SA pools. Therefore, ICS2- and phenylalanine ammonia lyase (PAL)-derived SA (Garcion et al., 2008)(Garcoin et al., 2008; Huang et al., 2010) might contribute to the early, *ICS1*-independent, transcriptional activation of *AtWRKY18* and *AtWRKY40* in the *G. orontii* interaction. *At*WRKY18 and *At*WRKY40 positively affect JA signalling (Wang et al., 2008) and the study by Pandey et al. (in press) suggests *At*WRKY18 and *At*WRKY40 to affect JA signalling by partly suppressing the expression of JAZ repressors. Thus, in At*wrky18 Atwrky40* pre- and post-invasive resistance towards *G. orontii* might be influenced through an altered balance in the SA and JA signalling pathways. This in turn could affect *At*WRKY40-regulated EDS1-dependent processes. Interestingly, EDS1 and SA were recently reported to fulfill redundant functions in HRT-mediated HR formation and *PR1* expression (Venugopal et al., 2009). However, *eds1* deficiency alone, in the *Atwrky18 Atwrky40* background, is sufficient to restore both pre- and post-invasive wild-type-like susceptibility towards the adapted powdery mildew *G. orontii*.

### 1.3.5 *PEN1* contributes to post- but not to pre-invasive *G. orontii* resistance in *Atwrky18 Atwrky40* mutant plants

The plasma membrane-resident syntaxin PEN1 acts together with the adaptor protein SNAP33 and the endomembrane-anchored VAMP721/722 in a vesicle-mediated secretory defence pathway (Collins et al., 2003; Kwon et al., 2008). PEN1 focal accumulation in papillae, formed underneath fungal entry sites of adapted and non-adapted powdery mildews but not in papillae triggered by the entry attempts of other ascomycetes or the oomycete

pathogen *H. arabidopsidis* (Assaad et al., 2004; Bhat et al., 2005; Shimada et al., 2006; Meyer et al., 2009). Nevertheless, restriction of invasive growth by PEN1 has been shown, so far, only for the non-adapted powdery mildews *Bgh* and *E. pisi* (Collins et al., 2003; Lipka et al., 2005). Thus, the mechanism underlying PEN1-mediated pre-invasive resistance appears to be rather specific for powdery mildew.

Since fungal entry-rates were unaffected in *Atwrky18 Atwrky40 pen1* mutant plants (Fig. 1.6a), *Atwrky18 Atwrky40*-mediated penetration resistance, most likely, utilizes a resistance pathway different from *PEN1*. However, at later infection stages (8 dpi) resistance in *Atwrky18 Atwrky40 pen1* plants was associated with the appearance of large necrotic leaf areas that were absent in resistant *Atwrky18 Atwrky40* plants (Fig. 1.6b). Although the papillary accumulation of PEN1 seems to be powdery mildew specific, post-invasive recruitment of PEN1 to haustorial encasements has been shown for other haustorium-forming non-adapted pathogens (Meyer et al., 2009). Post-penetration resistance is often associated with the appearance of an HR at the side of infection. Consistent with this, infections of non-adapted *Bgh* and *E. pisi* under conditions that enable them to overcome pre-invasive resistance and progress to form haustoria strongly trigger this form of hypersensitive cell death. Posthaustorial powdery mildew resistance was show to depend on genes including *EDS1*, *PAD4* and *SAG101* (Lipka et al., 2005; Stein et al., 2006). EDS1 is required for the promotion of leaf cell death (Rusterucci et al., 2001) and contributes to basal defence and systemic resistance (Vlot et al., 2008; Attaran et al., 2009). NUT7 was shown to exert negative regulation of EDS1 signalling (Bartsch et al., 2006) and both genes were differentially expressed in naïve and infected *Atwrky18 Atwrk40* mutant plants (Pandey et al., in press). Thus, the appearance of large necrotic areas in *Atwrky18 Atwrky40 pen1* mutant plants might be the consequence of altered basal and/or systemic defence program(s). Currently, the molecular basis of PEN1 action in contributing to *Atwrky18 Atwrky40*-mediated resistance remains elusive.

### 1.3.6 *Atwrky18 Atwrky40*-mediated pre-invasive resistance towards *G. orontii* requires CYP81F2, PEN2 and PAD3

Beside the rather powdery mildew-specific function of PEN1 in anti-microbial defence, the atypical myrosinase PEN2 together with the P450 enzyme CYP81F2 mediate broad spectrum anti-fungal defence. This second pathway depends on the breakdown of the CYP81F2-derived secondary metabolite 4MI3G by PEN2 in order to restrict fungal entry (Lipka et al., 2005; Bednarek et al., 2009). The loss of penetration resistance in *Atwrky18*

*Atwrky40 cyp81f2* and *Atwrky18 Atwrky40 pen2* mutants implicates a requirement of 4MI3G synthesis and/or hydrolysis in *wrky18 wrky40*-mediated pre-invasive resistance. Consistent with this, 4MI3G levels were found to be elevated in *Atwrky18 Atwrky40* mutant plants within hours post infection (Moritz Schön, personal communication). In *pen2* mutants fungal entry-rates and endogenous levels of the phytoalexin camalexin were elevated after infection with the non-adapted powdery mildews *Bgh* and *E.pisi*. However, in camalexin deficient *pad3* plants fungal entry-rates appeared wild-type-like. Therefore, 4MI3G hydrolysis and camalexin are thought to act sequentially in plant defence (Nürnberger and Lipka, 2005; Bednarek et al., 2009). Similar conclusions were drawn from *Arabidopsis* mutant studies employing the oomycete pathogen *Phythophthora brassicae* (Schlaeppi et al., 2010). Nevertheless, camalexin seems to be required for *Atwrky18 Atwrky40*-dependent fungal entry resistance, since the *pad3* mutant restored wild-type-like fungal entry-rates in the *Atwrky18 Atwky40* background (Fig. 1.6a). Notably, already uninfected *Atwrky18 Atwrky40* plants accumulate higher camalexin levels than the wild-type (Pandey et al., in press). Thus, deregulation in timing and magnitude of camalexin accumulation may at least in part be the molecular basis for the pre-invasive resistance observed in *Atwrky18 Atwrky40* double mutants.

The mutant analyses presented in this work provide genetic evidence for the requirement of the tryptophan-derived secondary metabolites, camalexin and 4MI3G, in *Atwrky18 Atwrky40*-mediated *G. orontii* host cell-entry restriction. Microarray analysis identified the transcription factor MYC2 as a negative regulator of tryptophan and indole glucosinolate (IG) biosynthesis during JA signalling. MeJA treated *myc2* plants accumulate higher amounts of 4MI3G and increased transcript levels of *MYB51* and *PAD3* (Dombrecht et al., 2007). Furthermore, MYC2 positively affects JA biosynthesis and the expression of genes encoding JAZ proteins (Lorenzo et al., 2004; Chini et al., 2007; Dombrecht et al., 2007). JAZ repressors in turn have been shown to target the MYC2 transcription factor in a negative feedback loop (Chini et al., 2007). *At*WRKY40 binds to W-box containing regions in the *JAZ8* promoter and transcripts of several JAZ family members accumulate in uninfected *Atwrky18 Atwrky40* mutants to higher levels than in wild-type. Notably, transcripts of *ASA1*, the rate-limiting enzyme in tryptophan biosynthesis, also accumulate to higher amounts in naïve *Atwrky18 Atwrky40* plants (Pandey et al., in press). Thus, stimulation of tryptophan-derived secondary metabolites through JAZ repressor-dependent inhibition of MYC2 might provide a testable working model by which enhanced fungal entry resistance in *Atwrky18 Atwrky40* mutant plants is achieved.

### 1.3.7 Post-invasive *Atwrky18 Atwrky40*-mediated *G. orontii* resistance elucidates a novel role of CYP81F2

Host cell entry restriction during the interaction of *G. orontii* with *Arabidopsis Atwrky18 Atwrky40* mutants appears to be rather weak (~60 % of fungal spores still enter the host tissue). Therefore, this host defence mechanism is insufficient to explain the explicit post-invasive resistance phenotype observed at later time points (8 dpi). Surprisingly, CYP81F2 was found to be required for *Atwrky18 Atwrky40*-mediated post-invasive resistance (Fig. 1.6b). Since *Atwrky18 Atwrky40 pen2* triple mutants were unaffected in persistence of *G. orontii* growth inhibition, post-invasive resistance appears independent of PEN2 function(s). In turn this implicates a so far unknown role of CYP81F2 or its product 4MI3G in plant defence. PEN2-dependent 4MI3G breakdown products have been suggested as possible signalling molecules in *flg22*-triggered callose deposition (Clay et al., 2009). Nevertheless such a scenario would depend on a so far unknown *PEN2* homologue in *Atwrky18 Atwrky40*-mediated powdery mildew resistance. The *Arabidopsis* genome encodes seven *PEN2*-like family 1 glycosyl hydrolases. The PEN2-related enzyme PYK10 was shown to restrict colonization by the soil-bourne fungus *Piriformospora indica* (Sherameti et al., 2008). However, PYK10 is a root specific protein. Alternatively, CYP81F2 compartmentation and/or existence of additional substrates might facilitate *PEN2*-independent but *CYP81F2*-mediated resistance in *Atwrky18 Atwrky40* double mutants.

### 1.3.8 The MLA-CC domain forms a homo-dimer

Self-association of NBS-LRR proteins, including their N-terminal and/or central NB-ARC domain, has been described in vertebrates (Danot et al., 2009; Qi et al., 2010). In plants, the immune sensors N, PRF and RPS5 have been implicated in forming homo-oligomers through self-association of their N-terminal domains (Mestre and Baulcombe, 2006; Ade et al., 2007; Gutierrez et al., 2010). The recently resolved crystal structure of the barley MLA CC domain identified this R protein as well to homo-dimerize through its N-terminal domain (Fig. 1.7b; Maekawa et al., under review in Cell Host & Microbe). The anti-parallel association of two MLA-CC monomers gives rise to a dimer with remarkable different electrostatic potentials for the opposing sides of the dimer (Maekawa et al., under review in Cell Host & Microbe). Interestingly, the "hinge" region between helix α1a and helix α1b, for which no electron density was found (Fig. 1.7), locates exactly opposite of the two most hydrophobic residues at the 3rd and 4th position within the EDVID motif (Rairdan et al. 2008). A molecular flexibility (MD) simulation of the CC dimer shows that the flexibility of the

"hinge" leaves both EDVID motifs largely exposed on the same side of the dimer structure (Maekawa et al., under review in Cell Host & Microbe). The 3rd and 4th residues of the EDVID motif are orientated into the dimeric structure and V80, at the 4th position, contributes to the hydrophobic interactions within the four helix bundle, whereas the 1st, 2nd and 5th positions provide the negative charges at the surface (Maekawa et al., under review in Cell Host & Microbe).

RPM1 confers resistance towards the bacterial pathogen *Pseudomaonas syringae* (Grant et al., 1995) and its CC domain shows 48,5 % sequence similarity and matching structural profiles to that of MLA (Maekawa et al., under review in Cell Host & Microbe). Maekawa et al. (under review in Cell Host & Microbe) therefore used the RPM1 CC domain for structural modeling. They identified the surface electrostatic properties to be conserved between both CC domains, especially in the region encompassing the EDVID motif. Thus, although not known for RPM1, these data indicate that a subset of CC domain-possessing NBS-LRR R proteins can form homo-dimers through their N-terminal domain. Beyond this, the data of Markawa et al. (under review in Cell Host & Microbe) suggest the "hinge" region together with the EDVID motif to connect inter- with intramolecular interactions within the MLA dimer, which could facilitate effector-triggered conformational changes, possibly allowing ATP loading to the central NB-ARC domain and/or subsequent interactions with downstream partners such as WRKY factors.

Both yeast 2-hybrid and co-IP analysis confirmed the dimerization of MLA-CC (Fig. 1.9; Maekawa et al., under review in Cell Host & Microbe). The yeast studies further identified three amino acids (I33, L36 and M43) of MLA-CC that are required for dimerization (Fig. 1.10). Maekawa et al. (under review in Cell Host & Microbe) showed in transient expression assays that the MLA10 wild-type CC domain alone is capable of inducing cell death, whereas the substitution variants I33E, L36E and M43E, which fail to dimerize, do not. Therefore the authors suggest the CC dimer as a module for cell death induction. So far several N-terminal TIR domains of NBS-LRR R proteins have been shown to induce effector-independent cell death (Frost et al., 2004; Swiderski et al., 2009). Recently, Krasileva et al. (2010) described that induction of HR by the TIR domain of RPP1 was dependent on the dimerization competence of its fusion partner GFP. MLA10 interacts through its CC domain located in helix α1 with the C-terminal domains of *Hv*WRKY1 and *Hv*WRKY2 upon effector stimulation (Shen et al., 2007; Fig. 1.2; Fig. 1.3). Both WRKY factors belong to a subgroup of WRKY transcription factors that can form homo- and hetero-dimers (Xu et al., 2006). Whether MLA10 interacts with these WRKY factors as a mono- or as a dimer remains to be tested. Helix α1, constituting the minimal portion of MLA10 required for WRKY interaction, did not

44

dimerize (Fig. 1.9) and was not sufficient to trigger cell death (Maekawa et al., under review in Cell Host and Microbe). In contrast to the self-association analysis of helix α1, all tested MLA-CC substitution variants retained reduced association abilities towards *Hv*WRKY1 in yeast (Fig. 1.11). These retained weak associations might be promoted by the yeast system itself, perhaps by a yeast bridging protein that forces the interaction partners together. MLA10 helix α1 appears to expose the surface relevant for the interaction with the WRKY factor but most likely lacks the regulatory parts that control this interaction *in vivo*. In any case, the MLA10-CC variant L18E was identified as the only targeted substitution that retained a wild-type-like *Hv*WRKY1 interaction phenotype and, together with the natural occurring variant G37R, wild-type-like resistance activity (Maekawa et al., under review in Cell Host and Microbe). Therefore, it is likely that effector triggered conformational changes of the MLA dimer induce proximity to distinct WRKY oligomers for induction of downstream signalling.

# Chapter II

**Dual function of Arabidopsis Glucan Synthase-Like genes *GSL8* and *GSL10* in male gametophyte development and plant growth**

Armin Töller, Lynette Brownfield, Christina Neu, David Twell and Paul Schulze-Lefert

**Contributions:**

**Figures, tables and corresponding experiments have been generated and performed by the authors as indicated below:**

Figure 1: Armin Töller; Table 1: Armin Töller; Table 2: Armin Töller; Figure 2: Armin Töller; Figure 3: Lynette Brownfield; Figure 4a-c: Armin Töller; Figure 4d: Lynette Brownfield; Figure 5: Lynette Brownfield; Figure 6: Lynette Brownflield; Figure 7: Lynette Brownfield Figure 8: Armin Töller; Table 3: Armin Töller

## 2.1 Introduction

Callose is a linear 1,3-ß-glucan polymer with some 1,6 branches that is widespread in cell walls of higher plants (Stone and Clarke, 1992). Callose deposits are formed during normal plant growth and development in sporophytic tissues including root hairs and sieve plates of dormant phloem, at plasmodesmata and as a transitory component at the cell plate in dividing cells as well as in male and female gametophytes (Stone and Clarke, 1992; Samuels et al., 1995). Callose is also rapidly deposited in response to wounding or pathogen challenge (Stone and Clarke, 1992).

Callose is an important structural component in male gametophyte development being deposited at several stages (Stone and Clarke, 1992; McCormick, 1993). Within the anther locule the pollen mother cells are surrounded by callose before entry into meiosis. Following meiosis callose is also deposited between the individual microspores during cytokinesis. This callose is important for exine patterning and is transient, being degraded to enable individual microspore release. The microspores then undergo an asymmetric division forming a large vegetative cell and a smaller generative cell, with callose forming a prominent, but transient cell wall that separates the two cells (Park and Twell, 2001). The generative cell migrates into the vegetative cytoplasm where it undergoes a further mitotic division to produce two sperm cells. After pollen germination the sperm cells are delivered to the ovule by the pollen tube in which callose forms a major component of the cell wall and the plugs that form along the length of the tube (Li et al., 1997; Ferguson et al., 1998; Nishikawa et al., 2005).

The highly impermeable 1,3-$\beta$-glucan polymer is also found in yeast and filamentous fungi, where it represents a major component of the cell wall. Formation of 1,3-$\beta$-glucan in *Saccharomyces cerevisiae* is dependent on the large partially functionally redundant and sequence-related *FKS1/FKS2* genes that encode integral plasma membrane proteins that appear to serve as substrate-binding catalytic subunit in heteromeric callose synthase complexes (Patel et al., 1994; Mazur et al., 1995; Mazur and Baginsky, 1996; Schimoler-O'Rourke et al., 2003). Homologs of fungal *FKS* genes are found in higher plants and compose a family of 12 glucan synthase-like (*GSL*) genes in *Arabidopsis* (Saxena and Brown, 2000; Woo et al., 2001). Molecular and biochemical evidence supports a role for GSL proteins in callose synthesis (Cui et al., 2001; Woo et al., 2001; Ostergaard et al., 2002; Li et al., 2003; Brownfield et al., 2007) and recessive mutations in few tested *Arabidopsis GSL* genes abolish either specific developmentally regulated or stress-induced callose deposits (Jacobs et al., 2003; Nishimura et al., 2003; Dong et al., 2005; Enns et al., 2005; Nishikawa et al., 2005) indicating potential functional diversification.

GSL5/PMR4 has been shown to direct the synthesis of wound- and pathogen-inducible callose in sporophytic tissue (Jacobs et al., 2003; Dong et al., 2005). In pollen development, GSL5 acts together with GSL1 where it is required for the formation of the callose wall that separates the microspores of the tetrad (Enns et al., 2005). Absence of *GSL5* and *GSL1* renders pollen infertile, demonstrating that the same gene family member can have unique as well as overlapping functions with another *GSL* family member in different biological processes. *GSL2* acts during pollen development and is essential for the formation of the callose wall surrounding pollen mother cells (Dong et al., 2005) and also contributes to the callose deposited in the wall and plugs of the growing pollen tube (Nishikawa et al., 2005).

To test the hypothesis that the proliferation of *GSL* genes across the Arabidopsis genome reflects functional diversification of family members, we isolated T-DNA insertion mutants of *GSL* genes whose biological functions are unknown. Our failure to recover homozygous mutant plants for two independent T-DNA insertion alleles for *GSL8* (*gsl8*-1 and *gsl8*-2) and *GSL10* (*gsl10*-1 and *gsl10*-2) and the observed pollen developmental defects in all mutants demonstrate essential male gametophytic functions for the respective wild-type genes. Moreover, transgenic lines expressing 35S promoter driven gene-specific dsRNAi constructs for *GSL8* or *GSL10* exhibited a dwarfed growth habit, thereby revealing dual and independent functions of both genes in gametophyte and sporophyte development. Our findings suggest for the first time that plant GSL family members might exert indirect regulatory functions through interactions with other proteins rather than through their catalytic activity alone.

## 2.2 Results

### 2.2.1 *GSL8* and *GSL10* have a gametophytic function

We isolated for each of the highly sequence-related *AtGSL8* (At2g36850) and *AtGSL10* (At3g07160) Glucan Synthase-Like family members two independent T-DNA insertion lines (Fig. 2.1). T-DNA lines SALK 111094 and GABI 851C04 contain an insertion in the *GSL8* coding region close to its 5' end and were named *gsl8*-1 and *gsl8*-2, respectively. T-DNA lines GABI 038F11 and GABI 054E08 contain an insertion in the *GSL10* coding region and were named *gsl10*-1 and *gsl10*-2, respectively. DNA isolated from selfed progeny of the hemizygous T-DNA lines was examined by PCR analysis using T-DNA left border and gene-specific PCR primers to identify homozygous insertion lines. We found among progeny of each of the four tested insertion lines only wild type or hemizygous T-DNA lines with a segregation ratio of about 1:1 (Tab. 2.1). There were no recognizable morphological differences between wild type and hemizygous *gsl8* or *gsl10* plants. The absence of homozygous T-DNA containing progeny and the observed distorted segregation ratio of wild type and hemizygous T-DNA plants provided the first evidence that homozygous *gsl8* and *gsl10* mutants could not be recovered due to essential gametophytic functions of the respective wild-type genes.
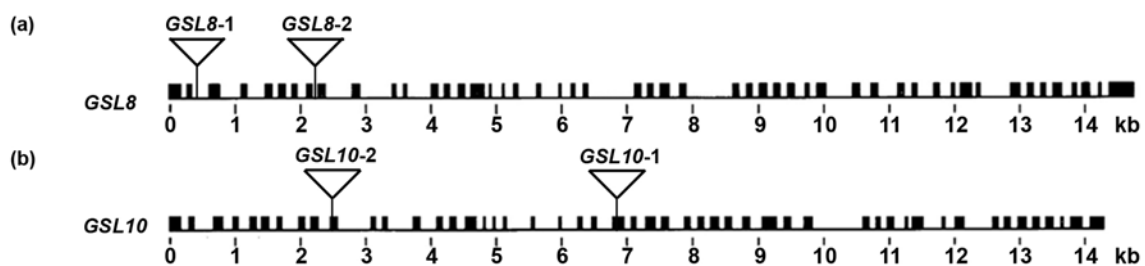


**Figure 2.1: Scheme of *GSL8* and *GSL10* gene structures.**
Gene structures of (a) *GSL8* and (b) *GSL10*. Black boxes represent exons and lines indicate introns. Triangles mark the T-DNA insertion sites of the indicated *gsl8* and *gsl10* mutant alleles.

**Table 2.1:** T-DNA segregation in progeny of selfed *GSL8/gsl8* and *GSL10/gsl10* mutant lines.

| | T-DNA Line | n plants tested | % plants heterozygous | % plants wild-type |
|---|---|---|---|---|
| *GSL8/gsl8*-2 | GK_851C04 | 76 | 63,2 | 36,8 |
| *GSL8/gsl8*-1 | SALK_111094 | 72 | 54,2 | 45,8 |
| *GSL10/gsl10*-1 | GK_038F11 | 86 | 48,8 | 51,2 |
| *GSL10/gsl10*-2 | GK_054E08 | 78 | 53,8 | 46,2 |

51

### 2.2.2  *GSL8* and *GSL10* T-DNA insertions lead to pollen sterility

Since callose deposition is known to occur at multiple stages during male gametophyte development, we investigated pollen development in each hemizygous *gsl8* and *gsl10* T-DNA line. Light microscopic analysis of mature pollen from *GSL8/gsl8* plants revealed over 40% collapsed pollen while pollen from *GSL10/gsl10* plants contained nearly 40% aberrant pollen, being either collapsed or mis-shapen (Tab. 2.2).  In contrast, only 1-2% aberrant pollen was found in *GSL8* or *GSL10* wild-type siblings and the increased frequency of aberrant pollen co-segregated with the respective T-DNA insertions.  Closer examination of the collapsed pollen phenotype by scanning electron microscopy revealed a shrunken appearance of pollen grains, although the characteristic reticulate exine architecture of wild-type pollen was clearly visible in the collapsed grains (Fig. 2.2).  Thus both GSL8 and GSL10 are required for normal pollen development.

**Table 2.2:** Light microscopic analyses of mature pollen from *GSL8/gsl8* and *GSL10/gsl10* lines.

| Line | total pollen | collapsed pollen | % collapsed | aberrant pollen | % aberrant |
|---|---|---|---|---|---|
| *GSL8/gsl8*-1 | 429 | 201 | 46.9 | 0 | 0 |
| *GSL8/gsl8*-2 | 428 | 188 | 43.9 | 0 | 0 |
| GSL10/gsl10-1 | 562 | 50 | 8.4 | 171 | 30.4 |
| GSL10/gsl10-2 | 410 | 98 | 23.9 | 63 | 15.4 |

We investigated the expression of *GSL8* and *GSL10* during pollen development using RT-PCR with RNA isolated from spores at different developmental stages (Fig. 2.3).  Both *GSL8* and *GSL10* are expressed throughout pollen development, with *GSL8* being most strongly expressed in bicellular and tricellular pollen and *GSL10* showing peak expression in bicellular pollen.  Since *GSL8* and *GSL10* are both expressed throughout pollen development, and mature pollen from *GSL8/gsl8* and *GSL10/gsl10* is aberrant, we conducted a detailed analysis of mutant pollen development to determine the role of *GSL8* and *GSL10* in male gametogenesis.
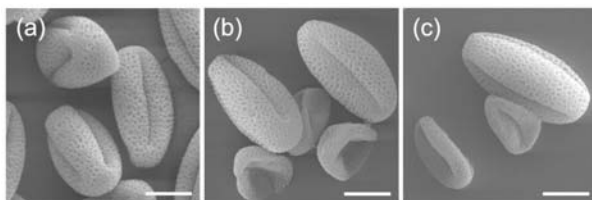


**Figure 2.2: Aberrant *gsl8* and *gsl10* pollen phenotypes.**
(a-c) Scanning electron micrographs of pollen isolated from (a) wild type, (b) *GSL8/gsl8*-1, and (c) *GSL10/gsl10*-2 mutant plants. Approximately half of the pollen grains of all tested heterozygous mutant lines exhibit an aberrant pollen phenotype. Bar=10μm.
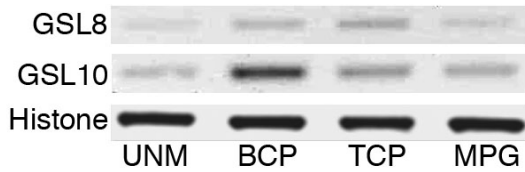
**Figure 2.3: Expression of *GSL8* and *GSL10* during pollen development.**
RT-PCR analysis of *GSL8* and *GSL10* transcripts in uninucleate microspores (UNM), bicellular pollen (BCP), tricellular pollen (TCP) and mature pollen grains (MPG). A histone gene is used as a control.

## 2.2.3  *GSL8* and *GSL10* are not required for microspore development

As extensive callose deposition is known to occur at the tetrad stage (McCormick, 1993) we visualized callose in the tetrads of the four hemizygous T-DNA insertion lines as well as wild-type tetrads by aniline blue staining. We failed to detect neither differences in callose deposition patterns nor in the shape of haploid microspores between tetrads from wild type and hemizygous *GSL8/gsl8* and *GSL10/gsl10* plants (Fig. 2.4a-c). This might indicate that *GSL8* and *GSL10* activities are redundant during tetrad formation and/or that both genes act gametophytically at a later stage of pollen development.
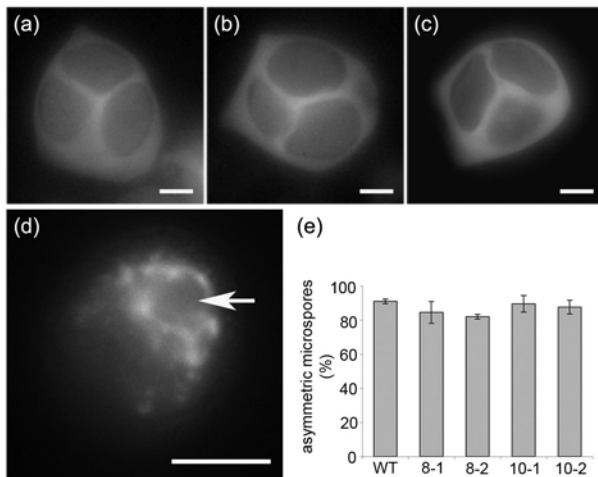


**Figure 2.4: Microspore development is not interrupted in *GSL8/gsl8*-1, and *GSL10/gsl10*-2 plants.** Isolated microspore tetrads of (a) wild type, (b) *GSL8/gsl8*-1 and (c) *GSL10/gsl10*-2 genotypes were stained with aniline blue. Callose deposition around and between microspores are indistinguishable in wild type and mutant lines. Bars=5µm. WT microspore with a polarized nucleus indicated with an arrow (d). Bar = 10 µm. Microspores from *GSL8/gsl8*-1 (8-1), *GSL8/gsl8*-2 (8-2), *GSL10/gsl10*-1 (10-1) and *GSL10/gsl10*-2 (10-2) become polarized to a similar level as WT (e).

Older microspores were isolated and nuclear DNA stained with DAPI. In buds containing free microspores all spores exhibited a single, brightly stained centrally located nucleus in both wild type and hemizygous T-DNA mutant lines (data not shown). During microspore development the nucleus migrates to the microspore wall before the asymmetric cell division, producing a highly polarized cell (Fig. 2.4d, arrow showing nucleus). In late microspore stage anthers from a wild type plant approximately 90% of microspores were polarized (Fig. 2.4e). Similarly in both *GSL8/gsl8* and *GSL10/gsl10* plants, over 80% of the microspores were

polarized (Fig. 2.4e), demonstrating that GSL8 or GSL10 deficient microspores can still establish polarity.

### 2.2.4 *GSL8* and *GSL10* exert essential functions associated with microspore division

Pollen was also examined after completion of the asymmetric microspore division at mid-bicellular stage when the generative cell had migrated into the vegetative cell cytoplasm (Fig. 2.5c). Only about half of the pollen from *GSL8/gsl8*-1 and *GSL8/gsl8*-2 plants was bicellular in comparison to almost 100 % of pollen from a wild type plant at this stage (Fig. 2.5a). Most of the remaining pollen had a single DAPI-staining nucleus, organelles that still stained with DAPI and were often slightly smaller and plasmolysed in comparison with bicellular pollen (Fig. 2.5c and d). Moreover nuclei were sometimes enlarged or displayed disordered chromatin structure. This aberrant pollen phenotypic class was termed 'mononuclear', and indicates that GSL8 is required for microspore entry into mitosis. There was also a small amount of pollen with two similar DAPI stained structures that resemble the vegetative nucleus with dispersed chromatin (Fig. 2.5c and e), indicating that these microspores had undergone mitosis but cytokinesis had been disrupted.

In contrast over 80% of pollen from the *GSL10/gsl10*-1 mutant resembled that of wild type pollen at mid-bicellular stage (Fig. 2.5a). Most of the remaining pollen was also bicellular, but rather than migrating into the vegetative cell cytoplasm the generative cell was positioned against the pollen wall, and was termed 'GC on wall' (Fig. 2.5f). Approximately half the pollen from *GSL10/gsl10*-2 plants was bicellular (Fig. 2.5a). Of the remaining pollen over half resembled *gsl8* pollen and was mononuclear, many contained two similar nuclei and in the rest the generative cell was against the wall (Fig. 2.5a). The mononuclear phenotype of *gsl10*-2 pollen indicates that like GSL8, GSL10 is also involved in entry into mitosis and the similar nuclei class suggest GSL10 is important for asymmetric division.

At later pollen stages all pollen was tricellular in wild type plants (Fig. 2.5b), consisting of the vegetative cell enclosing two sperm cells (Fig. 2.5g). Half the pollen from both *GSL8/gsl8-1* and *GSL8/gsl8-2* plants was tricellular (the *GSL8* portion of the pollen) while most of the remaining pollen had aborted (Fig. 2.5b). In aborted pollen, the pollen grains had collapsed and there was no or only residual DAPI staining (Fig. 2.5h). There were also small amounts of pollen that were still mononuclear or bicellular. This complementary decrease in the proportion of aberrantly stained mononuclear-like microspores and the associated

increase in the number of unstained and collapsed microspores likely reflect progressive cell death in *gsl8* mutant microspores.
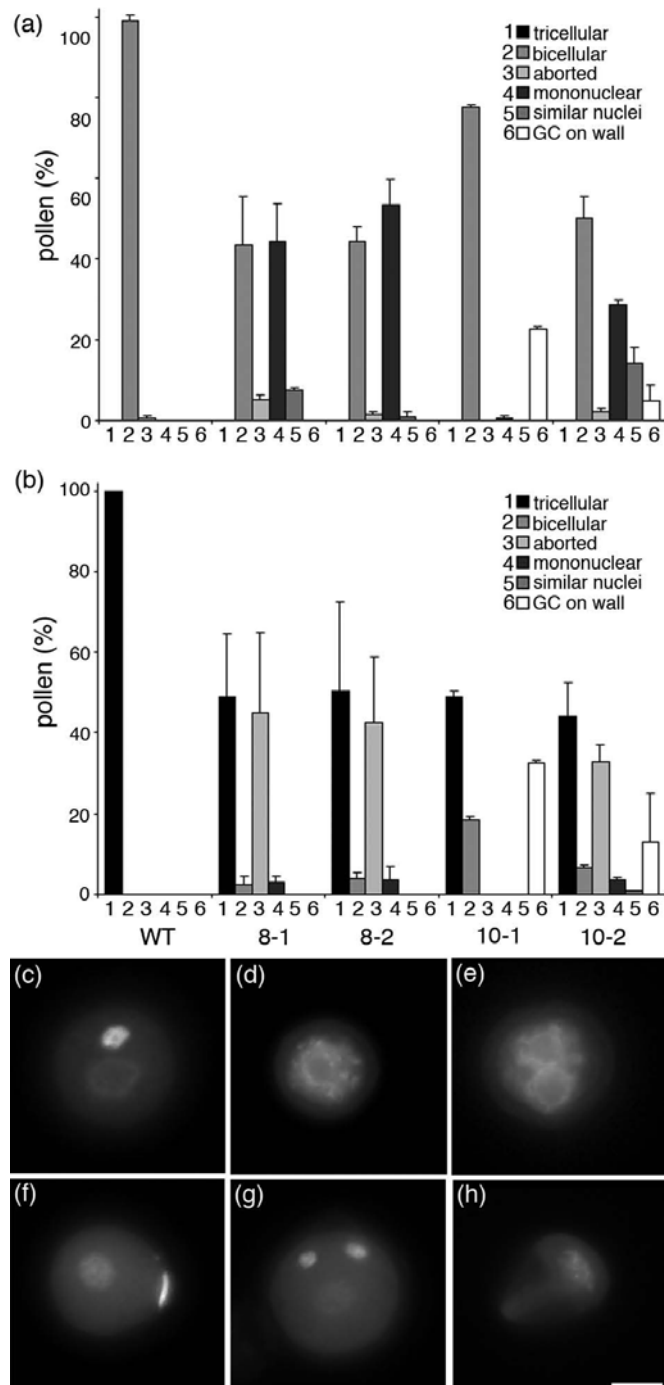


**Figure 2.5: Phenotypes of bicellular and tricellular pollen from *GSL8/gsl8*, and *GSL10/gsl10* plants.**
The phenotype of *GSL8/gsl8*-1 (8-1), *GSL8/gsl8*-2 (8-2), *GSL10/gsl10*-1 (10-1) and *GSL10/gsl10*-2 (10-2) pollen at mid bicellular stage (a) and tricellular stage (b) was analysed in pollen with DNA stained with DAPI. Pollen phenotypes observed are WT bicellular pollen (c), mononuclear pollen (d), pollen with 2 nuclei with a similar appearance (similar nuclei) (e), pollen with the generative cell stuck on the vegetative cell wall (GC on wall) (f), WT tricellular pollen (g) and aborted pollen (h). Bar = 10 µm.

Similarly, at tricellular pollen stage in *GSL10/gsl10*-1 and *GSL10/gsl10*-2 plants only 50% of the pollen was tricellular (Fig. 2.5b). The remaining pollen from *GSL10/gsl10*-1 was bicellular and in many cases the generative cell was tight against the wall (Fig. 2.5b). The amount of pollen with the generative cell against the wall was higher in the tricellular pollen than in the bicellular stage examined, presumably because at the bicellular stage the generative cell was often close to the wall but not noticeably flattened. Much of the mutant pollen from *GSL10/gsl10*-2 plants had aborted by the tricellular stage (Fig. 2.5b), and is likely to arise from pollen that was mononuclear or had two similar nuclei at bicellular stage. The remaining pollen was bicellular with the generative cell often tight against the wall, similar to that seen in *GSL10/gsl10*-1.

Collectively, these findings show that GSL8 is essential for microspore division as most *gsl8* microspores fail to enter mitosis and subsequently abort. In pollen from *GSL10/gsl10* some pollen also fails at mitosis entry (mainly in *GSL10/gsl10*-2), but a greater proportion of mutant pollen (mainly in *GSL10/gsl10*-1) passes through microspore division but shows phenotypes that may relate to incorrect cytokinesis. The differences observed between *gsl10*-1 and *gsl10*-2 may relate to allelic differences. As only 50% of the pollen from hemizygous plants for each of the four T-DNA lines becomes tricellular it appears that each line is fully penetrant and does not produce fertile pollen.

### 2.2.5  Aberrant callose synthesis and degradation in *gsl10* mutant pollen

As GSL proteins are involved in callose synthesis, pollen from *GSL8/gsl8* and *GSL10/gsl10* plants was further analysed by co-staining for callose with aniline blue and for DNA with DAPI. In wild-type pollen callose is transiently deposited after microspore mitosis between the newly formed generative and vegetative cell, and appears as a dome surrounding the generative cell (Fig. 2.6c and d). In early bicellular pollen this callosic dome can be detected in over 80% of pollen (Fig. 2.6a). By mid-bicellular pollen (2 buds older) virtually all aniline blue staining had disappeared reflecting degradation of the callose wall (Fig. 2.6b). This callose wall was not synthesized in aberrant *GSL8/gsl8* pollen that failed to enter pollen mitosis I (data not shown).  However, over 80% of early bicellular pollen from *GSL10/gsl10*-1 plants contained callose in a dome over the generative cell (Fig. 2.6a), indicating that these pollen grains can synthesize callose in a manner similar to wild type. The callose however appears to be more persistent as approximately 20% of pollen at the mid-bicellular stage in *GSL10/gsl10*-1 still contained an aniline blue-stained wall (Fig. 2.6b). The persistence of the callose wall therefore may interfere with the migration of the

generative cell, possibly leading to the generative cell being tightly stuck against the wall later in development.
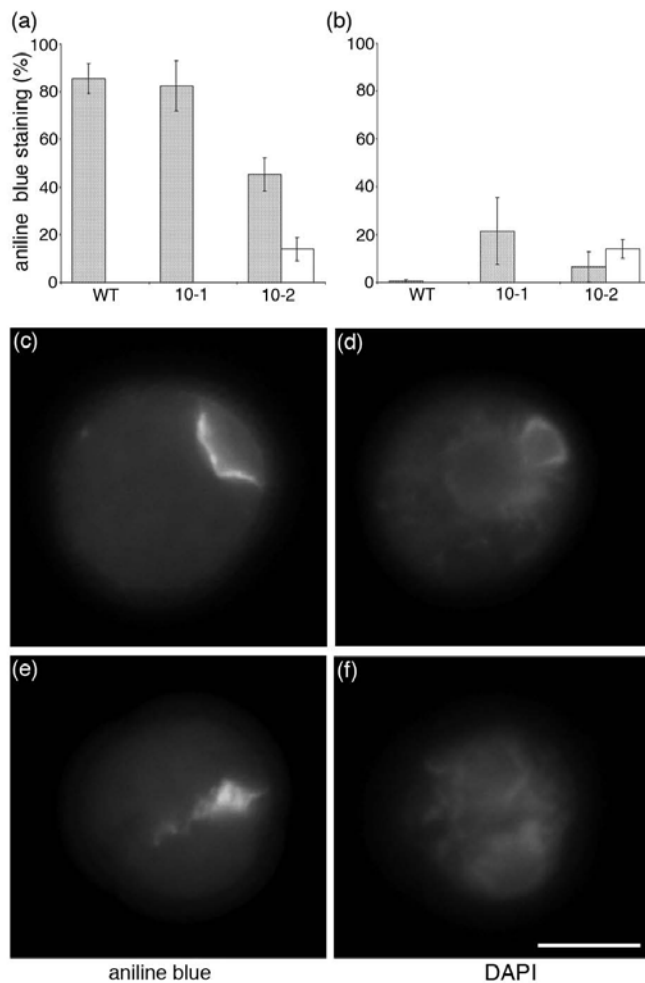


**Figure 2.6: Callose deposition in bicellular pollen from *GSL10/gsl10* plants.**
Pollen from early bicellular (a) and mid bicellular (b) stages were stained with aniline blue and DAPI. Shaded bars show the percentage of pollen with a WT callosic dome and empty bar indicates internal ectopic callose. In pollen from WT and *GSL10/gsl10*-1 plants the majority of pollen has a dome shaped callose wall (c) between the vegetative cell nucleus and the generative cell nucleus (d). In pollen from *GSL10/gsl10*-2 plants internal ectopic callose is sometimes observed (e), often between two nuclei with a similar appearance (f). Same pollen grains shown in (c) and (d) and in (e) and (f). Bar = 10 μm.

Aniline blue staining was also carried out on early bicellular pollen from *GSL10/gsl10*-2 plants. A callosic dome was observed in approximately 45% of early bicellular pollen (Fig. 2.6a), suggesting that many *gsl10*-2 pollen grains fail to make a wild type callosic wall. Ectopic callose was regularly observed (Fig. 2.6e). This callose was generally in a rough line, although not always complete, close to the centre of the pollen grain and often with regions where there appeared to be clumps of callose (Fig. 2.6e). This ectopic callose was often (27/29) in pollen grains which also had two similar nuclei and the callose was located

between the two nuclei (Fig. 2.6e and f). Ectopic callose was persistent in mid-bicellular pollen (Fig. 2.6b) and was still present in pollen with two similar nuclei (25/27). There was also a small amount of mid-bicellular pollen from *GSL10/gsl10*-2 plants with a callosic dome (Fig. 2.6b) similar to the persistence of aniline blue staining in *GSL10/gsl10*-1 pollen, suggesting some *gsl10*-2 pollen do make a callosic dome that persists and could also result in the generative cell marginalisation observed in tricellular stage pollen from these plants.


### 2.2.6  Transmission electron microscopy of pollen phenotype


To further analyse the phenotype of the mutant *gsl8* and *gsl10* pollen, buds containing early to mid bicellular pollen and buds containing tricellular pollen from *GSL8/gsl8* and *GSL10/gsl10* plants were examined by transmission electron microscopy. We observed two distinct classes of pollen from *GSL8/gsl8* plants in an anther locule containing early to mid bicellular pollen (Fig. 2.7a). A portion of pollen had dense cytoplasm including a generative and vegetative cell (Fig. 2.7b), similar to wild type pollen (Fig. 2.7e-h). The remaining pollen had less dense cytoplasm, disrupted cellular structure and a single, sometimes abnormally shaped nucleus (Fig. 2.7c and d). Such pollen grains were not seen in wild type and are likely to be the *gsl8* mutant pollen classified as mononuclear in Figure 5.

Unlike *GSL8/gsl8*, all pollen in a bicellular stage anther from *GSL10/gsl10*-1 had a density of cytoplasmic staining similar to the wild type (Fig. 2.7i and e). The *gsl10*-1 mutant pollen appears to often have a callose wall separating the generative and vegetative cell that, with aniline blue, appears similar to the wall in wild type pollen but persists (Fig. 2.6b). The ultrastructure of the wall in pollen from *GSL10/gsl10*-1 plants (Fig. 2.7 j-l) was compared to wild type pollen (Fig. 2.7 f-h). In wild type pollen the callosic wall is generally smooth and forms a dome around the generative cell (Fig. 2.7f). During the process of generative cell detachment the callosic wall becomes thinner in the central region with thickened stubs at junctions with the outer pollen grain wall, while the generative cell rounds up (Fig. 2.7 g and h). In some pollen from *GSL10/gsl10*-1 plants the wall separating the generative and vegetative cells was disturbed, being flattened rather than consistently dome-shaped and the wall was not always smooth and showed some invaginations (arrows Fig. 2.7 j and k). Also ectopic internal walls were observed that were not located between the generative and vegetative cells (Fig. 2.7l). Such ectopic walls may also have contributed to the number of persistent wild type-like wall seen with aniline blue staining (Fig. 2.6b).
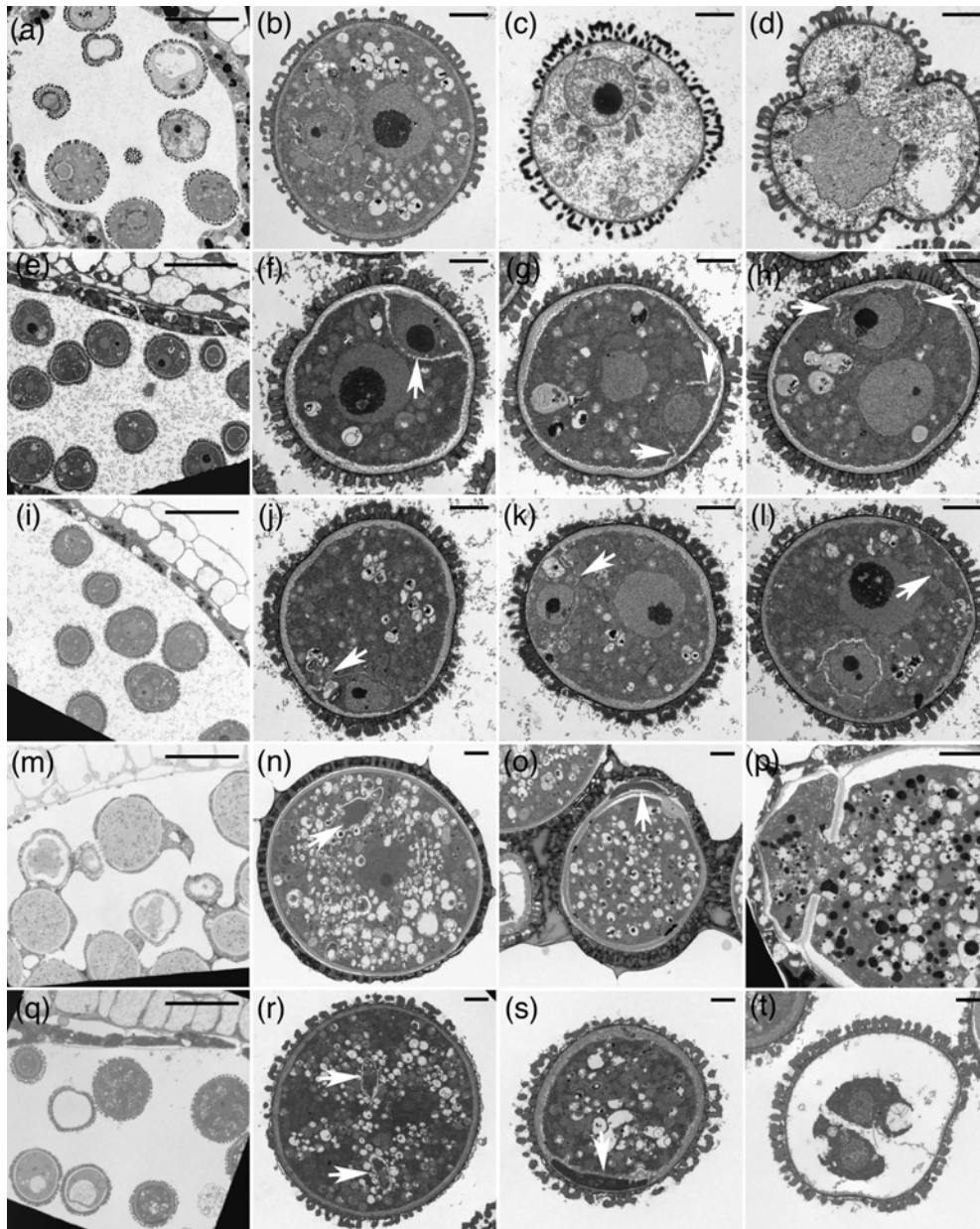
**Figure 2.7: TEM analysis of pollen phenotypes.**

Pollen from anthers at the early to mid bicellular stage from *GSL8/gsl8* plants (a-d), wild type plants (e-h) and *GSL10/gsl10-1* plants (i-l). Pollen from tricellular stage anthers from *GSL10/gsl10-1* (m-p) and *GSL10/gsl10-2* plants (q-t). Anther locule from *GSL8-1/gsl8-1* plant at the early to mid bicellular stage with light and dark staining of pollen (a), wild-type bicellular pollen grain from *GSL8/gls8*-1 bud (b), examples of reduced cytoplasmic density in *gsl8-1* (c) and gsl8-2 (d) pollen. Anther locule from a wildtype plant showing consistent cytoplasmic staining (e). Wildtype pollen grain with smooth domed shaped wall (arrow) between the newly divided generative and vegetative cells (f) and the generative cell migrating off the vegetative wall with rounded generative cells and callose wall stubs (arrow) (g and h). Anther locule from a *GSL10/gsl10-1* plant with consistent cytoplasmic staining (i). Examples of flattened and disrupted wall (arrow) between the generative and vegetative cells (j,k) and ectopic callose (arrow) in the *GSL10/gsl10-1* mutant (l). Anther locule from *GSL10/gsl10-1* (m) and *GSL10/gsl10-2* (q) showing wild type and mutant pollen. Wild type pollen grains at tricellular stage (n and r) sperm cells indicated by arrow, only one sperm cell visible in n. Examples of the generative cell stuck on wall phenotype (o and s), partial walls (p) and two similar nuclei (t).

Pollen was also observed from buds at the tricellular stage from *GSL10/gsl10*-1 (Fig. 2.7 m-p) and *GSL10/gsl10*-2 plants (Fig. 2.7 q-t). Pollen was not observed for the *gsl8* mutants because previous analysis had shown that the mutant pollen was aborted by this stage. Anther locules from *GSL10/gsl10*-1 and *GSL10/gsl10*-2 plants contained a mixture of pollen with dense cytoplasm filling the entire grain, and slightly smaller pollen grains where the cytoplasm was reduced or absent (Fig. 2.7m and q). The wild type pollen at this stage has dense cytoplasm with a vegetative nucleus and two sperm cells (Fig. 2.7n and r). In both mutants pollen grains with a marginalised, electron dense region separated from the main cytoplasm by wall-like material were present (Fig. 2.7o and s) and presumably represent the generative cell stuck on wall class seen with DAPI staining (Fig. 2. 5b). In some cases the wall separating this region was incomplete (Fig. 2.7p). Pollen with two similar nuclei was also seen in the *GSL10/gsl10*-2 mutant, although by this stage much of the cytoplasm is degraded (Fig. 2.7t), consistent with this class of pollen aborting (Fig. 2.5a, b).

### 2.2.7  *GSL8* and *GSL10* act independently in the sporophyte

The expression of *GSL8* and *GSL10* in diverse sporophytic tissues and organs (Zimmermann et al., 2004) prompted us to examine potential roles of *GSL8* and *GSL10* in sporophyte development. Since homozygous *gsl8* or *gsl10* mutant plants cannot be recovered, we chose a gene silencing approach to down-regulate *GSL8* or *GSL10* using 35S promoter driven gene-specific double-stranded RNA interference (dsRNAi) constructs. Since *GSL5* was previously shown to function both in the male gametophyte and in sporophytic tissue (Jacobs et al., 2003; Nishimura et al., 2003), the resulting dsRNAi constructs were transformed into the *gsl5* (*pmr4*-1) mutant background to examine potential gene interactions between *GSL5* and *GSL8* or *GSL10.* We recovered independent dsRNAi lines that showed a strong reduction of *GSL8* or *GSL10* leaf transcript levels (Fig. 2.8a). Although *GSL8* and *GSL10* are more closely related to each other than to any other *GSL* family member (63,7% DNA sequence identity, 63,4% protein sequence identity), the silencing effect appeared to be gene-specific as indicated by semi-quantitative RT-PCR analysis of the respective dsRNAi lines (Fig. 2.8a). dsRNAi lines containing a single locus integration event in the *gsl5* background were backcrossed with Col-0 wild-type plants to produce $F_2$ populations. Plants that were Basta resistant (indicating the presence of the dsRNAi transgene) were screened using a cleaved amplified polymorphism marker to determine if these were *GSL5/GSL5* (WT), *gsl5/gsl5* or *GSL5/gsl5* (Tab. 2.3). The effectiveness of *GSL8* dsRNAi or *GSL10* dsRNAi-mediated gene silencing, measured by semi-quantitative RT-PCR analysis of the

respective endogene-derived mRNA levels, was found to be indistinguishable in *GSL5* or *gsl5* backgrounds (Fig. 2.8a and b).
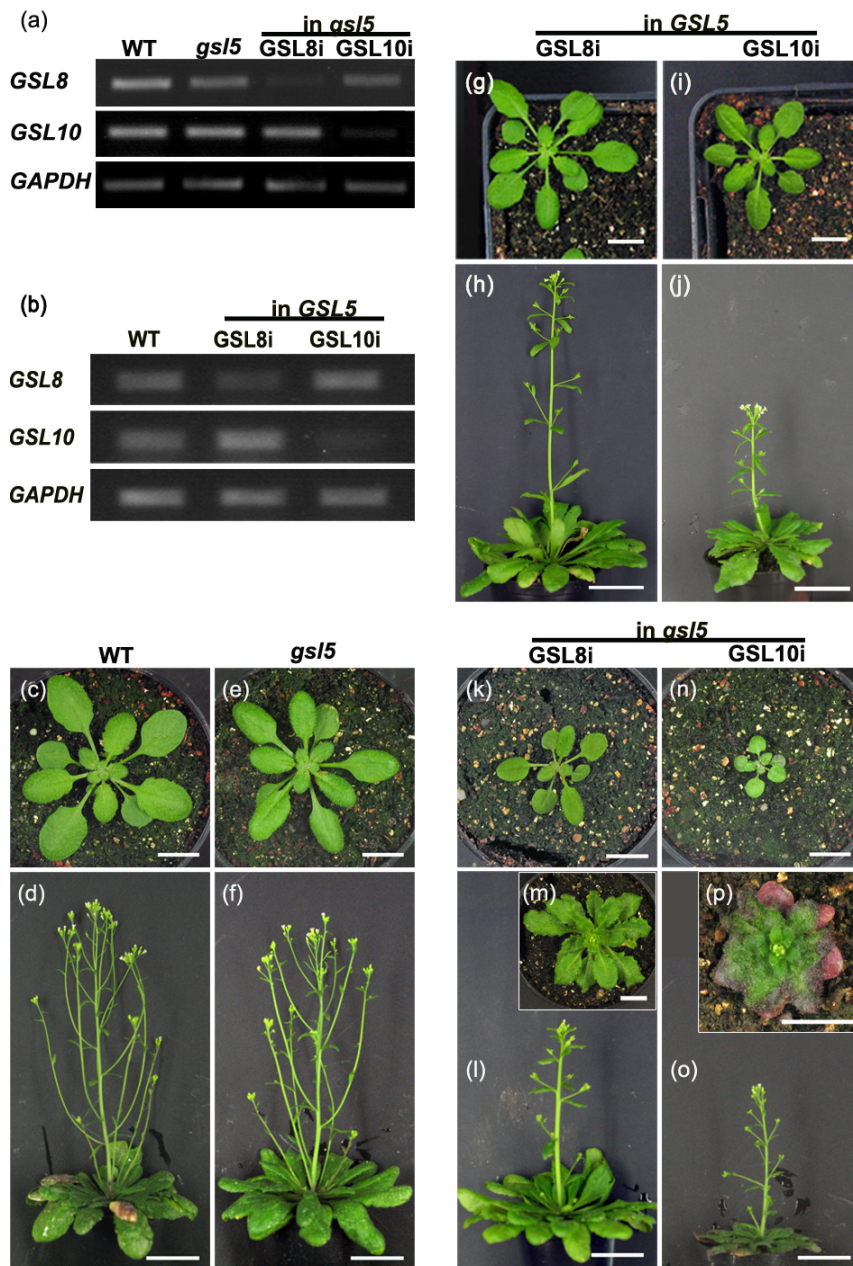


**Figure 2.8:  Silencing of *GSL8* and *GSL10* in wild type and *gsl5* mutant backgrounds.**

(a) Semi-quantitative RT-PCR of *GSL8* and *GSL10* transcripts in wild-type (WT), *gsl5* mutant plants, and transgenic lines expressing gene-specific GSL8 (GSL8i) and GSL10 (GSL10i) dsRNAi constructs in the *gsl5* background. (b) Semi-quantitative RT-PCR of *GSL8* and *GSL10* transcripts in wild-type (WT), *gsl5* mutant plants, and transgenic lines expressing gene-specific *GSL8* (GSL8i) and *GSL10* (GSL10i) dsRNAi constructs in the *GSL5* background. (c, e, g, i, k, n) Top-view of 28 day-old plants of the indicated genotypes. Bars=1 cm. (d, f, h, j, l, o) Side-view of 49 day-old plants of the indicated genotypes. Bars=3 cm. (m and p) Top-view of 49 day-old extreme dwarfs of the indicated genotypes. Bar=1 cm.

In *GSL5* wild type and *gsl5* mutant backgrounds we noticed a marked dwarf phenotype in both *GSL8* and *GSL10* dsRNAi lines. The dwarf phenotypes of *GSL8* dsRNAi- or *GSL10* dsRNAi-containing siblings were enhanced in the *gsl5* background (compare Fig. 2.8g-j with Fig. 2.8k-p). Dwarfism in the *GSL8* dsRNAi lines was consistently less severe compared to the *GSL10* dsRNAi-lines in wild type and mutant gsl5 backgrounds (Fig. 2.8c-d and g-j). These data demonstrate that *GSL8* and *GSL10* are independently required for normal growth of wild-type plants. Consistent with previous findings (Enns et al., 2005), homozygous *gsl5* mutants were slightly smaller compared to wild type plants.

**Table 2.3:** Segregation of dsRNAi transgenes in $F_2$ progeny of crosses between *GSL8* or *GSL10* dsRNAi transgenic lines (in *gsl5* background) and Col-0 wild-type.

| dsRNAi line | *n* plants germinated | *n* Basta survivors | *n* wild-type | *n gsl5* | *n* heterozygous |
|---|---|---|---|---|---|
| *GSL8*i #1 | 100 | 76 | 21 | 18 | 37 |
| *GSL10*i #1 | 97 | 72 | 19 | 12 | 41 |
| *GSL10i* #2 | 98 | 69 | 21 | 18 | 37 |

We could discriminate dwarf subtypes for both *GSL8* and *GSL10* dsRNAi lines among $T_2$ progeny in the *gsl5* background, designated 'moderate' or 'extreme' (compare Fig. 2.8l-m and Fig. 2.8o-p). To test whether the severity of dwarfism was dependent on transgene dosage, we examined the segregation of dwarf phenotypes. Since viable seeds of extreme dwarfs were difficult to recover in sufficient quantities, we restricted our analysis to $T_3$ progeny derived from moderately dwarfed $T_2$ plants with single locus insertions. Among the Basta resistant $T_3$ progeny we found moderate and extreme dwarfs in a ratio of approximately 2:1, which might dicate a dose-dependent effect of the dsRNAi transgene on the severity of dwarfed plant growth.

## 2.3    Discussion

To investigate the functional diversification and roles of GSL family members in *Arabidopsis*, two independent T-DNA insertion lines each for *GSL8* (*gsl8*-1 and *gsl8*-2) and *GSL10* (*gsl10*-1 and *gsl10*-2) were characterized. We have shown that both GSL8 and GSL10 are required gametophytically for pollen development and both GSL proteins also have a role in the sporophyte.

Previously reported mutations in genes of the glucan synthase-like family that act in male gametogenesis affect tetrad callose deposition and/or exine architecture. *GSL2* exerts an essential function in callose synthesis at the primary cell wall of meiocytes, tetrads, and microspores and is required for correct exine patterning (Dong et al., 2005). *GSL1* and *GSL5* play a partially redundant role in pollen development and are responsible for the formation of the callose wall that separates the microspores of the tetrad (Enns et al., 2005). Unlike these *GSL* family members, *GSL8* and *GSL10* are not required for microspore development, as mutant pollen has a reticulate exine, callose deposition in tetrads appears normal and microspores become polarized in preparation for asymmetric division. These previously reported *GSL* family members also act later in pollen development. *GSL2* is required for callose deposition in growing pollen tubes (Nishikawa et al., 2005) while *gsl1/gsl5* mutant pollen are reported to have a bicellular pollen phenotype (Enns et al., 2005). *GSL8* and *GSL10* also act during pollen development and independently have a role in the entry of polarized microspores into mitosis. Perturbation of generative cell engulfment, that involves spatially controlled synthesis and turnover of the separating callose wall, was mainly observed in *gsl10*-2 pollen.

Relatively few gametophytic mutants have been described in *Arabidopsis* that affect defined steps of microgametogenesis (Twell, 2006). Mutants and genes affecting microspore division symmetry and cytokinesis (Park et al., 1998; Twell et al., 2002) or that specifically block generative cell division have been isolated (Durbarry et al., 2005), but none that specifically block microspore division. *gsl8* and *gsl10*, therefore, present a new class of gametophytic mutants that act during microspore development to prevent mitotic entry. Interestingly the *limpet pollen* mutant, in common with *gsl10*, also fails to complete generative cell migration after microspore division (Howden et al., 1998), although the locus responsible remains unknown.

In both hemizygous *gsl8* and *gsl10* (mainly *gsl10*-2) lines some mutant pollen display a single DAPI-stained nucleus followed by progressive cell death (Fig. 2.5a and b), indicating a

63

role for GSL8 and GSL10 in entry into mitosis. Such a role for a GSL protein is intriguing and has not been shown before. Callose deposition before entry into mitosis, in the microspore or other cell types, has not been described. Thus the functions of GSL8 and GSL10 at this stage may be independent of their functions in callose synthesis. GSL8 and GSL10 may exert indirect regulatory functions through interactions with other proteins rather than through catalytic activity at this stage. Whether this regulatory function involves surveillance of cell wall integrity systems similar to those described in yeast in which FKS1/2 represent effector proteins remains to be tested (reviewed inLevin, 2005).

When *gsl8* (rarely) or *gsl10* microspores do divide there are common defects in cytokinesis. Callose deposition was previously shown to occur during cytokinesis in all higher plants (Scherp et al., 2001) where it consolidates the tubular network into a new cell plate (Samuels et al., 1995). In *gsl10* mutant pollen callose is still deposited but either in the wrong location in an irregular structure (mainly *gs10*-2) or as a dome surrounding the generative cell but with slight structural abnormalities (observed by TEM, Fig. 2.7) which persists (mainly in *gsl10*-1), indicating that GSL10 is not essential for callose production during pollen mitosis but may be required for correct temporal and spatial control of its deposition. GSL6 has been reported to be important in the cell plate between dividing cells in sporophytic tissues (Woo et al., 2001). Whether GSL6 is also involved in the production of callose after microspore division, and contributes to the callose deposited in *gsl10* mutant pollen, is unknown.

Although all four T-DNA lines show similar pollen phenotypes, the proportions of pollen that fail to enter mitosis or display cytokinetic phenotypes differs. The majority of *gsl8* mutant pollen fails to enter mitosis, indicating a requirement for GSL8 in this process and consistent with both *gsl8* alleles being nulls as the insertions occur close to the 5' end of the coding region (Fig. 2.1). The *gsl10*-2 insertion, which results in some mononuclear pollen, also occurs close to the 5' end of *GSL10* so is also likely to be a null allele, suggesting the requirement for GSL8 in microspore entry into mitosis is not absolute. The proportion of *gsl10*-1 and *gsl10*-2 pollen in different phenotypic classes differs and may be due to allelic differences. Consistent with this, the T-DNA insertion in *gsl10*-1 is located almost exactly in the middle of the 14 kb long *GSL10* gene, thus potentially giving rise to a truncated gene product with residual activity (Fig. 2.1). Since the *gsl10*-1 T-DNA insertion is located upstream of the region encoding the putative catalytic region (deduced amino acids 1064-1796) that is conserved among GSL family members, the residual GSL10-1 activity most likely lacks callose synthase activity. That there appears to be some function of GSL10 while

lacking the putative catalytic domain is consistent with the idea that these GSL proteins may have a function other than callose synthesis in entry into mitosis.

Both *GSL8* and *GSL10* are expressed throughout pollen development and may have roles after microspore division, in tricellular pollen for example, which are not apparent in these T-DNA lines. Several alleles of *GSL2* have been described, *gsl2*-1 and *gsl2*-2 both result in microspore collapse (Dong et al., 2005), but a weaker allele *gsl2*-3 revealed a role for *GSL2* in callose deposition during pollen tube growth (Nishikawa et al., 2005). Analysis of further alleles for *GSL8* and *GSL10* may also reveal additional roles for these proteins that may be masked by earlier phenotypic defects in strongly defective alleles.

Recently Huang and colleagues (2009) described two additional GLS10 alleles *(gsl10*-3 and *gsl10*-4), which also fail to transmit mutant *gsl10* through their pollen. Likewise the two *GSL10* alleles described above, *GSL10/gsl10*-3 and *GSL10/gsl10*-4 hemizygous plants display normal microspore growth but fail in asymmetric microspore division in a 1:1 ratio. Further more Chen et al. (2009) also failed to recover homozygous *gsl10* mutant lines. Thus it seems likely that the requirement for GSL10 is limiting in pollen mitosis and absence leads to male sterility. Current research work describes 10 newly isolated alleles for *gsl8* (Chen et al., 2009; Huang et al., 2009; Thiele et al., 2009; Guseman et al., 2010). All of them, including the two alleles characterized above, were described as seedling lethal by the authors. However permission of mutant *gsl8* though the pollen is reduced (Chen et al., 2009). These *gls8* alleles vary in the peculiarity of their mutant phenotypes. Varying segregation patterns in allelic *gsl8* null mutants let Thiele et al. (2009) speculate on putative second site mutations. Nevertheless also *gsl8*-1 and *gsl8*-2 have been described as homozygous seedling lethal (Chen et al., 2009; Huang et al., 2009). Partial seedling recovery of homozygous *gsl8* individuals (9.9% homozygous plants for *gsl8*-2) was always observed under sterile conditions by the use of high amounts of sucrose (up to 3%) and decreased dramatically in the absence of sucrose (Chen et al., 2009). Providing additional carbon sources such as sucrose has been previously shown to increase germination and post-germinational growth in mutant plants (Cernac et al., 2006; Eastmond, 2006). Interestingly a recent publication on *GSL10* describes residual precocious pollen germination (about 20%) of *gsl10* containing mircospores within the anther, which failed in migration of any nuclear-like structures into the growing pollen tube (Xie et al., 2010). This observation might explain why mutant alleles of closely related *GSL8* can be accidentally transferred by the male germline. For our segregation analysis we utilized the aberrant phenotype of bulk pollen from dehisced anthers of soil grown plants. In the post-bicellular stage analysis we mainly focused on *GSL10*. Therefore we unfortunately overlooked residual permission of *gls8* in hemizygous *GSL8/gsl8* plants.

In addition to their role in male gametophyte development, we have shown that *GSL8* and *GSL10* are independently required for normal plant growth (Figure 8). If the cellular function(s) of *GSL8* and *GSL10* in male gametophyte and sporophytic cells are conserved, then dwarfism in *GSL8* and *GSL10* dsRNAi plants could be the consequence of partially impaired entry into mitosis or cytokinesis defects. Indeed analysis of newly isolated seedling lethal *gsl8* alleles revealed strong defects in cytokinesis, cell-to-cell connectivity, stomatal patterning, root-hair morphology and reduced callose deposition at plasmodesmata (Thiele et al., 2009; Guseman et al., 2010). Alternatively, the dwarf phenotypes that are enhanced in the *gsl5* background may arise from deregulation of the salicylic acid (SA) pathway. *GSL5/PMR4* has been shown to negatively regulate the salicylic acid (SA) pathway (Nishimura et al., 2003) and deregulated SA levels can dramatically affect cell growth (Rate et al., 1999; Vanacker et al., 2001; Yang and Hua, 2004). Nevertheless in the light of seedling lethality and male sterility, *GSL8* and *GSL10* are the only GSL gene-family members without true functional redundancy through other GSLs.

A meta-analysis of publicly available data from 1,388 microarrays revealed highly correlated gene expression for *GSL8* and *GSL10* (Pearsons's correlation coefficient *r*=0.66; http://www.atted.bio.titech.ac.jp). This and the similar mutant phenotypes of *gsl8* and *gsl10* in both the gametophyte and sporophyte point to related or overlapping gene functions and suggest potential concerted co-action of these two most closely related GSL family members. Callose synthases may exist as complexes containing a number of catalytic domains as callose usually exists as triple helices (Stone and Clarke, 1992; Pelosi et al., 2003) and GSL proteins are present in very high molecular complexes on native gels (Li et al., 2003; Kjell et al., 2004). Thus, it is tempting to speculate that the strikingly similar severe phenotypes resulting from loss-of-function mutations in *GSL8* or *GSL10* reflect the existence of a GSL8 GSL10 heteromeric callose synthase-like complex in which the absence of one family member disrupts complex activity. This would also explain why both gene functions are genetically independent. Such heteromeric complexes have been shown for the cellulose synthase complexes with three different CESA proteins being present in one complex (Tsiamis et al., 2000; Gardiner et al., 2003). Notably loss of function in one of the three CESAs required for primary cell-wall cellulose synthesis (CESA1,-3 and -6) leads to pollen sterility (Persson et al., 2007).

# 3. Material and Methods

The Materials and Methods section is subdivided into two parts. In the first part (3.1) materials used throughout this study, including plant lines, pathogens, bacterial strains, chemicals, enzymes, media, buffers and solutions are listed. Methods applied in this work are described in the second part (3.2).

## 3.1. Material

### 3.1.1  Plant materials

Arabidopsis wild-type and mutant lines used in this study were listed in Table 3.1 and 3.2, respectively.

**Table 3.1: Wild-type *Arabidopsis* accessions used in this study**

| accession | abbreviation | source |
|-----------|--------------|--------|
| Columbia | Col-0 | J. Dangle[a] |
| Dijon | Di17 | H. Kang[b] |
| C24 | C24 | R. Panstruga[c] |

[a]University of North Carolina, Chapel Hill, NC, USA; [b]Boyce Thompson, Ithaca, NC, USA; [c]Max-Planck-Institut für Pflanzenzüchtungsforschung, Köln, Germany

**Table 3.2: Mutant *Arabidopsis* lines used in this study**

| gene | accession | mutagen | reference/source |
|------|-----------|---------|------------------|
| *wrky18 wrky40* | Col-0 | T-DNA/dSpm | Shen et al., 2007 |
| *eds1-2* | Col-0 (Ler-0)[a] | FN | Bartsch et al., 2006 |
| *pen1-1* | Col-0 | EMS | Collins et al., 2003 |
| *pen2-2* | Col-0 | T-DNA | Bednarek et al., 2009 |
| *pad-3-1* | Col-0 | EMS | Glazebrook and Ausubel, 1994 |
| *Cyp81f2-1* | Col-0 | T-DNA | Bednarek et al., 2009 |
| *pmr4-1* | Col-0 | EMS | Vogel and Sommerville, 2000 |
| *gsl8-1* | Col-0 | T-DNA | Töller et al., 2008/ this study |
| *gsl8-2* | Col-0 | T-DNA | Töller et al., 2008/ this study |
| *gsl10-1* | Col-0 | T-DNA | Töller et al., 2008/ this study |
| *gsl10-2* | Col-0 | T-DNA | Töller et al., 2008/ this study |

[a]Ler *eds1-2* allele introgressed into Col-0 genetic background 8th backcross generation, reffered to as Col *eds1-2* in this study; EMS: ethyl methane sulfonate; T-DNA: Transfer DNA; dSpm: defective Suppressor-mutator

## 3.1.2 Bacterial strains

Bacterial strains used for cloning and stabile transformation of *Arabidopsis* were listed in table 3.3.

**Table 3.3: Bacterial strains**

| name | strain | genotype |
|------|--------|----------|
| *Escherichia coli* | DH5a | F⁻ f80lacZDM15 D(lacZYA-argF) U169 deoR endA1 recA1 hsdR17 (r$_k^-$,m$_k$) sup44 thi-1 gyrA96 relA1 phoA |
| *Escherichia coli* | DB3.1 | F⁻ gyrA462 endA D(sr1-recA) mcrB mrr hsdS20 (r$_B^-$, m$_B^-$) supE44 ara14 galK2 lacY1 proA2 rpsL20(Sm$^r$) xyl5 Dleu mtl1 |
| *Agrobacterium tumefaciens* | GV3101 | PMP90RK Gm$^R$ Km$^R$ Rif$^R$ |

### 3.1.3  Yeast

All yeast 2-hybrid experiments were performed with strain EGY48 (*8op-LacZ*): Yeast strain EGY48 transformed with the autonomous replicating *p8op-LacZ* plasmide. Genotype: *MATa, ura3, his3, trp1, LexAop (6x)-Leu2*.

### 3.1.4  Pathogens

For Powdery mildew infections inoculum from *Golovinomyces orontii* present at the pathogen stock collection of the MPIPZ (Köln) was used.

### 3.1.5  Vectors

**Table 3.4 Vectors**

| name | reference |
|------|-----------|
| pDONR201 | Invitrogen, Heidelberg; Germany |
| pJawohl8-RNAi | Töller et al., 2008, this study |
| pLexA-GW | Shen et al., 2007 |
| pB42AD-GW | Shen et al., 2007 |
| p8op-LacZ | Clontech, Heidelber, Germany |

### 3.1.6  Oligonicleotides

Primers used in this study are listed below. Lyophilised primers, synthesized by Invitrogen, were resuspended in sterile water to a final concentration of 100µM. Working stock were diluted to 10µM and 5µM, respectively.

**Table 3.5 List of primers ueds in this study**

| name | sequence (5´- 3´) | purpose |
|---|---|---|
| HvW2WD-F | XACTCGCCGGCCAGGAAGCGCGC | *Hv*WRKY2: WRKY domain cloning |
| HvW2WD-R | XTCACGGTGCGTGGTTGTGGT | |
| HvW2CT-F | XACCCGCCCAAGCATCAAGGCTC | *Hv*WRKY2: CT domain cloning |
| HvW2CT-R | XTCAAGCAACAGGGATCCGAC | |
| HvW1CT-F | XACCCGCAGCAGCAGAACG | *Hv*WRKY1: CT domain cloning |
| HvW1CT-R | XTTAATTGATGTCCCTGGTCG | |
| W18CT-F | XACGCGTTGGAGAAAAACGAAAG | *At*WRKY18: CT domain cloning |
| W18CT-R | XTCATCATGTTCTAGATTGCTCCATTAAC | |
| W40CT-F | XACCTTGACTGTGCCGGTGACTA | *At*WRKY40: CT domain cloning |
| W40CT-R | XTCACTATTTCTCGGTATGATTCTGTTGA | |
| CC2-GW-F | XACATGGGCGGTTGTGTCTC | At1G12210: CC domain cloning |
| CC2-GW-R | XTCACAACTCTTCAACCTCAGC | |
| CC3-GW-F | XACATGGGAGGTTGTTTCTCTGTTT | At1G12220: CC domain cloning (RPS5) |
| CC3-GW-R | XTCATGTGGGTTGAAAAGGGATCT | |
| CC4-GW-F | XACATGGGAGCTTGTTTAACACTCTC | At1G12280: CC domain cloning |
| CC4-GW-R | XTCATTCTGTGAGACGGGTCCA | |
| CC5-GW-F | XACATGGGTGGTTGTGTCTCTGT | At1G12290: CC domain cloning |
| CC5-GW-R | XTCATGTTTCCTGACCAACAATCG | |
| CC9-GW-F | XACATGGCGGATTGGCTTCTACT | At1G51480: CC domain cloning |
| CC9-GW-R | XTCACTTATGCGCCACCACTTC | |
| CC10-GW-F | XACATGGCTGAGGCAGTTGTATC | At1G53350: CC domain cloning |
| CC10-GW-R | XTCACAACCCCACAAGATCACTCT | |
| CC11-GW-F | XACATGGCTGGAGAACTTGTGTC | At1G58390: CC domain cloning |
| CC11-GW-R | XTCAAAACGTTTGTCGCATCTCC | |
| CC14-GW-F | XACATGGCTGGGGAACTTATTTCG | At1G59124: CC domain cloning |
| CC14-GW-R | XTCAGCTGTCGTCGTCCTTAGAAAA | |

| CC16-GW-F | XACATGGCTGAGACACTTTTGTCATT | At1G59620: CC domain cloning |
| --- | --- | --- |
| CC16-GW-R | XTCACCTCTTACTTAGGCCTTCCATAT | |
| CC18-GW-F | XACATGCAGGACTTATATATGGTTGATT | At1G59780: CC domain cloning |
| CC18-GW-R | XTCAATGACGCAACTCCCTTTTCCT | |
| CC20-GW-F | XACATGGGAAATTTTGTGTGTATAGAAAT | At1G61190: CC domain cloning |
| CC20-GW-R | XTCATTGACCAATCGTAGGCTGAGT | |
| CC22-GW-F | XACATGGGGAGTTGTTTTTCTTTTC | At1G61310: CC domain cloning |
| CC22-GW-R | XTCAAGGCCTCTCTTCAACTTCAGA | |
| CC23-GW-F | XACATGGGTATTTCTTTCTCGATACC | At1G62630: CC domain cloning |
| CC23-GW-R | XTCACAACAATTGTCGGCTGAAGA | |
| CC24-GW-F | XACATGGGTATCTCTTTCTCGATACC | At1G63350: CC domain cloning |
| CC24-GW-R | XTCACGGTTGAAGTTGTTGTTCCTC | |
| CC25-GW-F | XACATGGGTATTTCTTTCTCGATACC | At1G63360: CC domain cloning |
| CC25-GW-R | XTCAGATTGTCGGTTGAAGAGGTC | |
| CC26-GW-F | XCAATGGCTTCGGCTACTGTTG | At3G07040: CC domain cloning (RPM1) |
| CC26-GW-R | XTCAGTTGTTCACCCACTTTGCAT | |
| CC27-GW-F | XACATGGCGAACTCCTATTTATCAAG | At3G14460: CC domain cloning |
| CC27-GW-R | XTCACGCTAGCTTATCTTCCACTCG | |
| CC28-GW-F | XACATGACCGGCATAGGAGAGAT | At3G14470: CC domain cloning |
| CC28-GW-R | XTCATTCAGATTCATCCACAAGAGATG | |
| CC30-GW-F | XACATGGTAGATGCGATCACGG | At3G46530: CC domain cloning |
| CC30-GW-R | XTCAAGATCGAGCACGCCGAAG | |
| CC34-GW-F | XACATGGGTAGTTGTATCTCTCTCCAA | At4G10780: CC domain cloning |
| CC34-GW-R | XTCAAATTGTTTCCCGACCCATAA | |
| CC41-GW-F | XACATGGCAGATATAATCGGCG | At5G04720: CC domain cloning |
| CC41-GW-R | XTCACAACATCTCCTTCACCTTCCTC | |
| CC44-GW-F | XACATGGCTGAAGCATTTGTGTC | At5G43470: CC domain cloning |

| | | |
|---|---|---|
| CC44-GW-R | XTCAATCGCTTTCAGAACTGTCAGG | (RPP8) |
| CC45-GW-F | XACATGGTGGACTGGCTTTCACT | At5G43730: CC domain cloning |
| CC45-GW-R | XTCAACCAACTGTGGTTTGTATATGCTTC | At5G43730: CC domain cloning |
| CC48-GW-F | XACATGAATTGCTGTTGGCAGGT | At5G47250: CC domain cloning |
| CC48-GW-R | XTCACGTCGTATCAAGACCGACTG | At5G47250: CC domain cloning |
| CC49-GW-F | XACATGGGAAATAATTTCTCAGTTGAAT | At5G47260: CC domain cloning |
| CC49-GW-R | XTCAAAGCAACTTTGCTTGAGAAACA | At5G47260: CC domain cloning |
| CC52-GW-F | XACATGGGAGGTTGTGTCTCTGTATC | At5G63020: CC domain cloning |
| CC52-GW-R | XTCATAGACGGTTCCACGCACTCTC | At5G63020: CC domain cloning |
| CC54-GW-F | XACATGAACGATTGGGCTAGTTTG | At5G66900: CC domain cloning |
| CC54-GW-R | XTCACTTGGGAACCGAACAAAGAT | At5G66900: CC domain cloning |
| CC60-GW-F | XACATGGCAGGGGAACTTGTGT | At9G58602: CC domain cloning |
| CC60-GW-R | XTCATGTTCGTCGTATCTCCCTTTC | At9G58602: CC domain cloning |
| Mla1-46-GW-F | XACATGGATATTGTCACCGGTGC | cloning of MLA10$_{1-46}$ |
| Mla1-46-GW-R | XTCAGGCAGCGTTCATGCTCTCAA | cloning of MLA10$_{1-46}$ |
| Mla10-523-R | XTCAGCCATCCAATAGATTCACAAA | cloning of MLA10$_{1-523}$ |
| Mla10-225-R | XTCACCGACAATCGAAATCACCTT | cloning of MLA10$_{1-225}$ |
| AG9:105/E2 | ACACAAGGGTGATGCGAGACA | *eds1-2* mutant detection |
| EDS4 | GGCTTGTATTCATCTTCTATCC | *eds1-2* mutant detection |
| EDS5 | GTGGAAACCAAATTTGACATTAG | *eds1-2* mutant detection |
| pad3-1-F | AATCTCGCCGAAATGTATGG | *pad3-1* mutant detection; digest with *HindIII* |
| pad3-1-R | TTGGGAGCAAGAGTGGAGTT | *pad3-1* mutant detection; digest with *HindIII* |
| cyp81F2-1-F | GGACCAACTCCGTTTCCTATC | *cyp81f2-1* mutant detection |
| cyp81F2-1-R | TTCATCGACCAATCTCTCTT | *cyp81f2-1* mutant detection |
| pen1-1-F | CAACGAAACACTCTCTTCATGTCACGC | *pen1-1* mutant detection |
| pen1-1-R | CATCAATTTCTTCCTGAGAC | *pen1-1* mutant detection |
| pen2-2-F | CTCTTTGGAACTGCTTCATCTTCT | *pen2-2* mutant |

| | | |
|---|---|---|
| pen2-2-R | CAGCAACACTAGCGCCATTA | detection |
| Wrky18-F | CGGATTTCGTCTGATCCATT | spans T-DNA insertion in *wrky18* |
| Wrky18-R | CGATTCATTTCGATGCAAAG | |
| W40-GW-F | XACATGGATCAGTACTCATCCTCTTTGG | spans dSpm insertion in *wrky40* |
| Wrky40-R2 | TCCACCAAAGCACTTGTCTG | |
| GK-LB8409 | ATATTGACCATCATACTCATTGC | left border detection (GK) |
| dSpm8 | GTT TTG GCC GAC ACT CCT TAC C | detection of dSpm insertion |
| Lba1 | TGGTTCACGTAGTGGGCCATCG | left border detection (SALK) |
| Gsl10-F1 | TGCTCAGAAACTGGATGACG | spans T-DNA (GK) in *gsl10-2* |
| Gsl10-R3 | TGTAATGGAACCCATCAAGAAA | |
| Gsl10-F2 | AATGTTGCTGTTGGGGTTTC | spans T-DNA (GK) in *gsl10-1* |
| Gsl10-R4 | TGAACCAATTCGAGCCTACC | |
| Gsl8-F2 | ATGCTGCACTAAACGCACAG | spans T-DNA (SALK) in *gsl8-1* |
| Gsl8-R1 | GGCGATCGGAGAAAATATGA | |
| Gsl08-F1 | TAGGTACGTGGTGCAGTCCA | spans T-DNA (GK) in *gsl8-2* |
| Gsl08-R2 | TGCAGAGACGATCAGATGCT | |
| pmr4-1 F | CAAGGACGGCATTCATAGGT | pmr4-1 mutant detection; digest with *NhiI* |
| pmr4-1 R | CCGTCTCGCCTCTAGATTCA | |
| Gsl08-RT-F | GGACTTAACCAGATTGCCCTA | *GSL8* RT-PCR |
| Gsl08-RT-R | ATACCTTTGCACCACCGTGA | |
| Gsl10-RT-F | GAGATGTTGGGCTCAATCAAA | *GSL10* RT-PCR |
| Gsl10-RT-R | CATTGGCACAGCAGTGAAGA | |
| Gsl8-S-F1 | XATGCTGCACTAAACGCACAG | *GSL8 ds*RNAi fragment amplification |
| Gsl8-S-R1 | XGGCGATCGGAGAAAATATGA | |
| Gsl10-S-F1 | XGTACCTTGCGTATGGCAA | *GSL10 ds*RNAi fragment amplification |
| Gsl10-S-R1 | XTAGCCTTGCTAGGGAACGAAT | |

X denotes forward or reverse Gateway[®] recombination sites.

### 3.1.7  Enzymes

Restriction enzymes were purchased from New England Biolabs (Frankfurt/Main, Germany) and Fermentas (St. Leon-Rot, Gernamy). Restriction digestions were performed following the manufactures recommendations, using the provided 10x reaction buffer.

Standard PCR reactions were performed using home made *Taq* DNA polymerase. High accuracy *Pfu* DNA polymerase (Fermentas, St. Leon-Rot, Germany) or *TaKaRa* DNA polymerase (Clontech, Heidelberg, Germany) was used to generate PCR products for cloning and/or sequencing.

### 3.1.8  Antibiotics

Antibiotic stock solutions (1000x) were prepared as indicated (Table 3.6) and stored at -20°C.

**Tabel 3.6. Antibiotic stock (1000x) solutions**

| name | description | source |
|------|-------------|--------|
| Ampliciline | 100mg/ml in dH$_2$O | Roth, Karlsruhe, Germany |
| Kanamycin | 50mg/ml in dH$_2$O | Serva, Heideberg, Germany |
| Carbencilin | 50mg/ml in dH$_2$O | Sigma, München, Germany |
| Rifampicin | 100mg/ml in DMSO | Fluka, Buchs, Switzerland |

### 3.1.9   Antibodies

**Table 3.7 Primary antibodies**

| name | source | dilution | source |
|------|--------|----------|--------|
| α-LexA | mouse | 1:1000 in PBST + 2% milk (w/v) | Santa Cruz, Heideberg, Germany |
| α-B42AD | rabbit | 1:1000 in PBST + 2% milk (w/v) | Santa Cruz, Heideberg, Germany |
| α-HA | rat | 1:2500 in PBST + 2% milk (w/v) | M. Roccaro[a] |

[a]Max-Planck-Institut für Pflanzenzüchtungsforschung, Köln

**Table 3.7 Secondary antibodys**

| name | lable | dilution | Source |
|---|---|---|---|
| α-mouse | HRP[b] | 1:4000 in PBST + 5% milk (w/v) | GE Healthcare, Freiburg, Germany |
| α-goat | HRP[b] | 1:4000 in PBST + 5% milk (w/v) | Santa Cruz, Heideberg, Germany |
| α-goat | HRP[b] | 1:5000 in PBST + 5% milk (w/v) | M. Roccaro[a] |

[a]Max-Planck-Institut für Planzenzüchtungsforschung, Köln; [b]horseradish peroxidase

### 3.1.10 Chemicals

Laboratory grade chemicals and reagents were purchased from Sigma-Aldrich (München, Germany), Roth (Karlsruhe, Germany), Merck (Darmstadt, Germany), Serva (Heidelberg, Germany) and Invitrogen™ (Karlsruhe, Germany) unless otherwise stated.

### 3.1.11 Media

Sterile media were used for the growth of bacteria yeast and Arabidopsis *in vitro* pollen germination as follows:

*Escherichia coli* medium:            Luria-Bertani (LB) broth or agar plates
*Agrobacterium tumefaciens* medium:     YEB broth or agar plates

For yeast the appropriate drop-out selection media were prepared according to the "Yeast Protocols Handbook" (Clontech, Heidelberg).

*Arabidopsis* pollen germination medium:
18% (w/v) sucrose, 0,5% (w/v) agar, 0,01% (v/v) boric acid,  1mM $MgSO_4$, 1mM $CaCl_2$, 1mM $Ca(NO_3)_2$

### 3.1.12 Buffer and solutions

General buffers and solutions are denoted in the following list. All buffers and solutions were prepared with Milli-Q® water. Buffers and solutions for molecular biological experiments were autoclaved or filter sterilized, respectively.

| DNA extraction buffer (quick prep) | Tris | 200 mM |
| --- | --- | --- |
| | NaCl | 250 mM |
| | EDTA | 25 mM |
| | SDS | 0,5 % |
| | pH 7,5 (HCl) | |
| | | |
| DNA loading dye (6x) | Succrose | 4 g |
| | EDTA (0,5 M) | 2 ml |
| | Bromphenole blue | 25 mg |
| | dH$_2$O to 10 ml | |
| | | |
| TAE buffer (x50) | Tris | 242 g |
| | EDTA | 18,6 g |
| | Glacial acetic acid | 57,1 ml |
| | dH$_2$O to 1000 ml | |
| | pH 8,5 | |
| | | |
| Ethidium bromid stock solution | Ethidium bromid | 10 mg/ml H$_2$O |
| | Dilute 1:20000 in Agarose solution. | |
| | | |
| PCR reaction buffer | Tris | 100 mM |
| | KCl | 500 mM |
| | MgCl$_2$ | 15 mM |
| | pH 9 | |

| TE buffer | Tris | 10 mM |
| | EDTA | 1 mM |
| | pH 8,0 (HCl) | |

| Resolving gel buffer (4x) | Tris | 1,5 M |
| | pH 8,8 (HCl) | |

| Stacking gel buffer (4x) | Tris | 0,5 M |
| | pH6,8 (HCl) | |

| Protein sample buffer (2x) | Tris | 0, 125 M |
| | SDS | 4 % |
| | Gycerol | 40 % (v/v) |
| | Bromphenol blue | 0,02 % |
| | pH 6,8 | |
| | 0,2 M Dithiothreitol (DTT) was added befor use | |

Ponceau S — Ponceau S working solution was prepared by diluting ATX Ponceau S (Fulka) 1:5 in $dH_2O$.

| Running buffer (10x) | Tris | 30,28 g |
| | Glycine | 144,13 g |
| | SDS | 10 g |
| | $dH_2O$ to 1000 ml | |

| Transfer buffer (10x) | Tris | 58,2 g |
|---|---|---|
| | Glycine | 29,3 g |
| | SDS (10%) | 12,5 ml |

dH$_2$O to 1000 ml
Before use dilute 80 ml in 720 ml dH$_2$O
and add 200 ml methanol.

| PBS buffer (10x) | NaCl | 80 g |
|---|---|---|
| | KCl | 2 g |
| | Na$_2$HPO$_4$ | 14,4 g |
| | KH$_2$PO$_4$ | 2,4 g |

pH 7,4 (HCl)

| PBS-T buffer | 0,1 % (v/v) Tween® 20 in PBS |
|---|---|

| DEPC-H$_2$O | Diethylpyrocarbonate | 0,1 % in H2O |
|---|---|---|

Shake vigorously, let stand O/N and
autoclave 30 min.

| ΦB | Yeast extract | 0,5 % |
|---|---|---|
| | Tryptone | 2 % |
| | MgSO$_4$ | 0,4 % |
| | KCl | 10 mM |

pH 7,6

autoclave

| | | |
|---|---|---|
| TFB1 | KAc | 30mM |
| | MnCl2 | 50 mM |
| | RbCl | 100 mM |
| | CaCl | 10 mM |
| | Glycerol | 15% |
| | ph 5,8 | |
| | filter sterile | |
| | | |
| TFB2 | MOPS | 10 mM |
| | CaCl2 | 75 mM |
| | RbCl | 10 mM |
| | Glycerol | 15% |
| | filter sterile | |
| | | |
| Yeast transformation mix | PEG 3350 (50 %) | 7 ml |
| | TE (10x) | 1 ml |
| | LiAc (10x) | 1 ml |
| | dH2O | 1 ml |
| | Prepared fresh before use. | |

## 3.2. Methods

### 3.2.1 Maintenance and cultivation of *Arabidopsis* plant material

*Arabidopsis* seeds were germinated by sowing directly onto moist compost (Stender AG, Schermbeck, Germany) or freshly moisture expanded Jiffy pots (Jiffy Products, Mölln). Seeds were stored for at least 3 days at 4°C before sawing or cold treated by incubating covered sawn pots in the dark at 4°C for 2-3 days. Pots were subsequently transferred to a controlled environment growth chamber, covered with a propagator lid and maintained under

short day conditions (10 hour photoperiod, light intensity of approximately 200 µEinsteins$^{-2}$ m sec$^{-1}$, 23°C day, 22° C night, and 65% humidity). Propagator lids were removed when seeds had germinated. For propagation, plants were transferred to long day conditions (16 hour photoperiod), to allow bolting and setting of seed. To collect seed, aerial tissue was enveloped with a paper bag and sealed with tape at its base until siliques shattered.

## 3.2.2 Generation of *Arabidopsis* F$_1$ and F$_2$ progeny

Fine tweezers and a magnifying-glass were used to emasculate an individual flower. To prevent self-pollination, only flowers that had a well-developed stigma but immature stamen were used for crossing purpose. Fresh pollen from donor stamens was dabbed onto each single stigma. Mature siliques containing F$_1$ seed were harvested and allowed to dry. Approximately five F$_1$ seeds per cross were grown as described above and allowed to self pollinate. Produced F$_2$ seeds from individual F$_1$ were collected and stored separately.

## 3.2.3 *Golovinomyces orontii* maintenance and infection procedure

*G.orontii* was maintained as mass conidiosporangia cultures on leaves of a genetically susceptible *Arabidopsis* genotype, under short day conditions (10 hour photoperiod, 23°C day, 22°C night, 70% humidity) in a controlled environment growth chamber. For infections, conidia were carefully brushed off infected donor plants, held over acceptor plants, with a soft paint brush. Inoculated acceptor plans were kept in the same growth chamber as maintenance cultures until analysis.

## 3.2.4 Agrobacterium-mediated stable transformation of *Arabidopsis*

The method for Agrobacterium-mediated stable transformation of Arabidopsis, use in this study, is based on the floral dip protocol described by Clough and Bent (Clough and Bent, 1998). Approximately 9-12 Arabidopsis plants were grown in 9 cm square pots (3 pots for each transformation) under short day conditions for 4 - 5 weeks. Then the plants were shifted to 16 h photoperiod conditions to induce flowering. Plants were used for transformation when they had a maximum number of young flower heads. Agrobacterium was streaked out onto selective YEB plates containing appropriate antibiotics (Table 3.6) and was grown at 28°C for 72 h. A 20 ml overnight culture was prepared in selective YEB medium and cultured at 28 °C

in an orbital shaker. The next day 200 ml YEB broth with appropriate antibiotics was inoculated with all of the overnight culture and grown overnight at 28°C in an orbital shaker until OD600 > 1.6. Cultures were spun down at 5000 rpm for 10 min at room temperature and the pellet was resuspended in 5% sucrose to OD600 ~ 0.8. Silwet L- 77 (Lehle seeds, USA) at 500µl/l was added as surfactant. Plants were inverted into the cell-suspension ensuring all flower heads were submerged. Plants were agitated carefully to release air bubbles and left in the solution for approximately 10-20 sec. Plants were then placed horizontal on a plastic tray and covered with bags. The plants were incubated overnight at RT without direct light. Afterwards bags were removed and pots were moved to direct light in the greenhouse and left to set seed.

### 3.2.5 Preparation of chemically competent *E. coli* cells

5 ml of an E. coli over night culture grown in ΦB was added to 400 ml of ΦB and shaken at 37°C until the bacterial growth reached an OD600 0,4 - 0,5. Cells were cooled on ice and all following steps were carried out on ice or in a 4°C cold room. The bacteria were pelleted at 5000 g for 15 min at 4°C. The pellet was gently resuspended in 120 ml ice-cold TFB1 solution and incubated on ice for 10 min. The cells were pelleted as before and carefully resuspended in 16 ml ice-cold TFB2 solution. Cells were transferred into 1.5 ml reaction tubes containing 50 µl aliquots. The cells were frozen in liquid nitrogen and stored at -80 °C until use.

### 3.2.6 Transformation of chemically competent *E. coli* cells

A 50 µl aliquot of chemically competent cells was thawed on ice. 10 to 100 ng of plasmid DNA (or 3 µl of BP or LB Gareway© reaction mixture) was mixed with the aliquot and incubated on ice for 30 min. The mixture was heat shocked for 40 sec at 42°C and immediately put on ice for 2 min. 500 µl of LB broth medium was added and the cells were incubated at 37°C for 1 h in an Eppendorf thermomixer. The transformation mixture was centrifuged for 1 min at full speed in a table top centrifuge. The Cells were resuspended in 50 µl LB broth and plated onto selective media plates.

### 3.2.7 Preparation of electro-competent *A. tumefaciens* cells

Agrobacterium was streaked out onto a YEB agar plate, containing adequate antibiotics and was incubated at 28°C for two days. A single colony was picked into a 5 ml YEB medium over night culture, containing the appropriate antibiotics, at 28°C. The whole overnight culture was added to 200 ml YEB (without antibiotics) and grown to an OD600 of 0,6. Subsequently, the culture was chilled on ice for 15 – 30 min. From this point onwards bacteria were maintained at 4°C. Bacteria were centrifuged at 6000 g for 15 min an 4°C and the pellet was resuspended in 200 ml of ice-cold sterile water. Bacteria were again centrifuged at 6000 g for 15 min and 4°C. Bacteria were resuspended in 100 ml of ice-cold sterile water and centrifuged as described above. The bacterial pellet was resuspended in 4 ml of ice-cold 10% glycerol and centrifuged as described above. Bacteria were resuspended in 600 µl of ice-cold 10% glycerol. 40 µl aliquots were frozen in liquid nitrogen and stored at -80°C.

### 3.2.8 Transformation of electro-competent *A. tumefaciens* cells

50-100 ng of plasmid DNA was mixed with 40 µl of electro-competent *A. tumefaciens* cells, and transferred to an electroporation cuvette on ice (2 mm electrode distance; Eurogentec, Seraing, Belgium). The BioRad Gene Pulse™ apparatus was set to 25 µF, 2.5 kV and 400 Ω. The cells were pulsed once at the above settings for a second, the cuvette was put back on ice and immediately 1 ml of YEB medium was added to the cuvette. Cells were quickly resuspended by slowly pipetting and transferred to a 2 ml microcentrifuge tube. The tube was incubated for 3 h in an Eppendorf thermomixer at 28°C and 600 rpm. A 5 µl fraction of the transformation mixture was plated onto selection YEB agar plates.

### 3.2.9 Transformation of yeast cells

Yeast was grown at 30°C on a platform shaker in the appropriate SD selection medium over night. Fresh SD medium was inoculated with 10% of the over night culture and cells were incubated again until the yeast growth reached log phase. The yeast was peleted by centrifugation at 4800 rpm for 5 min and was subsequently resuspended with SD medium in 10% of the harvesting volume. The carrier DNA was boiled for 5 min at 95 °C and was immediately chilled on ice. 20 µl of yeast cell suspension were incubated with 100 µg of carrier DNA for 2 min at RT. 1-5 µg prey and/or bait plasmid constructs were added. After

adding 500 µl of fresh prepared transformation mix each transformation reaction mixture was vortexed and incutated over night at RT. Afterwards cells were peleted for 1 min at 10000 x *g* in a table top centrifuge. Yeast cells were resuspended in 100 µl sterile $H_2O$ and plated onto appropriate SD selection medium. Plates were incubated for 72 h at 30°C.

### 3.2.10 Isolation of *Arabidopsis* genomic DNA

For DNA extraction 1-2 young frozen leafs were homogenized with a pre-cold pestle in a 1,5 centrifuge tube. Subsequent 200µl pre-warmed (65°C) DNA extraction buffer was added and samles were incubated at 65°C for 20 min. The solution was centrifuged at maximum speed for 5 min in a bench top microcentrifuge and the supernatant was transferred into a new centrifuge tube containing one volume cold (-20°C) isopropanol. Samples were mixed by inverting the tubes several times and incubated 30 min at -20°C for DNA precipitation. The DNA was peleted by additional centrifugation at 15.000 x g by 4°C for 20 min. The pellet was washed with 70% ethanol and air dried. Finally the DNA was dissolved in 50 µl sterile $H_2O$ and 2 µl of the DNA solution were used for a 25 µl PCR reaction mixture. Samples were stored at -20°C.

Alternatively genomic DNA was isolated with REDExtract-N-Amp™ Tissue PCR Kit (SIGMA), according to manufacturers instructions. Samples were stored at 4°C.

### 3.2.11 Plasmid DNA isolations

Plasmid DNA was isolated by using the alcaline lysis method (Birnboim and Doly, 1979). High quality plasmid DNA was isolated with the MACHEREY-NAGEL (MN) NucleoSpin® Mini-Kit according to the manufacturer's instruction.

### 3.2.12 Restriction endonuclease digestion of DNA

All reactions were carried out by using the manufactures recommended conditions. Typically, reactions were performed in 1,5 ml microfuge tubes by using 1-2 U of Enzyme per 20 µl reaction. All digestions were carried out at appropriate temperatures in proper incubators or at least 60 min.

## 3.2.13 Polymerase chain reaction (PCR) amplification

Standard PCR reactions were performed using homemade *Taq* DNA polymerase while for cloning of PCR products *Pfu* (Fermentas) or *TaKaRa* (Clontech) polymerases were used according to the manufacturer instructions.

**Table 1: PCR reaction mix**

| Reagent | amount per reaction |
|---------|---------------------|
| template DNA (genomic or plasmid) | 20-50 ng |
| PCR amplification buffer | 1/10 of the reaction volume |
| dNTP mix (dATP, dGTP, dTTP, dCTP) | 0,2 mM each |
| upstream (F) primer | 0,5 µM |
| downstream (R) primer | 0,5 µM |
| Taq DANN polymerase | 2,5 U |
| sterile water | variable |

**Table 2: PCR thermal profile**

| step | temperature (C°) | Time | No. of cycles |
|------|------------------|------|---------------|
| Initial denaturation | 94 | 3 min | |
| denaturation | 94 | 30 sec | |
| annealing | 50-58 | 10-30 sec | 20-35 x |
| extension | 72 | 1-5min | |
| final extension | 72 | 5min | |

## 3.2.14 Agarose gel electrophoresis of DNA

DNA fragments were separated by agarose gel electrophoresis in gels consisting of 1–2% (w/v) SeaKem® LE agarose (Cambrex, USA) in TAE buffer. Agarose was dissolved in TAE buffer by heating in a microwave. Molten agarose was cooled to 50° C before 2.5 µl of ethidium bromide solution (10 mg/ml) was added. The agarose was pored and allowed to solidify before being placed in TAE in an electrophoresis tank. DNA samples were loaded

onto an agarose gel after addition of 2 µl 6x DNA loading buffer to 10 µl PCR- or restrictionreaction. Separated DNA fragments were visualised by placing the gel on a 312 nm UV transilluminator and photographed.

### 3.2.15 Isolation of total RNA from *Arabidopsis*

Total RNA was prepared from 3- to 6-week-old plant materials. Liquid nitrogen frozen samples (approximately 100 mg) were homogenized for ~20 sec to a fine powder using a Mini- Bead-Beater-8™ (Biospec Products) and 1.0 mm Zirconia beads (Roth) in 2 ml centrifuge tubes. 1 ml of TRI® Reagent (Sigma) was added and samples were homogenised by vortexing for 1 min. For dissociation of nucleoprotein complexes the homogenised sample was incubated for 5 min at room temperature. 0.2 ml of chloroform was added and samples were shaken vigorously for 15 sec. After incubation for 3 min at room temperature samples were centrifuged for 20 min at 12000 $g$ and 4°C. The upper aqueous, RNA containing phase, was transferred to a new microcentrifuge tube and the RNA was precipitated by adding one volume of isopropanol and incubation for 10 min at room temperature. Subsequently, samples were centrifuged for 10 min at 12000 $g$ and 4°C. The supernatant was removed and the pellet was washed in 0,5 ml of 70% ethanol. Samples were again centrifuged for 5 min at 7500 g and 4°C, pellets were air dried for 10 - 30 min and dissolved in 50 µl DEPC-$H_2O$. All RNA extracts were adjusted to the same concentration with DEPC-$H_2O$. Samples were stored at -80°C.

### 3.2.16 Reverse transcription PCR

For first strand cDNA synthesis SuperScript™ II Reverse Transcriptase (Invitrogen) was used by combining 1 µg template total RNA, 1 µl primer $dT_{18}$ (0.5 µg/µl), 5 µl dNTP mix in a volume of 13 µl (deficit made up with sterile $H_2O$). Samples were incubated at 65°C for 10 minutes. Subsequently, the reactions were complemented with 4 µl of 5 x reaction buffer, 2 µl of 0.1 M DTT and 1 µl reverse transcriptase. The reactions were incubated at 42°C for 60 minutes before the enzyme was heat inactivated at 70°C for 10 minutes. For subsequent normal PCR appropriate dilutions of the cDNA were used.

### 3.2.17 DNA sequencing

DNA sequences were determined by the "Automatische DNA Isolierung und Sequenzierung" (ADIS) service unit at the MPIPZ on Applied Biosystems (Weiterstadt, Germany) Abi Prism 377 and 3700 sequencers using Big Dye-terminator chemistry (Sanger, 1977).

### 3.2.18 DNA sequence analysis

Sequencing data were analysed mainly using DNAStar Lasergene 8 (DNASTAR, Madison, USA) software.

### 3.2.19 Yeast crude protein extraction

Overnight yeast cultures were grown in the appropriate SD selection media on a platform shaker at 30°C. 4 ml of each cell culture was pelleted by centrifugation for 1 min at full speed in a tabletop centrifuge. Immediately the supernatant was discarded and the pelletes were frozen in liquid nitrogen. Subsequently, the samples were boiled for 5 min at 95°C. This "freez – thaw" procedure was repeated for at least 3 times. 200 µl of 2x loading buffer with freshly added DTT was mixed with the sample. Samples were stored at -20°C. Prior to use samples were boiled for 5 min at 95°C and centrifuged for 5 min at 13,000 rpm.

### 3.2.20 Denaturing SDS-polyacrylamide gel electrophoresis (SDS-PAGE)

Different percentage polyacrylamide (PAA) gels were used depending on the size of the protein to be resolved. The resolving gel was poured between two glass plates and overlaid with ~2 ml sterile $H_2O$. The gel was allowed to set for a minimum of 15 minutes. The water was removed and a stacking gel was poured onto the top of the resolving gel. After insertion of a comb and ensuring that no bubbles were trapped the whole gel was left to set for at least 15 minutes.

**Table 3.8 Formulation of different percentage resolving gels**

| component[a] | 7,5 % resolving gel | 10 % resolving gel |
|---|---|---|
| dH$_2$O | 4,28 ml | 4,1 ml |
| 30 % Acrylamide/Bis solution 20:1 (BioRad) | 2,5 ml | 3,3 ml |
| resolving gel buffer | 2,5 ml | 2,5 ml |
| 10 % SDS | 100 µl | 100 µl |
| TEMED (BioRad) | 5 µl | 5 µl |
| 10 % APS | 75 µl | 75 µl |

[a]Add in stated order.


**Table 3.9 Constituents of a protein stacking gel**

| component[a] | 4 % stacking gel |
|---|---|
| dH$_2$O | 6,1 ml |
| 30 % Acrylamide/Bis solution 20:1 (BioRad) | 1,3 ml |
| stacking gel buffer | 2,5 ml |
| 10 % SDS | 100 µl |
| TEMED (BioRad) | 10 µl |
| 10 % APS | 100 µl |

[a]Add in stated order.

After removing the combs, each PAA gel was placed into the electrophoresis tank and submerged in 1x running buffer. A pre-stained molecular weight marker (Precision plus protein standard dual colour, BioRad) and denatured protein samples were loaded onto the gel and run at 80–100 V until the marker line suggested the samples had resolved sufficiently.

### 3.2.21 Immuno-blot analysis

Proteins that had been resolved on PAA gels were transferred to Trans-Blot® nitrocellulose membrane (BioRad). After gels were released from the glass plates and stacking gels were removed with a scalpel. PAA gels were pre-equilibrated in 1x transfer buffers for 20 min on a rotary shaker and the blotting apparatus (Mini Trans-Blot® Cell, BioRad) was assembled according to the manufacturer instructions. Transfer was carried out at 100V for 120 min. The transfer cassette was dismantled and membranes were checked for equal loading by staining with Ponceau S before rinsing with deionised water. Ponceau S stained membranes were scanned and thereafter washed for 5-15 min in PBS-T before membranes were blocked for 1-2 h at room temperature in BBS-T containing 5% (w/v) non-fat dry milk (Roth). The blocking solution was removed and membranes were washed briefly with PBS-T. Incubation with primary antibodies was carried out overnight by slowly shaking on a rotary shaker at 4°C in PBS-T supplemented with 5% (w/v) non-fat dry milk. Next morning the primary antibody solution was removed and membranes were washed 3x 15 min with PBS-T at room temperature on a rotary shaker. Bound primary antibodies were detected using horseradish peroxidise (HRP)-conjugated secondary antibodies (for antibody details see 3.1.10) diluted in PBS-T containing 5% (w/v) non-fat dry milk. Membranes were incubated with the secondary antibody for at least 1 h at room temperature by slowly rotating. The antibody solution was removed and membranes were washed as described above. This was followed by chemiluminescence detection using the SuperSignal® West Pico Chemimuminescent kit or a 5:1 - 1:1 mixture of the SuperSignal® West Pico Chemimuminescent- and SuperSignal® West Femto Maximum Sensitivity-kits (Pierce) according to the manufacturer instructions. Luminescence was detected by exposing the membrane to photographic film.

### 3.2.22 Yeast two-hybrid analyses

Yeast 2-hybrid constructs were cloned from the pDonr201 vector containing the appropriate constructs and fused to the C-terminus of the LexA DNA binding domain and B42 activation domain as described in Shen et. al. (2007). Prey and Bait plasmid were co-transformed into yeast strain EGY48 by using the LiAc method over night (as described above). Interaction analyses were performed according to the user manual (MATCHMAKER LexA Two Hybrid System User manual, PT3040-1; Clontech, Heidelberg).

**3.2.23 Determination of the fungal host cell entry rate**

*Arabidosis* plants were inoculated with *G. orontii* (as described in 3.2.6). For each genotype three leafs of three independent plants were detached and detained in EtOH/ Acidic acid (3:1) for at least 24 h, respectively. To visualize the fungal structures on the leaf surface, leafs were rinsed in $dH_2O$ and fungal structures were stained by slewing the leafs in 0,6 % Coomassie® brilliant blue R250 (in EtOH; Fluka) for 15-20 seconds. The sample leafs were rinsed again in dH2O and mounted on a microscope slide with 50% glycerol of analyzis.

The host cell entry attempt of *G orontii* is characterized by the formation of the primary hyphae that forms the appressorium. After successfully invading the host cell the fungus starts forming secondary hyphae. Therefore the ratio of primary vs. secondary hyphae forming spores can be used to determine the efficiency of the fungal host cell entry. A minimum of 50 interaction sites per leaf were analyzed using a light microscope.

**3.2.24 Microscopic analyzes of *Arabidopsis* pollen**

Light microscopy: For analysis of spores during development anthers were dissected and spores stained with DAPI (4'-6-Diamidino-2-phenylindole) and 0.03% aniline blue as described in Park *et al*., (1998). For each line spores from buds from 2 or 3 inflorescences were analyzed with 80-200 spores observed per bud.

Scanning electron microscopy: Pollen grains were sputter coated with gold and observed with a Zeiss DSM 940 scanning electron microscope.

Transmission electron microscopy was conducted as in Park and Twell (2001).

# 4.    References

**Aarts, N., Metz, M., Holub, E., Staskawicz, B.J., Daniels, M.J., and Parker, J.E.** (1998). Different requirements for *EDS1* and *NDR1* by disease resistance genes define at least two *R* gene-mediated signaling pathways in *Arabidopsis*. Proceedings of the National Academy of Sciences of the United States of America **95,** 10306-10311.

**Ade, J., DeYoung, B.J., Golstein, C., and Innes, R.W.** (2007). Indirect activation of a plant nucleotide binding site-leucine-rich repeat protein by a bacterial protease. Proceedings of the National Academy of Sciences of the United States of America **104,** 2531-2536.

**Adie, B.A.T., Perez-Perez, J., Perez-Perez, M.M., Godoy, M., Sanchez-Serrano, J.-J., Schmelz, E.A., and Solano, R.** (2007). ABA is an essential signal for plant resistance to pathogens affecting JA biosynthesis and the activation of defenses in Arabidopsis. The Plant Cell **19,** 1665-1681.

**Aist, J.R.** (1976). Papillae and Related Wound Plugs of Plant-Cells. Annual Review of Phytopathology **14,** 145-163.

**Andreasson, E., Jenkins, T., Brodersen, P., Thorgrimsen, S., Petersen, N.H.T., Zhu, S., Qiu, J.-L., Micheelsen, P., Rocher, A., Petersen, M., Newman, M.-A., Nielsen, H.B., Hirt, H., Somssich, I., Mattsson, O., and Mundy, J.** (2005). The MAP kinase substrate MKS1 is a regulator of plant defense responses. The EMBO Journal **24,** 2579-2589.

**Asai, T., Tena, G., Plotnikova, J., Willmann, M.R., Chiu, W.-L., Gomez-Gomez, L., Boller, T., Ausubel, F.M., and Sheen, J.** (2002). MAP kinase signalling cascade in *Arabidopsis* innate immunity. Nature **415,** 977-983.

**Assaad, F.F., Qiu, J.-L., Youngs, H., Ehrhardt, D., Zimmerli, L., Kalde, M., Wanner, G., Peck, S.C., Edwards, H., Ramonell, K., Somerville, C.R., and Thordal-Christensen, H.** (2004). The PEN1 syntaxin defines a novel cellular compartment upon fungal attack and is required for the timely assembly of papillae. Molecular Biology of the Cell **15,** 5118-5129.

**Attaran, E., Zeier, T.E., Griebel, T., and Zeier, J.** (2009). Methyl salicylate production and jasmonate signaling are not essential for systemic acquired resistance in *Arabidopsis*. The Plant Cell **21,** 954-971.

**Austin, M.J., Muskett, P., Kahn, K., Feys, B.J., Jones, J.D.G., and Parker, J.E.** (2002). Regulatory role of *SGT1* in early *R* gene-mediated plant defense. Science **295,** 2077-2080.

**Axtell, M.J., and Staskawicz, B.J.** (2003). Initiation of *RPS2*-specified disease resistance in *Arabidopsis* is coupled to the AvrRpt2-directed elimination of RIN4. Cell **112,** 369-377.

**Axtell, M.J., McNellis, T.W., Mudgett, M.B., Hsu, C.S., and Staskawicz, B.J.** (2001). Mutational analysis of the *Arabidopsis RPS2* disease resistance gene and the corresponding *Pseudomonas syringae avrRpt2* avirulence gene. Molecular Plant-Microbe Interactions **14,** 181-188.

**Bailey, J.A., and Mansfield, J.W.** (1982). Phytoalexins. (Glasgow: Blackie).

**Bartsch, M., Gobbato, E., Bednarek, P., Debey, S., Schultze, J.L., Bautor, J., and Parker, J.E.** (2006). Salicylic acid-independent ENHANCED DISEASE SUSCEPTIBILITY1 signaling in Arabidopsis immunity and cell death is regulated by the monooxygenase FMO1 and the nudix hydrolase NUDT7. The Plant Cell **18,** 1038-1051.

**Bednarek, P., Pislewska-Bednarek, M., Svatos, A., Schneider, B., Doubsky, J., Mansurova, M., Humphry, M., Consonni, C., Panstruga, R., Sanchez-Vallet, A., Molina, A., and Schulze-Lefert, P.** (2009). A glucosinolate metabolism pathway in living plant cells mediates broad-spectrum antifungal defense. Science **323,** 101-106.

**Berger, M.F., Philippakis, A.A., Qureshi, A.M., He, F.S., Estep, P.W., and Bulyk, M.L.** (2006). Compact, universal DNA microarrays to comprehensively determine transcription-factor binding site specificities. Nature Biotechnology **24,** 1429-1435.

**Bhat, R.A., Miklis, M., Schmelzer, E., Schulze-Lefert, P., and Panstruga, R.** (2005). Recruitment and interaction dynamics of plant penetration resistance components in a plasma membrane microdomain. Proceedings of the National Academy of Sciences of the United States of America **102,** 3135-3140.

**Bieri, S., Mauch, S., Shen, Q.H., Peart, J., Devoto, A., Casais, C., Ceron, F., Schulze, S., Steinbiss, H.H., Shirasu, K., and Schulze-Lefert, P.** (2004). RAR1 positively controls steady state levels of barley MLA resistance proteins and enables sufficient MLA6 accumulation for effective resistance. Plant Cell **16,** 3480-3495.

**Birnboim, H.C., and Doly, J.** (1979). A rapid alkaline extraction procedure for screening recombinant plasmid DNA. Nucleic Acids Research **7,** 1513-1523.

**Bittel, P., and Robatzek, S.** (2007). Microbe-associated molecular patterns (MAMPs) probe plant immunity. Current Opinion in Plant Biology **10,** 335-341.

**Boller, T.** (1995). Chemoperception of microbial signals in plant cells. Annual Reviews of Plant Physiology and Plant Molecular Biology **46,** 189-214.

**Boller, T., and Felix, G.** (2009). A renaissance of elicitors: Perception of microbe-associated molecular patterns and danger signals by pattern-recognition receptors. Annual Review of Plant Biology **60,** 379-406.

**Boyd, L.A., Smith, P.H., Foster, E.M., and Brown, J.K.M.** (1995). The Effects of Allelic Variation at the Mla Resistance Locus in Barley on the Early Development of Erysiphe-Graminis F Sp Hordei and Host Responses. Plant Journal **7,** 959-968.

**Boyes, D.C., Nam, J., and Dangl, J.L.** (1998). The *Arabidopsis thaliana RPM1* disease resistance gene product is a peripheral plasma membrane protein that is degraded coincident with the hypersensitive response. Proceedings of the National Academy of Sciences of the United States of America **95,** 15849-15854.

**Brownfield, L., Ford, K., Doblin, M.S., Newbigin, E., Read, S., and Bacic, A.** (2007). Proteomic and biochemical evidence links the callose synthase in Nicotiana alata pollen tubes to the product of the NaGSL1 gene. Plant J **52,** 147-156.

**Burch-Smith, T.M., Schiff, M., Caplan, J.L., Tsao, J., Czymmek, K., and Dinesh-Kumar, S.P.** (2007). A novel role for the TIR domain in association with pathogen-derived elicitors. PLoS Biology **5,** e68.

**Cernac, A., Andre, C., Hoffmann-Benning, S., and Benning, C.** (2006). WRI1 is required for seed germination and seedling establishment. Plant Physiology **141,** 745-757.

**Chandra-Shekara, A.C., Navarre, D., Kachroo, A., Kang, H.G., Klessig, D., and Kachroo, P.** (2004). Signaling requirements and role of salicylic acid in HRT- and rrt-mediated resistance to turnip crinkle virus in Arabidopsis. Plant Journal **40,** 647-659.

**Chandran, D., Tai, Y.C., Hather, G., Dewdney, J., Denoux, C., Burgess, D.G., Ausubel, F.M., Speed, T.P., and Wildermuth, M.C.** (2009). Temporal global expression data reveal known and novel salicylate-impacted processes and regulators mediating powdery mildew growth and reproduction on *Arabidopsis*. Plant Physiology **149,** 1435-1451.

**Chen, X.Y., Liu, L., Lee, E., Han, X., Rim, Y., Chu, H., Kim, S.W., Sack, F., and Kim, J.Y.** (2009). The Arabidopsis Callose Synthase Gene GSL8 Is Required for Cytokinesis and Cell Patterning. Plant Physiology **150,** 105-113.

**Chini, A., Fonseca, S., Fernandez, G., Adie, B., Chico, J.M., Lorenzo, O., Garcia-Casado, G., Lopez-Vidriero, I., Lozano, F.M., Ponce, M.R., Micol, J.L., and Solano, R.** (2007). The JAZ family of repressors is the missing link in jasmonate signalling. Nature **448,** 666-671.

**Ciolkowski, I., Wanke, D., Birkenbihl, R., and Somssich, I.** (2008). Studies on DNA-binding selectivity of WRKY transcription factors lend structural clues into WRKY-domain function. Plant Molecular Biology **68,** 81-92.

**Clay, N.K., Adio, A.M., Denoux, C., Jander, G., and Ausubel, F.M.** (2009). Glucosinolate metabolites required for an *Arabidopsis* innate immune response. Science **323,** 95-101.

**Clough, S.J., and Bent, A.F.** (1998). Floral dip: a simplified method for Agrobacterium-mediated transformation of *Arabidopsis thaliana*. The Plant Journal **16,** 735-743.

**Collier, S.M., and Moffett, P.** (2009). NB-LRRs work a "bait and switch" on pathogens. Trends in Plant Science **14,** 521-529.

**Collins, N.C., Thordal-Christensen, H., Lipka, V., Bau, S., Kombrink, E., Qiu, J.L., Huckelhoven, R., Stein, M., Freialdenhoven, A., Somerville, S.C., and Schulze-Lefert, P.** (2003). SNARE-protein-mediated disease resistance at the plant cell wall. Nature **425,** 973-977.

**Consonni, C., Bednarek, P., Humphry, M., Francocci, F., Ferrari, S., Harzen, A., Ver Loren van Themaat, E., and Panstruga, R.** (2010). Tryptophan-derived metabolites are required for antifungal defense in the *Arabidopsis mlo2* mutant. Plant Physiology **152,** 1544-1561.

**Cooley, M.B., Pathirana, S., Wu, H.-J., Kachroo, P., and Klessig, D.F.** (2000). members of the Arabidopsis *HRT/RPP8* family of resistance genes confer resistance to both viral and oomycete pathogens. The Plant Cell **12,** 663-676.

**Cui, X., Shin, H., Song, C., Laosinchai, W., Amano, Y., and Brown, R.M., Jr.** (2001). A putative plant homolog of the yeast beta-1,3-glucan synthase subunit FKS1 from cotton (Gossypium hirsutum L.) fibers. Planta **213,** 223-230.

**Dangl, J.L., and Jones, J.D.G.** (2001). Plant pathogens and intergrated defence responses to infection. Nature **411,** 826-833.

**Danot, O., Marquenet, E., Vidal-Ingigliardi, D., and Richet, E.** (2009). Wheel of Life, Wheel of Death: A Mechanistic Insight into Signaling by STAND Proteins. Structure **17,** 172-182.

**Dinesh-Kumar, S.P., Tham, W.-H., and Baker, B.J.** (2000). Structure-function analysis of the tobacco mosaic virus resistance gene *N*. Proceedings of the National Academy of Sciences of the United States of America **97,** 14789-14794.

**Dombrecht, B., Xue, G.P., Sprague, S.J., Kirkegaard, J.A., Ross, J.J., Reid, J.B., Fitt, G.P., Sewelam, N., Schenk, P.M., Manners, J.M., and Kazan, K.** (2007). MYC2 differentially modulates diverse jasmonate-dependent functions in Arabidopsis. The Plant Cell **19,** 2225-2245.

**Dong, X., Hong, Z., Sivaramakrishnan, M., Mahfouz, M., and Verma, D.P.** (2005). Callose synthase (CalS5) is required for exine formation during microgametogenesis and for pollen viability in Arabidopsis. Plant J **42,** 315-328.

**Duan, M.-R., Nan, J., Liang, Y.-H., Mao, P., Lu, L., Li, L., Wei, C., Lai, L., Li, Y., and Su, X.-D.** (2007). DNA binding mechanism revealed by high resolution crystal structure of Arabidopsis thaliana WRKY1 protein. Nucleic Acids Research **35,** 1145-1154.

**Durbarry, A., Vizir, I., and Twell, D.** (2005). Male germ line development in Arabidopsis. duo pollen mutants reveal gametophytic regulators of generative cell cycle progression. Plant Physiol **137,** 297-307.

**Eastmond, P.J.** (2006). SUGAR-DEPENDENT1 encodes a patatin domain triacylglycerol lipase that initiates storage oil breakdown in germinating Arabidopsis seeds. Plant Cell **18,** 665-675.

**Eckey, C., Korell, M., Leib, K., Biedenkopf, D., Jansen, C., Langen, G., and Kogel, K.-H.** (2004). Identification of powdery midew-induced barley genes by cDNA-AFLP: functional assessment of an early expressed MAP kinase. Plant Molecular Biology **55,** 1-15.

**Enns, L.C., Kanaoka, M.M., Torii, K.U., Comai, L., Okada, K., and Cleland, R.E.** (2005). Two callose synthases, GSL1 and GSL5, play an essential and redundant role in plant and pollen development and in fertility. Plant Mol Biol **58,** 333-349.

**Erickson, F.L., Holzberg, S., Calderon-Urrea, A., Handley, V., Axtell, M., Corr, C., and Baker, B.** (1999a). The helicase domain of the TMV replicase proteins induces the N-mediated defence response in tobacco. Plant Journal **18,** 67-75.

**Erickson, F.L., Dinesh-Kumar, S.P., Holzberg, S., Ustach, C.V., Dutton, M., Handley, V., Corr, C., and Baker, B.J.** (1999b). Interactions between tobacco mosaic virus and the tobacco N gene. Philosophical Transactions of the Royal Society of London Series B-Biological Sciences **354,** 653-658.

**Eulgem, T., and Somssich, I.E.** (2007). Networks of WRKY transcription factors in defense signaling. Current Opinion in Plant Biology **10,** 366-371.

**Eulgem, T., Rushton, P.J., Robatzek, S., and Somssich, I.E.** (2000). The WRKY superfamily of plant transcription factors. Trends in Plant Science **5,** 199-206.

**Eulgem, T., Rushton, P.J., Schmelzer, E., Hahlbrock, K., and Somssich, I.E.** (1999). Early nuclear events in plant defense: rapid gene activation by WRKY transcription factors. The EMBO Journal **18,** 4689-4699.

**Falk, A., Feys, B.J., Frost, L.N., Jones, J.D.G., Daniels, M., and Parker, J.E.** (1999). *EDS1*, an essential component of R gene-mediated disease resistance in *Arabidopsis* has homolgy to eukaryotic lipases. Proceedings of the National Academy of Sciences of the United States of America **96,** 3292-3297.

**Felix, G., Duran, J.D., Volko, S., and Boller, T.** (1999). Plants have a sensitive perception system for the most conserved domain of bacterial flagellin. The Plant Journal **18,** 265-276.

**Ferguson, C., Teeri, T.T., Siika-aho, M., Read, S.M., and Bacic, A.** (1998). Location of cellulose and callose in pollen tubes and grains of Nicotiana tabacum. Planta **206,** 452-460.

**Ferrari, S., Galletti, R., Denoux, C., De Lorenzo, G., Ausubel, F.M., and Dewdney, J.** (2007). Resistance to *Botrytis cinerea* induced in Arabidopsis by elicitors is independent of salicylic acid, ethylene, or jasmonate signaling but requires PHYTOALEXIN DEFICIENT3. Plant Physiology **144,** 367-379.

**Feys, B.J., Moisan, L.J., Newman, M.-A., and Parker, J.E.** (2001). Direct interaction between the *Arabidopsis* disease resistance signaling proteins, EDS1 and PAD4. The EMBO Journal **20,** 5400-5411.

**Flor, H.H.** (1971). Current status of the gene-for-gene concept. Annual Review of Phytopathology **9,** 275-296.

**Freialdenhoven, A., Scherag, B., Hollricher, K., Collinge, D.B., Thordalchristensen, H., and Schulze-Lefert, P.** (1994). Nar-1 and Nar-2, 2 Loci Required for Mla(12)-Specified Race-Specific Resistance to Powdery Mildew in Barley. Plant Cell **6,** 983-994.

**García, A.V., Blanvillain-Baufumé, S., Huibers, R.P., Wiermer, M., Li, G., Gobbato, E., Rietz, S., and Parker, J.E.** (2010). Balanced nuclear and cytoplasmic activities of EDS1 are required for a complete plant innate immune response. PLoS Pathogens **6,** e1000970.

**Garcion, C., Lohmann, A., Lamodiere, E., Catinot, J., Buchala, A., Doermann, P., and Metraux, J.-P.** (2008). Characterization and biological function of the *ISOCHORISMATE SYNTHASE2* gene of Arabidopsis. Plant Physiology **147,** 1279-1287.

**Gardiner, J.C., Taylor, N.G., and Turner, S.R.** (2003). Control of cellulose synthase complex localization in developing xylem. The Plant Cell **15,** 1740-1748.

**Glawischnig, E.** (2007). Camalexin. Phytochemistry **68,** 401-406.

**Glazebrook, J.** (2005). Contrasting mechanisms of defense against biotrophic and necrotrophic pathogens. Annual Reviews of Phytopathology **43,** 205-227.

**Glazebrook, J., and Ausubel, F.M.** (1994). Isolation of phytoalexin-deficient mutants of *Arabidopsis thaliana* and characterization of their interactions with bacterial pathogens. Proceedings of the National Academy of Sciences of the United States of America **91,** 8955-8959.

**Gómez-Gómez, L., and Boller, T.** (2000). FLS2: an LRR receptor-like kinase involved in the perception of the bacterial elicitor flagellin in *Arabidopsis*. Molecular Cell **5,** 1003-1011.

**Grant, M.R., Godiard, L., Straube, E., Ashfield, T., Lewald, J., Sattler, A., Innes, R.W., and Dangl, J.L.** (1995). Structure of the *Arabidopsis RPMI* gene enabling dual specificity disease resistance. Science **269,** 843-846.

**Guseman, J.M., Lee, J.S., Bogenschutz, N.L., Peterson, K.M., Virata, R.E., Xie, B., Kanaoka, M.M., Hong, Z.L., and Torii, K.U.** (2010). Dysregulation of cell-to-cell connectivity and stomatal patterning by loss-of-function mutation in Arabidopsis CHORUS (GLUCAN SYNTHASE-LIKE 8). Development **137,** 1731-1741.

**Gutierrez, J.R., Balmuth, A.L., Ntoukakis, V., Mucyn, T.S., Gimenez-Ibanez, S., Jones, A.M.E., and Rathjen, J.P.** (2010). Prf immune complexes of tomato are oligomeric and contain multiple Pto-like kinases that diversify effector recognition. Plant Journal **61,** 507-518.

**Halkier, B.A., and Gershenzon, J.** (2006). Biology and biochemistry of glucosinolates. Annual Review of Plant Biology **57,** 303-333.

**Halterman, D., Zhou, F.S., Wei, F.S., Wise, R.P., and Schulze-Lefert, P.** (2001). The MLA6 coiled-coil, NBS-LRR protein confers AvrMla6-dependent resistance specificity to Blumeria graminis f. sp hordei in barley and wheat. Plant Journal **25,** 335-348.

**Halterman, D.A., and Wise, R.P.** (2004). A single-amino acid substitution in the sixth leucine-rich repeat of barley MLA6 and MLA13 alleviates dependence on RAR1 for disease resistance signaling. The Plant Journal **38,** 215-226.

**Heath, M.C.** (2000). Nonhost resistance and nonspecific plant defenses. Current Opinion in Plant Biology **3,** 315-319.

**Howden, R., Park, S.K., Moore, J.M., Orme, J., Grossniklaus, U., and Twell, D.** (1998). Selection of T-DNA tagged male and female gametophytic mutants by segregation distortion in Arabidopsis. Genetics **149,** 621-631.

**Hu, J., Barlet, X., Deslandes, L., Hirsch, J., Feng, D.X., Somssich, I., and Marco, Y.** (2008). Transcriptional responses of *Arabidopsis thaliana* during wilt disease caused by the soil-borne phytopathogenic bacterium, *Ralstonia solanacearum*. PLoS ONE **3,** e2589.

**Huang, L.J., Chen, X.Y., Rim, Y., Han, X., Cho, W.K., Kim, S.W., and Kim, J.Y.** (2009). Arabidopsis glucan synthase-like 10 functions in male gametogenesis. Journal of Plant Physiology **166,** 344-352.

**Hubert, D.A., Tornero, P., Belkhadir, Y., Krishna, P., Takahashi, A., Shirasu, K., and Dangl, J.L.** (2003). Cytosolic HSP90 associates with and modulates the *Arabidopsis* RPM1 disease resistance protein. The EMBO Journal**,** 5679-5689.

**Jacobs, A.K., Lipka, V., Burton, R.A., Panstruga, R., Strizhov, N., Schulze-Lefert, P., and Fincher, G.B.** (2003). An Arabidopsis Callose Synthase, GSL5, Is Required for Wound and Papillary Callose Formation. Plant Cell **15,** 2503-2513.

**Jeong, R.D., Chandra-Shekara, A.C., Barman, S.R., Navarre, D., Klessig, D.F., Kachroo, A., and Kachroo, P.** (2010). Cryptochrome 2 and phototropin 2 regulate resistance protein-mediated viral defense by negatively regulating an E3 ubiquitin ligase. Proceedings of the National Academy of Sciences of the United States of America **107,** 13538-13543.

**Jia, Y., McAdams, S.A., Bryan, G.T., Hershey, H.P., and Valent, B.** (2000). Direct interaction of resistance gene and avirulence gene products confers rice blast resistance. The EMBO Journal **19,** 4004-4014.

**Jirage, D., Tootle, T.L., Reuber, L.T., Frost, L.N., Feys, B.J., Parker, J.E., Ausubel, F.M., and Glazebrook, J.** (1999). *Arabidopsis thaliana PAD4* encodes a lipase-like gene that is important for salicylic acid signaling. Proceedings of the National Academy of Sciences of the United States of America **96,** 13583-13588.

**Jones, J.D.G., and Dangl, J.L.** (2006). The plant immune system. Nature **444,** 323-329.

**Jorgensen, J.H.** (1994). Genetics of Powdery Mildew Resistance in Barley. Critical Reviews in Plant Sciences **13,** 97-119.

**Journot-Catalino, N., Somssich, I.E., Roby, D., and Kroj, T.** (2006). The transcription factors WRKY11 and WRKY17 act as negative regulators of basal resistance in *Arabidopsis thaliana*. The Plant Cell **18,** 3289-3302.

**Kachroo, P., Yoshioka, K., Shah, J., Dooner, H.K., and Klessig, D.F.** (2000). Resistance to Turnip Crinkle Virus in Arabidopsis is regulated by two host genes and is salicylic acid dependent but *NPR1*, ethylene, and jasmonate independent. The Plant Cell **12,** 677-690.

**Kang, H.-G., Oh, C.-S., Sato, M., Katagiri, F., Glazebrook, J., Takahashi, H., Kachroo, P., Martin, G.B., and Klessig, D.F.** (2010). Endosome-associated CRT1 functions early in resistance gene-mediated defense signaling in *Arabidopsis* and Tobacco. The Plant Cell **22,** 918-936.

**Kang, H.G., Kuhl, J.C., Kachroo, P., and Klessig, D.F.** (2008). CRT1, an Arabidopsis ATPase that interacts with diverse resistance proteins and modulates disease resistance to turnip crinkle virus. Cell Host & Microbe **3,** 48-57.

**Kazan, K., and Manners, J.M.** (2009). Linking development to defense: auxin in plant-pathogen interactions. Trends in Plant Science **14,** 373-382.

**Kessler, S.A., Shimosato-Asano, H., Keinath, N.F., Wuest, S.E., Ingram, G., Panstruga, R., and Grossniklaus, U.** (2010). Conserved molecular components for pollen tube reception and fungal invasion. Science **330,** 968-971.

**Kjell, J., Rasmusson, A.G., Larsson, H., and Widell, S.** (2004). Protein complexes of the plant plasma membrane resolved by Blue Native PAGE. Physiologia Plantarum **121,** 546-555.

**Kliebenstein, D.J.** (2004). Secondary metabolites and plant/environment interactions: a view through Arabidopsis thaliana tinged glasses. Plant Cell and Environment **27,** 675-684.

**Knoth, C., Ringler, J., Dangl, J.L., and Eulgem, T.** (2007). Arabidopsis WRKY70 is required for full *RPP4*-mediated disease resistance and basal defense against *Hyaloperonospora parasitica*. Molecular Plant-Microbe Interactions **20,** 120-128.

**Kwon, C., Neu, C., Pajonk, S., Yun, H.S., Lipka, U., Humphry, M., Bau, S., Straus, M., Kwaaitaal, M., Rampelt, H., Kasmi, F.E., Jurgens, G., Parker, J., Panstruga, R., Lipka, V., and Schulze-Lefert, P.** (2008). Co-option of a default secretory pathway for plant immune responses. Nature **451,** 835-840.

**Lelpe, D.D., Koonin, E.V., and Aravind, L.** (2004). STAND, a class of P-loop NTPases including animal and plant regulators of programmed cell death: Multiple, complex domain architectures, unusual phyletic patterns, and evolution by horizontal gene transfer. Journal of Molecular Biology **343,** 1-28.

**Levin, D.E.** (2005). Cell wall integrity signaling in Saccharomyces cerevisiae. Microbiol Mol Biol Rev **69,** 262-291.

**Li, H., Bacic, A., and Read, S.M.** (1997). Activation of pollen tube callose synthase by detergents. Evidence for different mechanisms of action. Plant Physiol **114,** 1255-1265.

**Li, J., Brader, G., and Palva, E.T.** (2004). The WRKY70 transcription factor: a node of convergence for jasmonate-mediated and salicylate-mediated signals in plant defense. The Plant Cell **16,** 319-331.

**Li, J., Brader, G., Kariola, T., and Tapio Palva, E.** (2006). WRKY70 modulates the selection of signaling pathways in plant defense. The Plant Journal **46,** 477-491.

**Li, J., Burton, R.A., Harvey, A.J., Hrmova, M., Wardak, A.Z., Stone, B.A., and Fincher, G.B.** (2003). Biochemical evidence linking a putative callose synthase gene with (1 --> 3)-beta-D-glucan biosynthesis in barley. Plant Mol Biol **53,** 213-225.

**Lipka, U., Fuchs, R., and Lipka, V.** (2008). Arabidopsis non-host resistance to powdery mildews. Current Opinion in Plant Biology **11,** 404-411.

**Lipka, V., Dittgen, J., Bednarek, P., Bhat, R., Wiermer, M., Stein, M., Landtag, J., Brandt, W., Rosahl, S., Scheel, D., Llorente, F., Molina, A., Parker, J., Somerville, S., and Schulze-Lefert, P.** (2005). Pre- and postinvasion defenses both contribute to nonhost resistance in *Arabidopsis*. Science **310,** 1180-1183.

**Liu, Y., Schiff, M., and Dinesh-Kumar, S.P.** (2004a). Involvement of MEK1 MAPKK, NTF6 MAPK, WRKY/MYB transcription factors, COI1 and CTR1 in *N*-mediated resistance to tobacco mosaic virus. The Plant Journal **38,** 800-809.

**Liu, Y.L., Burch-Smith, T., Schiff, M., Feng, S.H., and Dinesh-Kumar, S.P.** (2004b). Molecular chaperone Hsp90 associates with resistance protein n and its signaling proteins SGT1 and Rar1 to modulate an innate immune response in plants. Journal of Biological Chemistry **279,** 2101-2108.

**Lopez-Maury, L., Marguerat, S., and Bahler, J.** (2008). Tuning gene expression to changing environments: from rapid responses to evolutionary adaptation. Nature Review Genetics **9,** 583-593.

**Lorenzo, O., Chico, J.M., Sanchez-Serrano, J.J., and Solano, R.** (2004). JASMONATE-INSENSITIVE1 encodes a MYC transcription factor essential to discriminate between different jasmonate-regulated defense responses in Arabidopsis. Plant Cell **16,** 1938-1950.

**Mackey, D., III, H.B.F., Wiig, A., and Dangl, J.L.** (2002). RIN4 interacts with *Pseudomonas syringae* type III effector molecules and is required for RPM1-mediated resistance in *Arabidopsis*. Cell **108,** 743-754.

**Mackey, D., Belkhadir, Y., Alonso, J.M., Ecker, J.R., and Dangl, J.L.** (2003). *Arabidopsis* RIN4 is a target of the type III virulence effector AvrRpt2 and modulates RPS2-mediated resistance. Cell **112,** 379-389.

**Mazur, P., and Baginsky, W.** (1996). In vitro activity of 1,3-beta-D-glucan synthase requires the GTP-binding protein Rho1. J Biol Chem **271,** 14604-14609.

**Mazur, P., Morin, N., Baginsky, W., el-Sherbeini, M., Clemas, J.A., Nielsen, J.B., and Foor, F.** (1995). Differential expression and function of two homologous subunits of yeast 1,3-beta-D-glucan synthase. Mol Cell Biol **15,** 5671-5681.

**McCormick, S.** (1993). Male Gametophyte Development. Plant Cell **5,** 1265-1275.

**McDowell, J.M., Dhandaydham, M., Long, T.A., Aarts, M.G.M., Goff, S., Holub, E.B., and Dangl, J.L.** (1998). Intragenic recombination and diversifying selection contribute to the evolution of the downy mildew resistance at the *RPP8* locus of Arabidopsis. The Plant Cell **10,** 1861-1874.

**Menke, F.L.H., Kang, H.-G., Chen, Z., Park, J.M., Kumar, D., and Klessig, D.F.** (2005). Tobacco transription factor WRKY1 is phosphorylated by the MAP kinase SIPK and mediates HR-like cell death in tobacco. Molecular Plant-Microbe Interactions **18,** 1027-1034.

**Mestre, P., and Baulcombe, D.C.** (2006). Elicitor-mediated oligomerization of the tobacco N disease resistance protein. Plant Cell **18,** 491-501.

**Meyer, D., Pajonk, S., Micali, C., O'Connell, R., and Schulze-Lefert, P.** (2009). Extracellular transport and integration of plant secretory proteins into pathogen-induced cell wall compartments. Plant Journal **57,** 986-999.

**Meyers, B.C., Kozik, A., Griego, A., Kuang, H.H., and Michelmore, R.W.** (2003). Genome-wide analysis of NBS-LRR-encoding genes in Arabidopsis (vol 15, pg 809, 2003). Plant Cell **15,** 1683-1683.

**Mohr, T.J., Mammarella, N.D., Hoff, T., Woffenden, B.J., Jelesko, J.G., and McDowell, J.M.** (2010). The Arabidopsis downy mildew resistance gene *RPP8* is induced by pathogens and salicylic acid and is regulated by W box *cis* elements. Molecular Plant-Microbe Interactions **23,** 1303-1315.

**Murray, S.L., Ingle, R.A., Petersen, L.N., and Denby, K.J.** (2007). Basal resistance against *Pseudomonas syringae* in *Arabidopsis* involves WRKY53 and a protein with homology to a nematode resistance protein. Molecular Plant-Microbe Interactions **20,** 1431-1438.

**Nafisi, M., Goregaoker, S., Botanga, C.J., Glawischnig, E., Olsen, C.E., Halkier, B.A., and Glazebrook, J.** (2007). Arabidopsis cytochrome P450 monooxygenase 71A13 catalyzes the conversion of indole-3-acetaldoxime in camalexin synthesis. The Plant Cell **19,** 2039-2052.

**Nimchuk, Z., Eulgem, T., Holt III, B.F., and Dangl, J.L.** (2003). Recognition and response in the plant immune system. Annual Reviews in Genetics **37,** 579-609.

**Nishikawa, S., Zinkl, G.M., Swanson, R.J., Maruyama, D., and Preuss, D.** (2005). Callose (beta-1,3 glucan) is essential for Arabidopsis pollen wall patterning, but not tube growth. BMC Plant Biol **5,** 22.

**Nishimura, M.T., Stein, M., Hou, B.-H., Vogel, J.P., Edwards, H., and Somerville, S.C.** (2003). Loss of a callose synthase results in salicylic acid–dependent disease resistance. Science **301,** 969-972.

**Noutoshi, Y., Ito, T., Seki, M., Nakashita, H., Yoshida, S., Marco, Y., Shirasu, K., and Shinozaki, K.** (2005). A single amino acid insertion in the WRKY domain of the Arabidopsis TIR-NBS-LRR-WRKY-type disease resistance protein SLH1 (sensitive to low humidity 1) causes activation of defense responses and hypersensitive cell death. The Plant Journal **43,** 873-888.

**Nürnberger, T., and Lipka, V.** (2005). Non-host resistance in plants: new insights into an old phenomenon. Molecular Plant Pathology **6,** 335-345.

**Nürnberger, T., Brunner, F., Kemmerling, B., and Piater, L.** (2004). Innate immunity in plants and animals: striking similarities and obvious differences. Immunological Reviews **198,** 249-266.

**Ostergaard, L., Petersen, M., Mattsson, O., and Mundy, J.** (2002). An Arabidopsis callose synthase. Plant Mol Biol **49,** 559-566.

**Pandey, A., and Mann, M.** (2000). Proteomics to study genes and genomes. Nature **405,** 837-846.

**Pandey, S.P., and Somssich, I.E.** (2009). The role of WRKY transcription factors in plant immunity. Plant Physiology **150,** 1648-1655.

**Pandey, S.P., Roccaro, M., Schön, M., Logemann, E., and Somssich, I.E.** (in press). Transcriptional reprogramming regulated by WRKY18 and WRKY40 facilitates powdery mildew infection of *Arabidopsis*. The Plant Journal.

**Park, S.K., and Twell, D.** (2001). Novel patterns of ectopic cell plate growth and lipid body distribution in the Arabidopsis gemini pollen1 mutant. Plant Physiol **126,** 899-909.

**Park, S.K., Howden, R., and Twell, D.** (1998). The Arabidopsis thaliana gametophytic mutation gemini pollen1 disrupts microspore polarity, division asymmetry and pollen cell fate. Development **125,** 3789-3799.

**Parker, J.E., Holub, E.B., Frost, L.N., Falk, A., Gunn, N.D., and Daniels, M.J.** (1996). Characterization of *eds1*, a mutation in Arabidopsis suppressing resistance to *Peronospora parasitica* specified by several different *RPP* genes. The Plant Cell **8,** 2033-2046.

**Patel, V.K., Shanklin, J., and Furtek, D.B.** (1994). Changes in fatty-acid composition and stearoyl-acyl carrier protein desaturase expression in developing *Theobroma cacao* L. embryos. Planta **193,** 83-88.

**Peart, J.R., Cook, G., Feys, B.J., Parker, J.E., and Baulcombe, D.C.** (2002a). An *EDS1* orthologue is required for *N*-mediated resistance against tobacco mosaic virus. The Plant Journal **29,** 569-579.

**Peart, J.R., Lu, R., Sadanandom, A., Malcuit, I., Moffett, P., Brice, D.C., Schauser, L., Jaggard, D.A.W., Xiao, S., Coleman, M.J., Dow, M., Jones, J.D.G., Shirasu, K., and Baulcombe, D.C.** (2002b). Ubiquitin ligase-associated protein SGT1 is required for host and nonhost disease resistance in plants. Proceedings of the National Academy of Sciences of the United States of America **99,** 10865-10869.

**Pedras, M.S.C., Yaya, E.E., and Hossain, S.** (2010). Unveiling the phytoalexin biosynthetic puzzle in salt cress: unprecedented incorporation of glucobrassicin into wasalexins A and B. Organic & Biomolecular Chemistry **8,** 5150-5158.

**Pelosi, L., Imai, T., Chanzy, H., Heux, L., Buhler, E., and Bulone, V.** (2003). Structural and morphological diversity of (1-->3)-beta-D-glucans synthesized in vitro by enzymes from Saprolegnia monoica. Comparison with a corresponding in vitro product from blackberry (Rubus fruticosus). Biochemistry **42,** 6264-6274.

**Persson, S., Paredez, A., Carroll, A., Palsdottir, H., Doblin, M., Poindexter, P., Khitrov, N., Auer, M., and Somerville, C.R.** (2007). Genetic evidence for three unique components in primary cell-wall cellulose synthase complexes in Arabidopsis. Proceedings of the National Academy of Sciences of the United States of America **104,** 15566-15571.

**Petutschnig, E.K., Jones, A.M.E., Serazetdinova, L., Lipka, U., and Lipka, V.** (2010). The lysin motif receptor-like kinase (LysM-RLK) CERK1 is a major chitin-binding protein in *Arabidopsis thaliana* and subject to chitin-induced phosphorylation. Journal of Biological Chemistry **285,** 28902-28911.

**Pieterse, C.M.J., and Dicke, M.** (2007). Plant interactions with microbes and insects: from molecular mechanisms to ecology. Trends in Plant Science **12,** 564-569.

**Qi, S.Q., Pang, Y.X., Hu, Q., Liu, Q., Li, H., Zhou, Y.L., He, T.X., Liang, Q.L., Liu, Y.X., Yuan, X.Q., Luo, G.A., Li, H.L., Wang, J.W., Yan, N., and Shi, Y.G.** (2010). Crystal Structure of the Caenorhabditis elegans Apoptosome Reveals an Octameric Assembly of CED-4. Cell **141,** 446-457.

**Rafiqi, M., Bernoux, M., Ellis, J.G., and Dodds, P.N.** (2009). In the trenches of plant pathogen recognition: Role of NB-LRR proteins. Seminars in Cell & Developmental Biology **20,** 1017.

**Rairdan, G.J., Collier, S.M., Sacco, M.A., Baldwin, T.T., Boettrich, T., and Moffett, P.** (2008). The coiled-coil and nucleotide binding domains of the potato Rx disease resistance protein function in pathogen recognition and signaling. The Plant Cell **20,** 739-751.

**Rate, D.N., Cuenca, J.V., Bowman, G.R., Guttman, D.S., and Greenberg, J.T.** (1999). The gain-of-function Arabidopsis *acd6* mutant reveals novel regulation and function of the salicylic acid signaling pathway in controlling cell death, defenses, and cell growth. The Plant Cell **11,** 1695-1708.

**Riedl, S.J., Li, W.Y., Chao, Y., Schwarzenbacher, R., and Shi, Y.G.** (2005). Structure of the apoptotic protease-activating factor 1 bound to ADP. Nature **434,** 926-933.

**Ross, C.A., Liu, Y., and Shen, Q.J.** (2007). The WRKY gene family in rice (*Oryza sativa*). Journal of Integrative Plant Biology **49,** 827-842.

**Rushton, P.J., Somssich, I.E., Ringler, P., and Shen, Q.J.** (2010). WRKY transcription factors. Trends in Plant Science **15,** 247-258.

**Rushton, P.J., Torres, J.T., Parniske, M., Wernert, P., Hahlbrock, K., and Somssich, I.E.** (1996). Interaction of elicitor-induced DNA binding proteins with elicitor response elements in the promoters of parsley PR1 genes. The EMBO Journal **15,** 5690-5700.

**Rusterucci, C., Aviv, D.H., Holt, B.F., Dangl, J.L., and Parker, J.E.** (2001). The disease resistance signaling components EDS1 and PAD4 are essential regulators of the cell death pathway controlled by LSD1 in arabidopsis. Plant Cell **13,** 2211-2224.

**Sacco, M.A., Mansoor, S., and Moffett, P.** (2007). A RanGAP protein physically interacts with the NB-LRR protein Rx, and is required for Rx-mediated viral resistance. The Plant Journal **52,** 82-93.

**Samuels, A.L., Giddings, T.H., Jr., and Staehelin, L.A.** (1995). Cytokinesis in tobacco BY-2 and root tip cells: a new model of cell plate formation in higher plants. J Cell Biol **130,** 1345-1357.

**Sanchez-Vallet, A., Ramos, B., Bednarek, P., Lopez, G., Pislewska-Bednarek, M., Schulze-Lefert, P., and Molina, A.** (2010). Tryptophan-derived secondary metabolites in Arabidopsis thaliana confer non-host resistance to necrotrophic Plectosphaerella cucumerina fungi. Plant Journal **63,** 115-127.

**Sanger, F.** (1977). Nucleotide sequence of bacteriophage phi X174 DNA. Nature **265,** 687.

**Sarkar, P., Bosneaga, E., and Auer, M.** (2009). Plant cell walls throughout evolution: towards a molecular understanding of their design principles. Journal of Experimental Botany **60,** 3615-3635.

**Saxena, I.M., and Brown, R.M., Jr.** (2000). Cellulose synthases and related enzymes. Curr Opin Plant Biol **3,** 523-531.

**Scherp, P., Grotha, R., and Kutschera, U.** (2001). Occurrence and phylogenetic significance of cytocinesis-related callose in green algea, ferns and seed plants. Plant Cell Reports **20,** 143-149.

**Schimoler-O'Rourke, R., Renault, S., Mo, W., and Selitrennikoff, C.P.** (2003). Neurospora crassa FKS protein binds to the (1,3)beta-glucan synthase substrate, UDP-glucose. Curr Microbiol **46,** 408-412.

**Schlaeppi, K., Abou-Mansour, E., Buchala, A., and Mauch, F.** (2010). Disease resistance of Arabidopsis to *Phytophthora brassicae* is established by the sequential action of indole glucosinolates and camalexin. The Plant Journal **62,** 840-851.

**Schmelzer, E.** (2002). Cell polarization, a crucial process in fungal defence. Trends in Plant Science **7,** 411-415.

**Schuhegger, R., Nafisi, M., Mansourova, M., Petersen, B.L., Olsen, C.E., Svatos, A., Halkier, B.A., and Glawischnig, E.** (2006). CYP71B15 (PAD3) catalyzes the final step in camalexin biosynthesis. Plant Physiology **141,** 1248-1254.

**Schulze-Lefert, P.** (2004). Plant immunity: the origami of receptor activation. Current Biology **14,** R22-R24.

**Seeholzer, S., Tsuchimatsu, T., Jordan, T., Bieri, S., Pajonk, S., Yang, W.X., Jahoor, A., Shimizu, K.K., Keller, B., and Schulze-Lefert, P.** (2010). Diversity at the Mla Powdery Mildew Resistance Locus from Cultivated Barley Reveals Sites of Positive Selection. Molecular Plant-Microbe Interactions **23,** 497-509.

**Sekine, K.T., Ishihara, T., Hase, S., Kusano, T., Shah, J., and Takahashi, H.** (2006). Single amino acid alterations in Arabidopsis thaliana RCY1 compromise resistance to Cucumber mosaic virus, but differentially suppress hypersensitive response-like cell death. Plant Molecular Biology **62,** 669-682.

**Shang, Y., Yan, L., Liu, Z.-Q., Cao, Z., Mei, C., Xin, Q., Wu, F.-Q., Wang, X.-F., Du, S.-Y., Jiang, T., Zhang, X.-F., Zhao, R., Sun, H.-L., Liu, R., Yu, Y.-T., and Zhang, D.-P.** (2010). The Mg-chelatase H subunit of *Arabidopsis* antagonizes a group of WRKY transcription repressors to relieve ABA-responsive genes of inhibition. The Plant Cell **22,** 1909-1935.

**Shao, F., Golstein, C., Ade, J., Stoutemyer, M., Dixon, J.E., and Innes, R.W.** (2003). Cleavage of *Arabidopsis* PBS1 by a bacterial type III effector. Science **301,** 1230-1233.

**Shen, Q.-H., and Schulze-Lefert, P.** (2007). Rumble in the nuclear jungle: compartmentalization, trafficking, and nuclear action of plant immune receptors. The EMBO Journal **26,** 4293-4301.

**Shen, Q.-H., Saijo, Y., Mauch, S., Biskup, C., Bieri, S., Keller, B., Seki, H., Ulker, B., Somssich, I.E., and Schulze-Lefert, P.** (2007). Nuclear activity of MLA immune receptors links isolate-specific and basal disease-resistance responses. Science **315,** 1098-1103.

**Shen, Q.H., Zhou, F.S., Bieri, S., Haizel, T., Shirasu, K., and Schulze-Lefert, P.** (2003). Recognition specificity and RAR1/SGT1 dependence in barley Mla disease resistance genes to the powdery mildew fungus. Plant Cell **15,** 732-744.

**Sherameti, I., Venus, Y., Drzewiecki, C., Tripathi, S., Dan, V.M., Nitz, I., Varma, A., Grundler, F.M., and Oelmuller, R.** (2008). PYK10, a B-glucosidase located in the endoplasmatic reticulum, is crucial for the beneficial interaction between *Arabidopsis thaliana* and the endophytic fungus *Piriformospora indica*. The Plant Journal **54,** 428-439.

**Shimada, C., Lipka, V., O'Connel, R., Okuno, T., Schulze-Lefert, P., and Takano, Y.** (2006). Nonhost resistance in Arabidopsis-colletotrichum interactions acts at the cell periphery and requires actin filament function. Molecular Plant-Microbe Interactions **19,** 270-279.

**Stein, M., Dittgen, J., Sanchez-Rodriguez, C., Hou, B.-H., Molina, A., Schulze-Lefert, P., Lipka, V., and Somerville, S.** (2006). Arabidopsis PEN3/PDR8, an ATP binding cassette transporter, contributes to nonhost resistance to inappropriate pathogens that enter by direct penetration. The Plant Cell **18,** 731-746.

**Stone, B.A., and Clarke, A.E.** (1992). Chemistry and Physiology of higher plant 1,3-b-glucans (Callose). B. A. Stone and A. E. Clarke (Eds.) Chemistry and Biology of (1-3)-b-Glucans, La Trobe Universety Press, Bundoora, Australia**,** 365-429.

**Suarez-Rodriguez, M.C., Adams-Phillips, L., Liu, Y., Wang, H., Su, S.-H., Jester, P.J., Zhang, S., Bent, A.F., and Krysan, P.J.** (2007). MEKK1 is required for flg22-induced MPK4 activation in Arabidopsis plants. Plant Physiology **143,** 661-669.

**Takahashi, A., Casais, C., Ichimura, K., and Shirasu, K.** (2003). HSP90 interacts with RAR1 and SGT1 and is essential for RPS2-mediated disease resistance in Arabidopsis. Proceedings of the National Academy of Sciences of the United States of America **100,** 11777-11782.

**Takahashi, H., Miller, J., Nozaki, Y., Sukamto, Takeda, M., Shah, J., Hase, S., Ikegami, M., Ehara, Y., and Dinesh-Kumar, S.P.** (2002). *RCY1*, an *Arabidopsis thaliana RPP8/HRT* family resistance gene, confering resistance to cucumber mosaic virus requires salicylic acid, ehtylene and a novel signal transduction mechanism. The Plant Journal **32,** 655-667.

**Takemoto, D., Jones, D.A., and Hardham, A.R.** (2003). GFP-tagging of cell components reveals the dynamics of subcellular re-organization in response to infection of *Arabidopsis* by oomycete pathogens. The Plant Journal **33,** 775-792.

**Takken, F.L.W., Albrecht, M., and Tameling, W.I.L.** (2006). Resistance proteins: molecular switches of plant defence. Current Opinion in Plant Biology **9,** 383-390.

**Tameling, W.I.L., and Baulcombe, D.C.** (2007). Physical association of the NB-LRR resistance protein Rx with a Ran GTPase-activating protein is required for extreme resistance to *potato virus X*. The Plant Cell **19,** 1682-1694.

**Tameling, W.I.L., Elzinga, S.D.J., Darmin, P.S., Vossen, J.H., Takken, F.L.W., Haring, M.A., and Cornelissen, B.J.C.** (2002). The tomato R gene products I-2 and Mi-1 are functional ATP binding proteins with ATPase activity. Plant Cell **14,** 2929-2939.

**Tao, Y., Yuan, F., Leister, T.R., Ausubel, F.M., and Katagiri, F.** (2000). Mutational analysis of the Arabidopsis nucleotide binding site-leucine-rich repeat resistance gene *RPS2*. The Plant Cell **12,** 2541-2554.

**Thiele, K., Wanner, G., Kindzierski, V., Jurgens, G., Mayer, U., Pachl, F., and Assaad, F.F.** (2009). The timely deposition of callose is essential for cytokinesis in Arabidopsis. Plant Journal **58,** 13-26.

**Thordal-Christensen, H.** (2003). Fresh insights into processes of nonhost resistance. Current Opinion in Plant Biology **6,** 351-357.

**Tsiamis, G., Mansfield, J.W., Hockenhull, R., Jackson, R.W., Sesma, A., Athanassopoulos, E., Bennett, M.A., Stevens, C., Vivian, A., Taylor, J.D., and Murillo, J.** (2000). Cultivar-specific avirulence and virulence functions assigned to *avrPphF* in *Pseudomonas syringae* pv. *phaseolicola*, the cause of bean halo-blight disease. The EMBO Journal **19,** 3204-3214.

**Turck, F., Zhou, A., and Somssich, I.E.** (2004). Stimulus-dependent, promoter-specific binding of transcription factor WRKY1 to its native promoter and the defense-related gene *PcPR1-1* in parsley. The Plant Cell **16,** 2573-2585.

**Twell, D.** (2006). A blossoming romance: gamete interactions in flowering plants. Nat Cell Biol **8,** 14-16.

**Twell, D., Park, S.K., Hawkins, T.J., Schubert, D., Schmidt, R., Smertenko, A., and Hussey, P.J.** (2002). MOR1/GEM1 has an essential role in the plant-specific cytokinetic phragmoplast. Nat Cell Biol **4,** 711-714.

**Ülker, B., and Somssich, I.E.** (2004). WRKY transcription factors: from DNA binding towards biological function. Current Opinion in Plant Biology **7,** 491-498.

**van der Biezen, E.A., and Jones, J.D.G.** (1998). The NB-ARC domain: A novel signalling motif shared by plant resistance gene products and regulators of cell death in animals. Current Biology **8,** R226-R227.

**van Ooijen, G., Mayr, G., Kasiem, M.M.A., Albrecht, M., Cornelissen, B.J.C., and Takken, F.L.W.** (2008). Structure-function analysis of the NB-ARC domain of plant disease resistance proteins. Journal of Experimental Botany **59,** 1383-1397.

**Vanacker, H., Lu, H., Rate, D.N., and Greenberg, J.T.** (2001). A role for salicylic acid and NPR1 in regulating cell growth in Arabidopsis. Plant J **28,** 209-216.

**Venugopal, S.C., Jeong, R.-D., Mandal, M.K., Zhu, S., Chandra-Shekara, A.C., Xia, Y., Hersh, M., Stromberg, A.J., Navarre, D., Kachroo, A., and Kachroo, P.** (2009). Enhanced disease susceptibility 1 and salicylic acid act redundantly to regulate resistance gene-mediated signaling. PLoS Genetics **5,** e1000545.

**Vlot, A.C., Klessig, D.F., and Park, S.-W.** (2008). Systemic acquired resistance: the elusive signal(s). Current Opinion in Plant Biology **11,** 436-442.

**Vlot, A.C., Dempsey, D.M.A., and Klessig, D.F.** (2009). Salicylic acid, a multifaceted hormone to combat disease. Annual Review of Phytopathology **47,** 177-206.

**Vogel, J., and Somerville, S.** (2000). Isolation and characterization of powdery mildew-resistant *Arabidopsis* mutants. Proceedings of the National Academy of Sciences of the United States of America **97,** 1897-1902.

**Wang, L., Mitra, R.M., Hasselmann, K.D., Sato, M., Lenarz-Wyatt, L., Cohen, J.D., Katagiri, F., and Glazebrook, J.** (2008). The genetic network controlling the *Arabidopsis* transcriptional response to *Pseudomonas syringae* pv. *maculicola*: roles of major regulators and the phytotoxin Ccoronatine. Molecular Plant-Microbe Interactions **21,** 1408-1420.

**Whenham, R.J., Fraser, R.S.S., and Snow, A.** (1985). Tobacco Mosaic Virus-Induced Increase in Abscisic-Acid Concentration in Tobacco-Leaves - Intracellular Location and Relationship to Symptom Severity and to Extent of Virus Multiplication. Physiological Plant Pathology **26,** 379-387.

**Wiermer, M., Feys, B.J., and Parker, J.E.** (2005). Plant immunity: the EDS1 regulatory node. Current Opinion in Plant Biology **8,** 383-389.

**Wildermuth, M.C., Dewdney, J., Wu, G., and Ausubel, F.M.** (2001). Isochorismate synthase is required to synthesize salicylic acid for plant defence. Nature **414,** 562-565.

**Wirthmueller, L., Zhang, Y., Jones, J.D.G., and Parker, J.E.** (2007). Nuclear accumulation of the *Arabidopsis* immune receptor RPS4 is necessary for triggering EDS1-dependent defense. Current Biology **17,** 2023-2029.

**Woo, H.R., Chung, K.M., Park, J.-H., Oh, S.A., Ahn, T., Hong, S.H., Jang, S.K., and Nam, H.-G.** (2001). ORE9, an F-box protein that regulates leaf senescence in Arabidopsis. The Plant Cell **13,** 1779-1790.

**Xiao, S., Ellwood, S., Calis, O., Patrick, E., Li, T., Coleman, M., and Turner, J.G.** (2001). Broad-spectrum Mildew Resistance in *Arabidopsis thaliana* mediated by *RPW8*. Science **291,** 118-120.

**Xie, B., Wang, X.M., and Hong, Z.L.** (2010). Precocious pollen germination in Arabidopsis plants with altered callose deposition during microsporogenesis. Planta **231,** 809-823.

**Xu, X., Chen, C., Fan, B., and Chen, Z.** (2006). Physical and functional interactions between pathogen-induced *Arabidopsis* WRKY18, WRKY40, and WRKY60 transcription factors. The Plant Cell **18,** 1310-1326.

**Yamasaki, K., Kigawa, T., Inoue, M., Tateno, M., Yamasaki, T., Yabuki, T., Aoki, M., Seki, E., Matsuda, T., Tomo, Y., Hayami, N., Terada, T., Shirouzu, M., Tanaka, A., Seki, M., Shinozaki, K., and Yokoyama, S.** (2005). Solution structure of an Arabidopsis WRKY DNA binding domain. The Plant Cell **17,** 944-956.

**Yan, N., Chai, J.J., Lee, E.S., Gu, L.C., Liu, Q., He, J.Q., Wu, J.W., Kokel, D., Li, H.L., Hao, Q., Xue, D., and Shi, Y.G.** (2005). Structure of the CED-4-CED-9 complex provides insights into programmed cell death in Caenorhabditis elegans. Nature **437,** 831-837.

**Yang, S., and Hua, J.** (2004). A haplotype-specific Resistance gene regulated by BONZAI1 mediates temperature-dependent growth control in Arabidopsis. Plant Cell **16,** 1060-1071.

**Zheng, Z., Qamar, S.A., Chen, Z., and Mengiste, T.** (2006). Arabidopsis WRKY33 transcription factor is required for resistance to necrotrophic fungal pathogens. The Plant Journal **48,** 592-605.

**Zimmermann, P., Hirsch-Hoffmann, M., Hennig, L., and Gruissem, W.** (2004). GENEVESTIGATOR. Arabidopsis microarray database and analysis toolbox. Plant Physiol **136,** 2621-2632.

**Zipfel, C., and Felix, G.** (2005). Plants and animals: a different taste for microbes? Current Opinion in Plant Biology **8,** 353-360.

**Zipfel, C., Robatzek, S., Navarro, L., Oakeley, E.J., Jones, J.D.G., Felix, G., and Boller, T.** (2004). Bacterial disease resistance in Arabidopsis through flagellin perception. Nature **428,** 764-767.

**Zipfel, C., Kunze, G., Chinchilla, D., Caniard, A., Jones, J.D.G., Boller, T., and Felix, G.** (2006). Perception of the bacterial PAMP EF-Tu by the receptor EFR restricts *Agrobacterium*-mediated transformation. Cell **125,** 749-760.

# Danksagung

Vielen Dank an Paul Schulze-Lefert für die Möglichkeit, am MPIPZ zu promovieren.

Danke an Dich, Imre, für Deine Unterstützung und die stets offene Bürotür.

Großer Dank gilt den vielen lieben Kollegen, die den Weg dieser Arbeit begleitet und mir mit Rat und kritischem Verstand zur Seite gestanden haben.
Besonders möchte ich mich bei Elke, Lydia, Moritz, Rainer und Mario für die gute Atmosphäre im Labor und Ihre Hilfsbereitschaft bedanken.

Danke an die alte Container-Mannschaft: Dorit, Doris, Ana und Simone für gemeinsam geteilte Freuden und Frust - in heißen Sommern und kalten Wintern.

Einige Menschen waren maßgeblich - ohne es zu wissen - an dem Gelingen dieser Arbeit beteiligt. Ich danke Dave, Tom, Patrick, Micha, Chris und Gabi für ihre Freundschaft, die vielen Konzerte, das ein oder andere Bier und die Tatsache, dass es Euch gibt –
Rock' n Roll!

Mein besonderer Dank gilt meinen Eltern für Ihre Liebe und Ihr Vertrauen sowie für ihre große Hilfsbereitschaft.

Zum Schluß möchte ich dem Menschen danken, der mir wie kein andererer in den letzten Wochen zur Seite stand und mir den Rücken freigehalten hat. Der sich trotz aller Widrigkeiten nie beschwert und mich immer wieder motiviert hat.  Danke Bille, für Deine Liebe und Dein Vertrauen!

# Erklärung

Ich versichere, dass ich die von mir vorgelegte Dissertation selbständig angefertigt, die benutzten Quellen und Hilfsmittel vollständig angegeben und die Stellen der Arbeit - einschließlich Tabellen, Karten und Abbildungen -, die anderen Werken im Wortlaut oder dem Sinn nach entnommen sind, in jedem Einzelfall als Entlehnung kenntlich gemacht habe; dass diese Dissertation noch keiner anderen Fakultät oder Universität zur Prüfung vorgelegen hat; dass sie - abgesehen von den unten angegebenen Teilpublikationen noch nicht veröffentlicht worden ist sowie, dass ich eine solche Veröffentlichung vor Abschluss des Promotionsverfahrens nicht vornehmen werde. Die Bestimmungen dieser Promotionsordnung sind mir bekannt. Die von mir vorgelegte Dissertation ist von Prof. Dr. Paul Schulze-Lefert betreut worden.

Köln, Januar 2011          _____

(Armin Töller)

# Curriculum vitae

## Angaben zur Person:

| | |
|---|---|
| Name: | Armin Töller |
| Anschrift: | Kaiserstraße 18a |
| | 50321 Brühl |
| Telefon: | 02232/577429 |
| | |
| Geburtsdatum, - ort: | 14. Januar 1978 in Brühl |
| Familienstand: | verheiratet |

## Schulbildung:

1988 – 1994      Elisabeth-von-Thüringen Realschule, Brühl

1994 – 1997      St. Ursula Gymnasium, Brühl
                 Abschluss: Allgemeine Hochschulreife

## Zivildienst:

09/1997 – 10/1998      Altenzentrum Johannesstift, Brühl

## Studium:

10/1999 –02/2006      Diplomstudium an der Universität zu Köln,
                      Fachbereich Biologie

03/2005 – 04/ 2006      Diplomarbeit am Max-Planck-Institut für
                        Pflanzenzüchtungsforschung in Köln unter Leitung von Prof.
                        Dr. Paul Schulz-Lefert: „ Funktionale Analyse von 1,3- β
                        Glucan-Synthasen in Pflanzen Pathogen Interaktionen"

04/2006 – 12/2006     Weiterführung der im Rahmen der Diplomarbeit  begonnenen Forschungsarbeit am Max-Planck-Institut für Pflanzenzüchtungsforschung in Köln

Seit 01/2007          Bearbeitung des Dissertationsthemas am Max-Planck-Institut für Pflanzenzüchtungsforschung in Köln, unter Leitung von Prof. Dr. Paul Schulze-Lefert im Labor von Dr. I. Somssich